Plant aromatic amino acid decarboxylases: Evolutionary divergence, physiological function, structure function relationships and biochemical properties.

Michael Patrick Spence

Dissertation submitted to the faculty of the Virginia Polytechnic Institute and State University in partial fulfillment of the requirements for the degree of

Doctor of Philosophy

In

Biochemistry

Chair Jianyong Li

Glenda E. Gillaspy

Timothy J. Larson

David R. Bevan

June 3, 2014

Blacksburg, Virginia

Keywords: Type II PLP decarboxylases; aromatic amino acid decarboxylase; aromatic acetaldehyde syntheses

Plant aromatic amino acid decarboxylases: Evolutionary divergence, physiological function, structure function relationships and biochemical properties.

Michael Patrick Spence

ABSTRACT

Plant aromatic amino acid decarboxylases (AAADs) are a group of economically important enzymes categorically joined through their pyridoxal 5'-phosphate (PLP) dependence and sequence homology. Extensive evolutionary divergence of this enzyme family has resulted in a selection of enzymes with stringent aromatic amino acid substrate specificities. Variations in substrate specificities enable individual enzymes to catalyze key reactions in a diverse set of pathways impacting the synthesis of monoterpenoid indole alkaloids (including the pharmacologically active vinblastine and quinine), benzylisoquinoline alkaloids (including the pharmacologically active papaverine, codeine, morphine, and sanguinarine), and antioxidant and chemotherapeutic amides. Recent studies of plant AAAD proteins demonstrated that in addition to the typical decarboxylation enzymes, some annotated plant AAAD proteins are actually aromatic acetaldehyde synthases (AASs). These AASs catalyze a decarboxylation-oxidative deamination process of aromatic amino acids, leading to the production of aromatic acetaldehydes rather than the AAAD derived arylalkylamines. Research has implicated that plant AAS enzymes are involved in the production of volatile flower scents, floral attractants, and defensive phenolic acetaldehyde secondary metabolites. Historically, the structural elements responsible for differentiating plant AAAD substrate specificity and activity have been difficult

to identify due to strong AAAD and AAS inter-enzyme homology. Through extensive bioinformatic analysis and experimental verification of plant AAADs, we have determined somestructural elements unique to given types of AAADs. This document highlights structural components apparently responsible for the differentiation of activity and substrate specificity. In addition to producing primary sequence identifiers capable of AAAD activity and substrate specificity differentiation, this work has also demonstrated applications of AAAD enzyme engineering and novel activity identification.

TABLE OF CONTENTS

List of Figures

List of Tables

Chapter 1

1.1 Introduction

Due to their sessile nature, plants have developed a broad variety of chemical compounds responsible for mitigating interactions with their biotic and abiotic environments. These secondary metabolites differ from so called primary metabolites due to their dispensable nature. Although, secondary metabolites aid in the growth and development of plants, they are not vital for survival under desirable growth conditions. Biosynthetic enzymes responsible for the synthesis of secondary metabolites were originated from primary metabolic pathways. Due to their non-vital nature, secondary metabolite biosynthetic enzymes generally display greater evolvability and mechanistic elasticity compared to their primary metabolism counterparts. The resulting plasticity of secondary metabolite enzymes has enabled the evolution of a broad selection of enzymes for the production of thousands of diverse chemicals frequently involved in plant defense mechanisms.

In plants, aromatic amino acid decarboxylases (AAADs) are an integral part of the pathways for the biosynthesis of a spectrum of alkaloid and volatile secondary metabolites. Like many other secondary metabolite biosynthesis genes, plant AAADs have undergone gene duplication events to generate significant functional and genetic redundancy. For example, the opium poppy (*Papaver somniferum)* contains approximately 15 AAAD sequences with apparently identical enzymatic functions. The resulting functional redundancy further increases the plasticity of the AAAD sequences by reducing the evolutionary consequences of genetic mutations. Although many mutations may generate non-functional or non-soluble proteins, occasionally mutations arise which grant new enzymatic activities that increase the evolutionary fitness of the organisms. Within plant AAADs, these functional divergence events have occurred on several occasions to generate a spectrum of activities and substrate specificities. Thus far, plant AAADs

have generated at least three distinct categories. These AAAD sub-categories include tryptophan decarboxylases (TDCs), tyrosine decarboxylases (TyDCs) and aromatic acetaldehyde synthases (AASs). TDCs and TyDCs catalyze the decarboxylation of indolic and phenolic amino acids respectively to generate their corresponding aromatic arylalkylamines. AAS catalyzes a more involved decarboxylation-oxidative deamination process to produce aromatic acetaldehydes from their phenolic amino acid substrates. It is clear that the physiological functions of plant AAADs are closely related to their respective activities and substrate specificities. However, due to the subtlety of the enzymatic divergence of these AAAD subcategories, the sequences between these categories remain almost identical. Due to this high sequence homology, it has historically been difficult to predict the function of any given plant AAAD through sequence comparison. This extensive homology has lead to a major problem in distinguishing activity and substrate specificity from a primary sequence standpoint. The structural elements responsible for differentiating plant AAAD substrate specificity and activity have been difficult to identify due to high TyDC, TDC and AAS inter-enzyme homology. In this dissertation, the evolutionary divergence and physiological functions of AAAD enzymes are investigated. Results from these studies have identified specific structural elements capable of differentiating the variable activities and substrate specificities of plant AAADs.

Chapter 2

Biochemical evaluation of a parsley tyrosine decarboxylase results in a novel 4-hydroxyphenylacetaldehyde synthase enzyme.

Reprinted from Biochemical and Biophysical Research Communications with permission

Torrens-Spence, M.P., Gillaspy, G., Zhao, B., Harich, K., White, R.H. and Li, J. (2012) Biochemical evaluation of a parsley tyrosine decarboxylase results in a novel 4-hydroxyphenylacetaldehyde synthase enzyme. *Biochem Biophys Res Commun.* 418(2): 211-216

Author Contributions

Michael P. Torrens-Spence[1] wrote the article and performed all the research except for the experiments mentioned below.

Glenda Gillaspy[1] assisted in the growing mRNA extraction and cDNA production from the involved plant models. Additionally, this author assisted in the real time PCR analysis.

Bingyu Zhao[2] assisted in the jasmonic acid elicitation.

Kim Harich[1] performed the LC MS and GC MS analyses.

Robert H. White was responsible for the synthesis of the 4-hydroxyphenyl acetaldehyde standard.

Jianyong Li[1] oversaw and directed the research and helped write the article.

[1] Department of Biochemistry, Virginia Tech, Blacksburg, Virginia, United States of America,

[2] Department of Horticulture, Virginia Tech, Blacksburg, Virginia, United States of America

2.1 Abstract

Plant aromatic amino acid decarboxylases (AAADs) are effectively indistinguishable from plant aromatic acetaldehyde syntheses (AASs) through primary sequence comparison. Spectroscopic analyses of several characterized AASs and AAADs were performed to look for absorbance spectral identifiers. Although this limited survey proved inconclusive, the resulting work enabled the reevaluation of several characterized plant AAS and AAAD enzymes. Upon completion, a previously reported parsley AAAD protein was demonstrated to have AAS activity. Substrate specificity tests demonstrate that this novel AAS enzyme has a unique substrate specificity towards tyrosine (km 0.46 mM) and dopa (km 1.40 mM). Metabolite analysis established the abundance of tyrosine and absence of dopa in parsley extracts. Such analysis indicates that tyrosine is likely to be the sole physiological substrate. The resulting information suggests that this gene is responsible for the in vivo production of 4-hydroxyphenylacetaldehyde (4-HPAA). This is the first reported case of an AAS enzyme utilizing tyrosine as a primary substrate and the first report of a single enzyme capable of producing 4-HPAA from tyrosine.

2.2 Keywords

Aromatic amino acid decarboxylases; aromatic acetaldehyde syntheses; tyrosine decarboxylase; 4-hydroxyphenylacetaldehyde

2.3 Introduction

Aromatic amino acid decarboxylase (AAAD) is an eponym originally applied to mammalian dopa decarboxylase (DDC). This enzyme catalyzes the respective decarboxylation of dopa and 5-hydroxytryptophan to dopamine and 5-hydroxytryptamine. The AAAD designation has subsequently been used for annotating similar enzymes from many other species. Such

annotations are appropriate for species that have a single AAAD protein with well-defined substrate specificity. This same annotation is vague or inaccurate for organisms with multiple divergent AAAD-like proteins. For example, an expansion of the AAAD gene within insect and plant species results in a multiplicity of functionally diverse AAAD enzymes. A single AAAD annotation does not accurately represent the selection of activities and substrate specificities. This can be illustrated through our recent study of some predicted *Drosophila* and mosquito AAAD sequences. Resulting research determined that these AAAD like sequences catalyze a complicated decarboxylation-deamination process of dopa to 3,4-dihydroxy-phenylacetaldehyde (DHPA) [1]. These enzymes, unlike their names imply, have nothing to do with the production of arylalkylamines, but rather catalyze the production of their corresponding aromatic acetaldehydes. Consequently, their AAAD name provides misleading functional implications. This issue with ambiguous AAAD annotation also applies to plants. Database and literature searches reveal that plants have similarly diverse AAAD groups. For example, one particular plant AAAD group catalyzes the same decarboxylation-deamination process as the aforementioned insect AAAD proteins.

Despite the major difference in catalytic processes between amine and aldehyde producing AAADs, this enzyme family in general retains great homology. This sequence similarity makes for problematic primary sequence differentiation of the amine producing AAADs and aldehyde producing aromatic acetaldehyde syntheses (AASs). In particular, this large level of homology makes it difficult to distinguish plant AASs from plant tyrosine decarboxylases (TyDCs). To investigate an alternate AAAD differentiation approach, we have been investigating the spectral characteristics of various AAAD enzymes. During this analysis, we observed no consistent spectral pattern for the differentiation of AAADs and AASs. This investigation did however enable characterizations of several previously investigated plant AAADs and AASs. Upon completion, we determined that contrary to previous reporting [2], parsley (*Petroselinum*

crispum) enzyme (NCBI accession Q06086) is not capable of catalyzing the conversion of tyrosine to tyramine and dopa to dopamine, but rather catalyzes the conversion of tyrosine to 4-hydroxyphenylacetaldehyde (4-HPAA) and dopa to DHPA. This substrate specificity for tyrosine and dopa makes parsley Q06086 unique amongst all other previously characterized plant AASs. To clearly differentiate this novel AAS activity from a typical AAAD we performed a side-by-side comparison of this parsley AAS enzyme to a highly homologous (70% identity) *Thalictrum flavum* TyDC (NCBI accession AAG60665). We also provide data showing that tyrosine is the sole physiological substrate for Q06086. The resulting information reveals the first plant AAS with tyrosine as a substrate. Q06086 and AAG60665 also serve as great examples illustrating that AAAD-like proteins sharing high sequence homology may have completely different biochemical functions.

2.4 Materials and Methods

Reagents

Tyrosine, tyramine, dopa, dopamine, benzaldehyde, 4-hydroxybenaldehyde, 3,4-dihydroxybenaldehyde, 4-hydroxyphenylethanol, 3,4-dihydroxyphenylethanol, pyridoxal 5-phsophate (PLP), formic acid, and acetonitrile were purchased from Sigma (St. Louis, MO). The IMPACT-CN protein expression system was purchased from New England Biolabs (Ipswich, MA).

Plant material, growth conditions, and jasmonic acid elicitation.

P. crispum seeds were obtained from www.burpee.com. *T. flavum* seeds were obtained from www.dianeseeds.com. Seeds were germinated in Sunshine Pro Premium potting soil and were grown under a 16-hr photoperiod at 23 degrees C at 100 microeinsteins. 10 mL of a 2.5 mM

Jasmonic acid (1.2% EtOH, 0.2% Triton X-100) solution was injected into the soil surrounding the stem of the parsley plant. In addition, 0.25 mL of 5 mM Jasmonic acid solution was rubbed onto parsley leaves and stems.

RNA isolation, cDNA production, and RT-PCR

Total RNA was isolated from whole parsley plants (12 weeks) and *T. flavum* plants (12 weeks) using Ambion®® mirVana™ miRNA Isolation Kit. RNA samples were subsequently DNase-treated using Ambion TURBO DNA-free™ Kit. cDNAs were produced using Invitrogen™ SuperScript™ III First-Strand Synthesis System for RT-PCR. Specific parsley Q06086 forward (5'-CTATGGAGTTGGTCAGCTGAG-3') and reverse primer (5'-CACCGAC TCCAACAACTTC-3') and control parsley polyubiquitin (*ubi*4) forward (5'-CTTCGTCT CCGTGGTGGT-3') and reverse primer (5'-GCTAGGGTCCTTCCATCCTC-3') were synthesized and used for RT-PCR with reagents and procedures from Invitrogen™ Platinum® SYBR® Green qPCR SuperMix-UDG. Each data point represented the average of three independent biological samples with three technical replicates.

Protein expression and purification.

A forward and reverse parsley Q06086 CDS primer pair (5'-ACTGACTAGTATGGGCTCCATCGATAATC-3' and 5'-ACTGCTCGAGTTAGGATAAAA TATTCACGATCTTCT-3') and a forward and reverse *Thalictrum* AAG60665 CDS primer pair (5'-ACTGACTAGTATGGGTAGCCTCCATGTT-3' and 5'-ACTGCTCGAGTTAAAATGTAG CAAGTACAGCATC -3') were synthesized and used to amplify cDNA. Amplified products were cloned into an Impact-CN protein expression vector (New England Biolabs). All proteins were expressed and purified according to the previous methods used in *D. melanogaster* DDC

recombinant production [3] with modifications. Protein concentration was determined using the Bradford method [4].

Activity assays

Reaction mixtures of 100 μl, containing 15 μg Q06086 or 5 μg AAG60665 and 2 mM tyrosine or dopa, were prepared in 50 mM phosphate buffer (pH 6.8) and incubated at 25^{o} C in a water bath. At different time periods after incubation (usually 10-60 min) the reaction of individual reaction mixtures was stopped by mixing an equal volume of 0.8 M formic acid. Supernatants of the reaction mixtures, obtained by centrifugation, were analyzed by HPLC with electrochemical detection (ED) as previously described [1]. Some reaction mixtures were treated with an equal volume of $NaBH_4$ saturated ethanol, incubated for 5 min at 25^{o} C, treated with 0.8 M formic acid (decompose remaining $NaBH_4$), and then analyzed by HPLC-ED similar to those described in a previous report [1]. The mobile phase consisted of 50 mM monopotassium phosphate (pH 4.6) containing 13% (v/v) acetonitrile and 0.5 mM octyl sulfate.

GC/MS analysis of parsley Q06086-catalyzed product from tyrosine

Enzyme activity assay strongly indicated the production of 4-HPAA from tyrosine and DPHA from dopa by parsley Q06086. To further verify the identity of the product, a tyrosine and parsley Q06086 reaction mixture was derivatized with O-(4-nitrobenzyl)hydroxylamine. The derivatized sample was injected onto an RTX5MS GC column (30 m x 0.32 mm) installed in a HP 5890 GC. Oven temperature was programmed from 80 to 280 deg at 8 deg/min. EI mass spectrometry was performed on a VG70SE mass spectrometer operated at 70 eV with the mass range scanned from 50-400 amu. The molecular ion and its EI spectrum of the enzymatic product derivative was compared with those of chemically synthesized 4-HPAA-*O*-(4-nitrobenzyl) derivative obtained at identical GC/MS analysis conditions. The 4-HPAA standard was

chemically synthesized from DL-4-hydroxyphenyllactic acid methanol. Supplement material provideds details about 4-HPAA synthesis/ derivatization.

Kinetic analysis

After the substrate specificity and catalytic reaction of parsley Q06086 were verified, its kinetic parameter to tyrosine and dopa were analyzed. Reaction mixtures of 100 μl containing 10 μg of parsley AAS (Q06086 protein) and a varying concentration (0.1 – 5 mM) of tyrosine or dopa were prepared in 50 mM phosphate buffer (pH 7.0) and incubated at 25^{o} C. An equal volume of borohydride-saturated ethanol was added to the reaction mixtures at 5 min after incubation (stopped reaction by protein denaturation and reduction of 4-HPAA to 4-HPEA by borohydride). The mixtures were acidified by mixing equal volume of 0.8 M formic acid (decomposition of remaining borohydride) and supernatants were injected for HPLC-ED analysis. The amounts of products in reaction mixtures containing different concentrations of substrate were quantitated based on a standard curve generated using authentic 4-PHEA standard (or DPHA standard) at identical conditions of HPLC-ED analysis.

Analysis of endogenous tyrosine and dopa in parsley extracts by LC/MSMS

Enzyme activity assays determined that parsley Q06086 could use tyrosine and dopa as its substrates. To determine the presence and relative amounts of tyrosine and dopa in parsley, whole adult plants (12 weeks) were frozen and ground to homogeneity in liquid nitrogen using a mortar and pestle. Ground plant powder was extracted with 80% ethanol at 1:25 (tissue powder weight versus volume of ethanol solution) for 30 min at room temperature. The soluble fraction was then removed and lyophilized. The lyophilized samples were re-dissolved in 0.1% formic acid and analyzed by a LC-3200 Q Trap MS/MS system (Applied Biosciences) at positive ion mode. Identification of tyrosine and dopa in parsley extracts was based on their retention time

and MS/MS spectra in comparison with those of authentic tyrosine and dopa standards at identical analytic conditions.

2.5 Results

Spectral characteristics

*S*pectral analysis of purified recombinant parsley Q06086 protein and *Thalictrum* AAG60665 protein revealed the presence of an ultraviolet (UV) absorbance peak with a λ_{max} around 330 – 340 nm and a visible absorbance peak with a λ_{max} around 398 to 422 nm (Fig. 2.1).

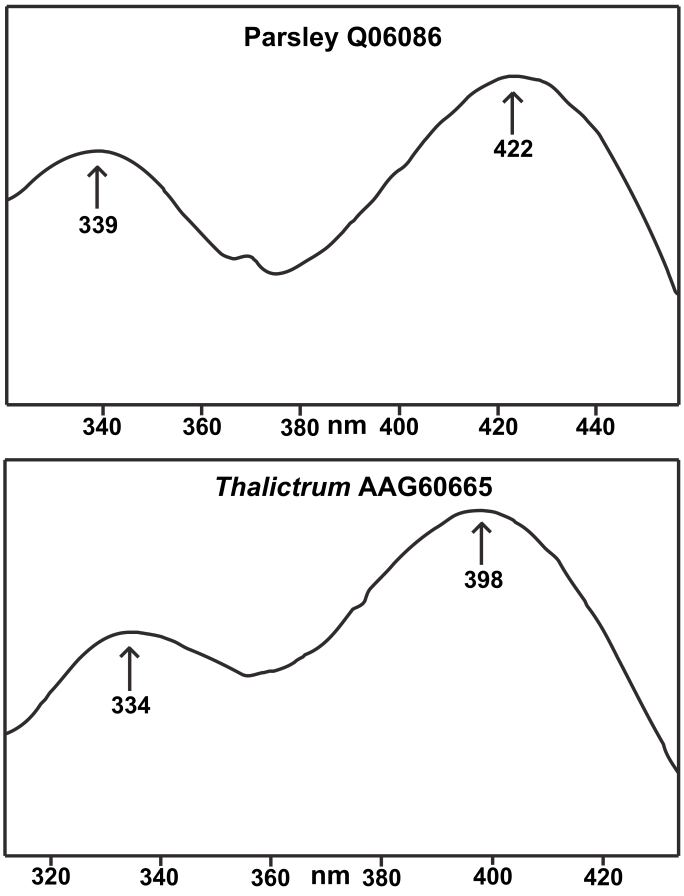

Figure 2.1. Spectral characteristics of recombinant Q06086 and AAG60665 proteins. Purified proteins were prepared in 50 mM phosphate buffer (pH 7.5) and their absorbance spectrum were determined using a Hitachi U2001 UVVisible spectrophotometer. Arrows indicate peak

maximum.

These two absorbance peaks are typical for PLP-containing proteins. The presence of the two absorbance peaks indicated that parsley Q06086 and *Thalictrum* AAG60665 were PLP-containing proteins. During ion exchange and gel filtration chromatographies, no PLP was added to buffers used for protein purification, indicating that PLP cofactor was tightly associated with their polypeptides.

AAAD assays

When recombinant Q06086 protein was first assayed using tyrosine as a substrate, a very broad peak was detected in the reaction mixture by HPLC-ED (Fig. 2.2A). The peak dimension was proportionally increased as the incubation time increased (Fig. 2.2B), indicating that the broad peak corresponds to the reaction product. Experimental repetition with dopa indicates a similar broad peak corresponding to the dopa enzymatic product. When phenylalanine was used a substrate, the broad peak essentially was not observed. This data was consistent with the previously reported Q06086 substrate specificity [2]. Under identical HPLC-ED analysis conditions, a sharp product peak was detected in a *Thalictrum* AAG60665 protein and tyrosine (Fig. 2.2D) or dopa reaction mixture (not shown).

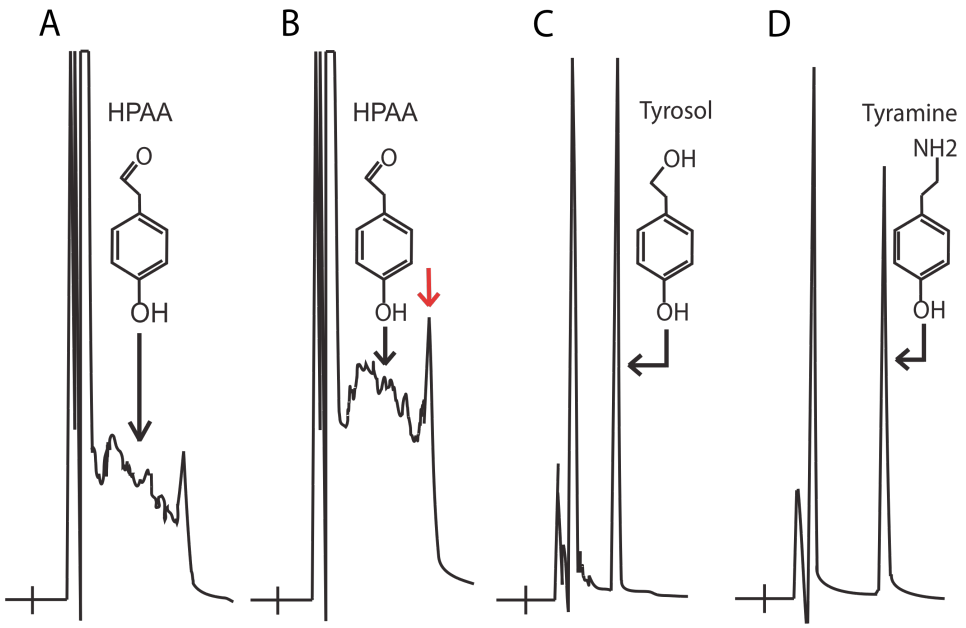

Figure 2.2. Q06086 and AAG60665 activity chromatograms. A & B illustrate the accumulation of 4-HPAA (the broad peak) in 0.1 ml reaction mixture containing 2 mM tyrosine and 15 µg Q06086 at 30 min (A) and 60 min (B) incubation. C shows the reduction of 4-HPAA to 4-HPEA by borohydride (the sample was prepared as in B, but it was treated with NaBH4 before HPLC-ED analysis). D illustrates the production of tyramine in 0.1 ml reaction mixture containing 2 mM tyrosine and 5 µg AAG60665 during 10 min incubation. Under identical conditions, the retention times of tyrosine, 4-HPEA and tyramine were 3.0, 5.1, and 6.9 min, respectively. The peak indicated by a red arrow in B with a retention time of 8.2 min (that might be presumed as tyramine) was part of the broad peak and became a single 4-HPEA peak after borohydride reduction.

Product identification

The product peak in the recombinant *Thalictrum* AAG60665 protein and tyrosine reaction mixture was identified as tyramine based on its coelution with tyramine standard at different chromatographic conditions. Production of dopamine in *Thalictrum* AAG60665 protein and dopa reaction mixtures was verified by the same procedures. Results demonstrate that *Thalictrum* AAG60665 protein catalyzes the standard decarboxylation reaction of tyrosine to tyramine and dopa to dopamine. This indicates that AAG60665 gene encodes a true TyDC.

The peak shapes resulting from parsley Q06086 protein incubated with tyrosine or dopa were similar to the chromatographic behavior of aromatic acetaldehyde produced by *Drosophila* DHPA synthase [1]. This peak similarity suggests that the Q06086 enzyme might function in aromatic aldehyde synthase activity rather than the previously reported aromatic decarboxylase activity. Aldehydes can be reduced to their corresponding alcohol by borohydride. When the incubated Q06086 and tyrosine reaction mixture was treated with $NaBH_4$ prior to HPLC-ED analysis, the broad product peak (Fig. 2.2A-B) was converted to a sharp peak (Fig. 2.2C) that coeluted with authentic 4-hydroxyphenylethanol (4-HPEA) standard at different chromatographic conditions. When incubated Q06086 protein and dopa was treated by $NaBH_4$, the broad product peak became a sharp peak that coeluted with 3,4-dihydroxyphenylethanol (DHPEA) at different chromatographic conditions (not shown).

The conversion of the broad product peak to a sharp peak by borohydride (Fig. 2.2) and its coelution with authentic 4-HPEA provide sufficient basis to suggest the 4-HPAA identity of the broad product peak (seen during HPLC-ED analysis of the parsley Q06086 protein and tyrosine reaction mixtures). To further verify the identity of the enzymatic product, incubated parsley Q06086 and tyrosine reaction mixtures were derivatized with O-(4-nitrobenzyl)hydroxylamine and analyzed by GC/MS. Under the applied GC/MS analysis conditions, a molecular ion of 286 was observed and its EI spectrum displayed 77, 107, 133, 150 product ions (Fig. 2.3C & 2.3D). The chemically synthesized 4-HPAA derivative produced the same molecular ion elution time and EI spectrum when analyzed under identical conditions (Fig. 2.3A & 2.3B). The identical molecular ion elution time and EI fragmentation pattern of the derivatized tyrosine enzymatic product and the derivatized chemically synthesized 4-HPAA standard further proves Q06086s role in the catalysis of tyrosine to 4-HPAA. These data clearly demonstrate the true AAS identity of the previously reported parsley TyDC. Under the applied conditions of kinetic analysis, parsley AAS showed a higher affinity to tyrosine (K_m = 0.46 mM) than to dopa (K_m = 1.4 mM) and also a higher V_{max} to tyrosine (V_{max} = 1.117 μmol min^{-1} mg^{-1}) than to dopa (V_{max} = 0.318 μmol min^{-1} mg^{-1}).

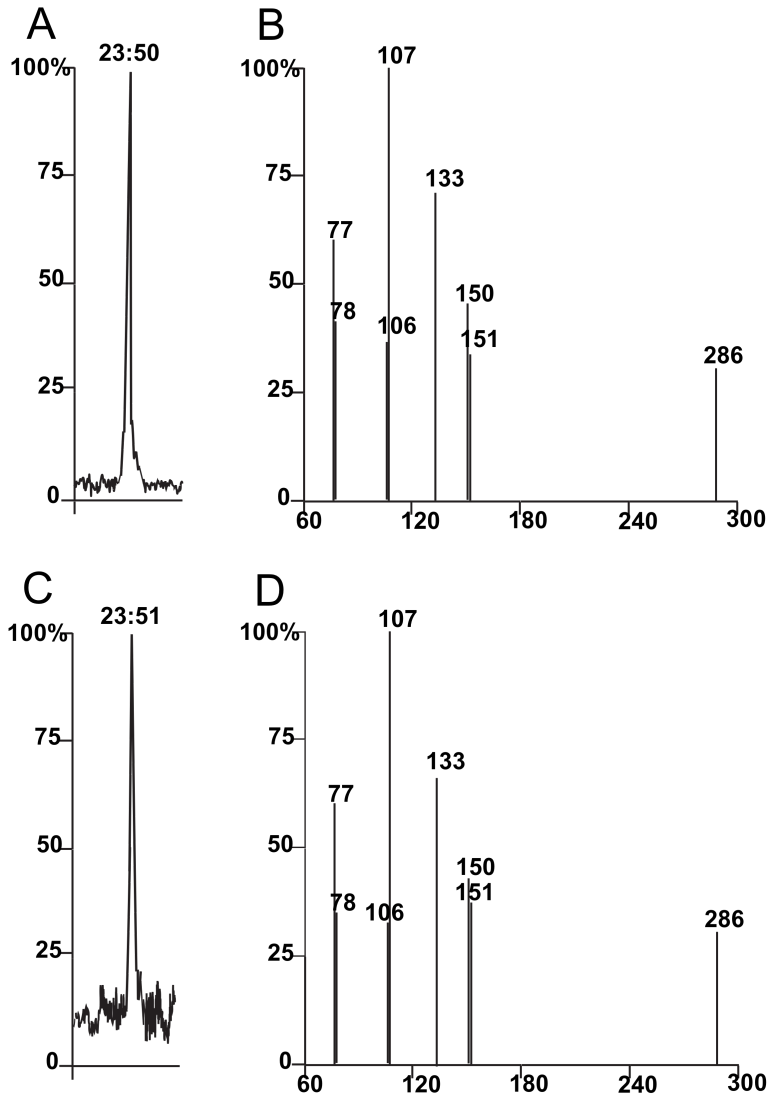

Figure 2.3. GC-MS chromatograms and ions spectra for chemically and enzymatically synthesized 4-HPAA derivatives. A represents the total ion count chromatography peak resulting from the chemically synthesized derivatized 4-HPAA. B represents the spectra resulting from the chemically synthesized derivatized 4-HPAA. C represents the total ion count chromatography peak resulting from the enzymatically synthesized derivatized 4-HPAA. D represents the spectra resulting from the enzymatically synthesized derivatized 4-HPAA. The ion spectra from both products B and C are highly similar. B and C illustrate key ions including the molecular ion (286) and strong product ions (77, 107, 133, 150). Ions below the 25% mark were not included to maintain figure clarity.

Physiological Substrate Identification

To determine the availability of physiological substrates within parsley, LC/MS was utilized to measure the presence of internal tyrosine and dopa levels. Assay development resulted in unique multiple reaction monitoring (MRM) chromatographs for both the tyrosine standard (Fig. 2.4A) and the dopa standard (Fig. 2.4C). The assay was then utilized to measure tyrosine and dopa from whole parsley extracts. Results demonstrated the presence of tyrosine (Fig. 2.4B) and the absence of dopa (Fig. 2.4D). This suggests parsley Q06086s potential role in 4-HPAA production and that tyrosine is likely the sole physiological substrate for Q06086.

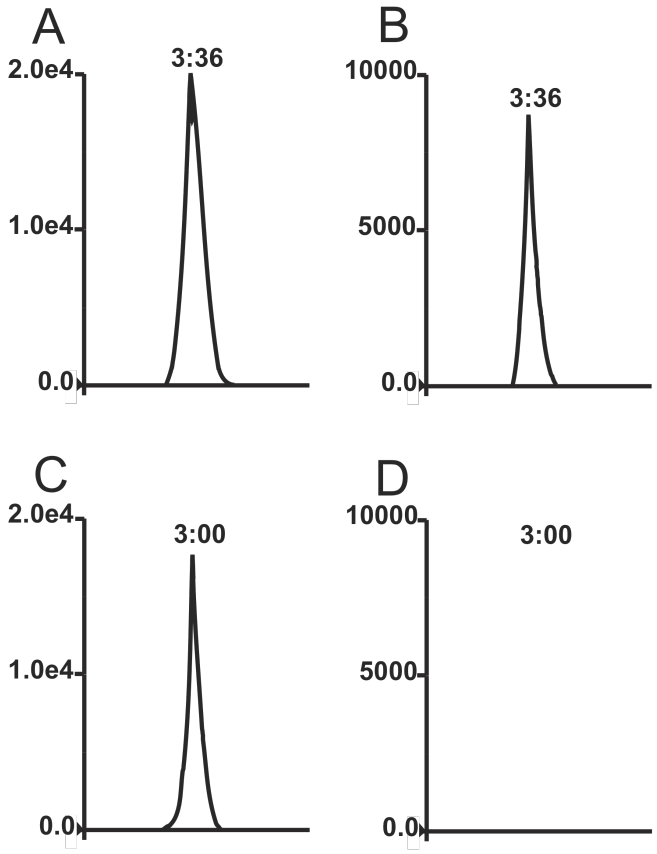

Figure 2.4. Parsley extract LCMS chromatograms of tyrosine and dopa. A and C represent the respective chromatography peaks resulting from select MRM ions of tyrosine and dopa standards. B and D represent the respective chromatography peaks resulting from select MRM ions of tyrosine and dopa measured from parsley metabolite extracts. This figure illustrates the relative abundance of tyrosine and absence of dopa with in parsley metabolite extracts. The y axis represents intensity in cps.

Potential function of parsley AAS in defense/stress responses

Q06086 was previously characterized as a pathogen-responsive gene because fungal infection or elicitor treatment led to a rapid increase in its gene transcription in parsley cell suspension culture [2]. To verify if Q06086 is a defense/stress responsive gene in whole plants, parsley plants were treated with jasmonic acid (JA) for a 10 hr-, 24 hr-, and 48 hr- time period. RT-PCR analyses of Q06086 transcript levels in comparison to polyubiquitin (*ubi*4) demonstrate a 4-fold transcript increase after 10 hrs, a 2.9 fold transcript increase at 24 hrs, and a return to control transcript level at 48 hrs. Up-regulation of the Q06086 transcription by JA suggests that it is a stress/defense responsive gene.

Parsley extract 4-HPAA measurements

GCMS analysis was used to measure internal levels of 4-HPAA from non-elicited plants and JA elicited plants. The GCMS assay developed to measure the chemically synthesized 4-HPAA derivative was utilized to measure derivatized 4-HPAA in extracts from both non-elicited plants and JA elicited plants. When parsley extracts were analyzed, no 4-HPAA was detected in either the non-elicited sample or the JA elicited sample. This absence of 4-HPAA may indicate that the 4-HPAA formed in parsley is rapidly converted to downstream compounds.

2.6 Discussion

In protein databases, proteins of the AAAD family are grouped together through their high homology, pyridoxal-5'-phosphate (PLP) dependence, and aromatic substrate requirements. Despite their shared homology AAADs actually represent several distinct enzyme groups. Each group is capable of catalyzing either the production of monoamines or formation of aromatic acetaldehydes on varied but stringent combinations of aromatic substrates. Variation in product formation equates to diverse physiological functions. This is particularly true for AAAD enzymes from plants and insects. For example, some insect AAADs that use dopa as a substrate

play very different physiological roles as compared to those that use tyrosine as a primary substrate [1,5,6]. Plant AAADs that catalyze tyrosine to tyramine conversion play essential roles in the biosynthesis of benzylisoquinoline alkaloids and many other secondary metabolites [7-9] and those that catalyze the decarboxylation of tryptophan and 5-HTP to tryptamine and 5-hydroxytryptamine (5-HT), respectively, may regulate the biosynthesis of thousands of indole alkaloid compounds [10-12]. Plant and insect AAADs that catalyze the production of aromatic acetaldehydes have completely different functions as compared to those that produce arylalkylamines [1,13,14]; as a result, their generic AAAD name provides misleading functional implications.

To link AAADs with functionally relevant information, efforts have been made to further classify plant and insect AAADs according to their substrate specificity. Due to high level of sequence homology of AAADs across species, annotation through primary sequence comparison is highly inaccurate. For example, until recently insects AAS proteins have been considered as DDC isozymes [1]. Comparison of Q06086 and AAG60665 especially exemplifies the sequence ambiguity of AAADs in plants. Despite different catalytic reactions and broad evolutionary divergence Q06086 and AAG60665 retain 70% sequence identity and 83% sequence homology. Evaluations of Q06086 and AAG60665 respective spectra further illustrate their conformity. In AAADs, the PLP cofactor is associated with their proteins by a Schiff-base linkage formed between the aldehyde group of PLP and the ε-amino group of a conserved active site lysine. Because this linkage is universal for all PLP-containing decarboxylases, the differences in spectral characteristics among distinct AAADs suggest some differences in the active site residues surrounding the PLP cofactor. Since comparison of Q06086 and AAG60665 (Fig. 2.1) yield minor variations, one must speculate that their respective PLP surrounding residues are highly similar. This spectral similarity illustrates that the Q06086 vs AAG60665 activity differentiating resides are truly quite subtle.

Another major problem in plant AAAD classification also includes the presence of incorrectly identified distinct plant AAAD proteins. Our initial intention in this study was to utilize Q06086 as a TyDC standard (because it has been experimentally verified [2]) to compare with AAS enzymes. Characterization work with Q06086 ultimately led us to its identification as a plant AAS. An extensive literature search suggests that misidentification of plant AAAD might be due to the method used for AAAD activity assays. Detection of CO_2 release has commonly been used in AAAD assays [2]. The method is valid once the decarboxylative nature of the reaction is established, but CO_2 release itself cannot distinguish AAS activity from TyDC activity. This may have been partly responsible for some plant AAAD misidentifications. For example, the first reported *Cytisus scoparius* DDC about 40 years ago [15] likely is an AAS because oxygen is necessary for CO_2 release by the enzyme (oxygen is required for oxidative deamination by AASs).

We previously proposed that the chromatographic behavior of the DHPA peak during HPLC-ED analysis was due to the keto-enol tautomerization [1]. The same phenomenon might also be responsible for the odd peak dimensions observed for 4-HPAA in this study. The chromatographic behavior of benzaldehyde, 4-hydroxybenzaldehyde and 3,4-dihydroxybenzaldehyde supports this suggestion. These aromatic aldehydes elute as sharp peak during HPLC-ED analysis under similar conditions and treatment of these compounds with $NaBH_4$ reduced them to their corresponding aromatic alcohols. In these aromatic aldehydes, formation of their side chain enol tautomers requires a series electron shift of their benzene, phenyl or catechol ring, which may not be favored. In contrast, the keto-enol tautomerization does not cause apparent change of the ring structure in DHPA and 4-HPAA, which may proceed relatively easily under acidic conditions during reverse-phase separation.

The instability/reactivity of the 4-HPAA product might be partly responsible for the misidentification of Q06086. This also might explain in part why plant and insect AASs were identified just recently [1,13] (while other types of AAADs have been established for many years [16,17]). In a previous study, we illustrated the instability of DHPA produced by insect AAS with dopa as a substrate [1]. The commercial availability of the aromatic aldehydes and the absence of the commercial aromatic acetaldehydes further imply the reactivity/instability of the aromatic acetaldehydes. There have been many reports that discussed the toxicity of DHPA in the development of human neurodegenerative diseases [18-19]. The chemical would have been available as a standard (because there is a need for clinical studies) if it were stable after synthesis. The odd peak dimensions might also contribute to AAS misidentification. Depending upon the amount of enzyme incorporated into the reaction mixture and the incubation time, the shallow broad peak we defined in this work could be easily presumed to be baseline noises due to contaminants from substrate or protein samples.

Q06086 was previously proposed to be a defense response gene because fungal infection or fungal extract treatment up-regulated its transcription in about an hour [2]. We did observed a similar significant up-regulation Q06086 transcription when JA was applied to the plant. This provides a basis to suggest that this AAS is a defense/stress responsive gene because JA regulates plant responses to abiotic and biotic stresses [20]. An apparent increase in AAS transcription should lead to an increased level of the AAS protein, which should in general be reflected by the increased content of 4-HPAA in parsley. Despite this rational, analysis of parsley extracts from both elicited or control samples did not result in the detection of 4-HPAA. Data from this study allows us to propose a positive relationship between Q06086 expression and defense/stress conditions of the parsley plant. The overall specific functions of this intriguing enzyme remain to be substantiated.

In summary, results from this study provide solid evidence demonstrating that the previously identified Q06086 parsley TyDC is a plant AAS that uses tyrosine as a primary substrate. Up-regulation of Q06086 transcription by JA indicates that Q06086 is a defense/stress responsive gene. Although details concerning the molecular regulation of the Q06086 gene and the precise functions of its protein remain to be established, our data provide a foundation towards achieving a comprehensive understanding of the biochemistry and molecular biology of this interesting protein. In addition, the aforementioned reactivity and instability of aromatic acetaldehydes should serve as a useful reference in studies dealing with the activity of similar AAS proteins.

2.7 Acknowledgements

This study was supported through Virginia Tech Biochemistry college of Agricultural and Life Sciences funding.

References

[1] Vavricka C., Han Q., Huan Y., et al. (2011) From Dopa to dihydroxyphenylacetaldehyde: a toxic biochemical pathway plays a vital physiological function in insects. PLoS One 6(1): e16124.

[2] Kawalleck P., Keller H., Hahlbrok K., et al. (1993) A pathogen-responsive gene of parsley encodes tyrosine decarboxylase. J Biol Chem,. 268(3): 2189-2194

[3] Han Q., Ding H., Robinson H., et al. (2010) Crystal Structure and Substrate Specificity of Drosophila 3,4-Dihydroxyphenylalanine Decarboxylase. PLOS ONE 5 (1): e8826.

[4] Bradford M.M (1976) A rapid and sensitive method for the quantitation of microgram quantities of protein utilizing the principle of protein-dye binding. Analytical Biochemistry 72 (1-2) 248-254

[5] Roeder T., Tyramine and octopamine: ruling behavior and metabolism. Annu Rev Entomol, 2005. 50: p. 447-77.

[6] Cole S.H., Carney G.E, McClung C.A., et al., Two functional but noncomplementing Drosophila tyrosine decarboxylase genes: distinct roles for neural tyramine and octopamine in female fertility. J Biol Chem, 2005. 280(15): p. 14948-55.

[7] Stadler R., Kutchan T.M., Loe,er S., et al. (1987) Revision of the early steps of reticuline biosynthesis Tetrahedron Letters 28: 1251.

[8] Hagel J.M. and P.J. Facchini (2005) Elevated tyrosine decarboxylase and tyramine hydroxycinnamoyltransferase levels increase wound-induced tyramine-derived hydroxycinnamic acid amide accumulation in transgenic tobacco leaves. Planta. 221(6): 904-14.

[9] Facchini P.J. and De Luca V. (1995) Phloem-Specific Expression of Tyrosine/Dopa Decarboxylase Genes and the Biosynthesis of Isoquinoline Alkaloids in Opium Poppy. PlantCell 7(11): 1811-1821.

[10] Yamazaki Y., Sudo H., Yamazaki M., et al. (2003) Camptothecin biosynthetic genes in hairy roots of Ophiorrhiza pumila: cloning, characterization and differential expression in tissues and by stress compounds. Plant Cell Physiol 44(4): 395-403.

[11] Tanaka E., Tanaka C., Mori N., et al. (2003) Phenylpropanoid amides of serotonin accumulate in witches' broom diseased bamboo. Phytochemistry 64(5): 965-9.

[12] Pasquali, G., Goddijn, O.J., de Waal, A., Verpoorte, R., Schilperoot, R.A., Hoge, J.H. and Memelink, J. (1992) Coordinated regulation of two indole alkaloid biosynthetic genes from cataranthus ruseus by auxin and elicitors. Plant molecular biology 18(6): 1121-1131

[13] Kaminaga, Y., Schnepp J., Peel G., et al. (2006) Plant phenylacetaldehyde synthase is a bifunctional homotetrameric enzyme that catalyzes phenylalanine decarboxylation and oxidation. J Biol Chem,. 281(33): 23357-23366.

[14] Gutensohn M., Lkempien A., Kaminaga Y., et al. (2011) Role of aromatic aldehyde synthase in wounding/herbivory response and flower scent production in different Arabidopsis ecotypes. Plant J. 66(4): 591-602.

[15] Tocher R.D., Tocher C.S. (1972) Dopa decarboxylase in Cytisus scoparius. Phytocheimstry. 11(5): 1661-1667.

[16] Leete E., Kirkwood S. and Marion L. (1952) The biogenesis of Alkaloids. VI. The formation of hordenine and N-methyltyramine from tyramine in barley. Can. Jour. Chem. 30: 749-760.

[17] Gibson R.A., Barret G. and Wightman F. (1972) Biosynthesis and metabolism of indol-3ylaceticacid: I II. Partial purification and properties of a tryptamine-forming L-tryptophan decarboxylase from tomato shoots. J. Exp. Bot. 23:775-786

[18] Lamensdorf I., Eisenhofer G., Harvey-White J., et al. (2000) Metabolic stress in PC12 cells induces the formation of the endogenous dopaminergic neurotoxin, 3,4-dihydroxyphenylacetaldehyde. J. Neurosci. Res. 60:552–558.

[19] Mattammal M.B., Haring J.H., Chung H.D., et al. (1995) An endogenous dopaminergic neurotoxin: implication for Parkinson's disease. Neurodegeneration 4: 271–281.

[20] Leon J., Rojo E., Sanchez-Serrano J.J. 2000. Wound signalling in plants. Journal of Experimental Botany. 52(354) :1-9

Chapter 3

Biochemical evaluation of the decarboxylation and decarboxylation-deamination activities of plant aromatic amino acid decarboxylases

Reprinted from the Journal of Biological Chemistry with permission

Torrens-Spence, M.P., Liu, P., Ding, H., Harich, K., Gillaspy, G., and Li, J. (2013) Biochemical evaluation of the decarboxylation and decarboxylation-deamination activities of plant aromatic amino acid decarboxylases. J Biol Chem 288: 2376-87

Author Contributions

Michael P. Torrens-Spence[1] wrote the article and performed all the research except for the experiments mentioned below.

Pingyang Liu[1] assisted in the model generation and analysis.

Haizhen Ding[1] assisted in the molecular cloning and protein expression.

Kim Harich[1] performed the LC MS and GC MS analyses.

Glenda Gillaspy[1] assisted in the mRNA extraction and cDNA production from the involved plant models.

Jianyong Li[1] oversaw and directed the research and helped write the article.

[1] Department of Biochemistry, Virginia Tech, Blacksburg, Virginia, United States of America

3.1 Abstract

Plant aromatic amino acid decarboxylase (AAAD) enzymes are capable of catalyzing either decarboxylation or decarboxylation-deamination on various combinations of aromatic amino acid substrates. These two different activities result in the production of arylalkylamines and the formation of aromatic acetaldehydes respectively. Variations in product formation enable individual enzymes to play different physiological functions. Despite these catalytic variations, arylalkylamine and aldehyde synthesizing AAADs are indistinguishable without protein expression and characterization. In this study, extensive biochemical characterization of plant AAADs was performed to identify residues responsible for differentiating decarboxylation AAADs from aldehyde synthase AAADs. Results demonstrated that a tyrosine residue located on a catalytic loop proximal to the active site of plant AAADs is primarily responsible for dictating typical decarboxylase activity whereas a phenylalanine at the same position is primarily liable for aldehyde synthase activity. Mutagenesis of the active site phenylalanine to tyrosine in *Arabidopsis thaliana* and *Petroselinum crispum* aromatic acetaldehyde synthases primarily converts the enzymes activity from decarboxylation-deamination to decarboxylation. The mutation of the active site tyrosine to phenylalanine in the *Catharanthus roseus* and *Papaver somniferum* aromatic amino acid decarboxylases changes the enzymes decarboxylation activity to a primarily decarboxylation-deamination activity. Generation of these mutant enzymes enables the production of unusual AAAD enzyme products including indole-3-acetaldehyde, 4-hydroxyphenylacetaldehyde, and phenylethylamine. Our data indicates that the tyrosine and phenylalanine in the catalytic loop region could serve as a signature residue to reliably distinguish plant arylalkylamine and aldehyde synthesizing AAADs. Additionally, the resulting data enables further insights into the mechanistic roles of active site residues.

3.2 Keywords

Aromatic acetaldehyde synthase; Phenylacetaldehyde synthase; Aromatic amino acid decarboxylase; Tryptophan decarboxylase; Indole-3-acetaldehyde; Phenylethylamine; Auxin.

3.3 Introduction

In many species, including humans, there is only one decarboxylase that selectively catalyzes the decarboxylation of aromatic amino acids. This enzyme is commonly named aromatic amino acid decarboxylase (AAAD). Within plants and insects, however, the similar enzyme has undergone extensive evolutionary divergence, resulting in multiple paralogs with divergent functions. The divergent functions of plant and insect AAADs are closely related to their corresponding substrate selectivity and catalytic reactions. For example, tyramine derived from tyrosine is the essential precursor for the biosynthesis of many plant secondary metabolites (including N-hydroxycinnamic acid amides and benzylisoquinoline alkaloids) [1-5]. Tryptamine and 5-hydroxytryptamine (5HT), produced by specific plant AAADs, are precursors for the synthesis of thousands of indole alkaloid compounds [1,6-7]. Because their substrate specificity provides functional relevant information, some AAADs have been further annotated on their principle substrate as tyrosine decarboxylases (TyDC) and tryptophan decarboxylases (TDC) [8-9].

Recent studies of AAAD proteins demonstrated that in addition to the typical decarboxylation activity established in TyDCs and TDCs, some annotated plant and insect AAAD proteins are actually aromatic acetaldehyde synthases (AASs) [10-12]. These AASs catalyze a rather complicated decarboxylation-oxidative deamination process of aromatic amino acids, leading to the production of aromatic acetaldehydes, CO_2, ammonia, and hydrogen peroxide rather than the AAAD derived arylalkylamines and CO_2 (Fig. 3.1).

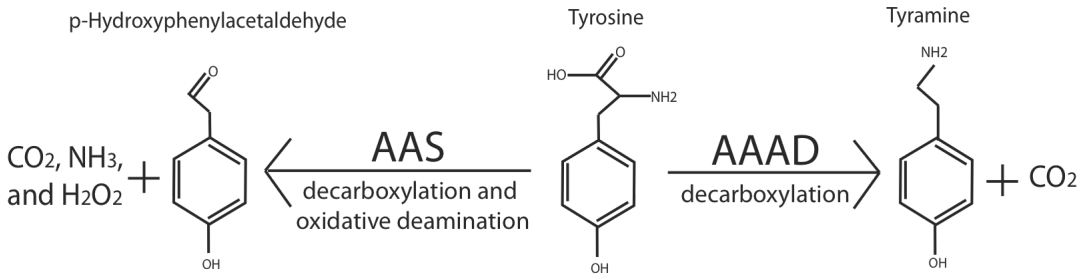

FIGURE 3.1. Relative activities of aromatic amino acid decarboxylase (AAAD) and aromatic acetaldehyde synthases (AAS).

Research has implicated plant AAS enzymes in the production of volatile flower scents, floral attractants, and defensive phenolic acetaldehyde secondary metabolites [10-12] and insect AAS in soft cuticle hardening [13]. While the physiological functions of true AAADs vary with their substrate selection, AAS proteins perform additional distinct physiological roles as compared with true AAADs. Consequently, it is essential to be able to distinguish AAS proteins from true AAAD enzymes. Despite variations in substrate specificity and catalytic reactions, plant AAS proteins share great sequence similarity to true AAADs. Such high homology is specifically emphasized through the comparison of a characterized *Arabidopsis thaliana* AAS and a *Capsicum annuum* TDC [11,14]. Although the *C. annuum* TDC only catalyzes decarboxylation of indolic substrates and the *A. thaliana* AAS only catalyzes aldehyde synthesis on phenolic substrates, these two enzymes retain 74% identity and 84% homology. This extensive homology has lead to a major problem in distinguishing AAS enzymes from typical AAAD proteins. For example, all currently verified plant AAS proteins were initially annotated as TyDCs. Additionally, our recent study showed that even experimentally investigated AAAD enzymes are capable of inaccurate characterization. In the aforementioned study we demonstrate that the previously characterized *Petroselinum crispum* TyDC (Q06086) [15] is actually an AAS that principally catalyzes the conversion of tyrosine to *p*-hydroxyphenylacetaldehyde [12].

To narrow the location of activity dictating AAAD and AAS residues we initiated this study by generating a chimeric enzyme, containing the N-terminal half of the *Thalictrum flavum* TyDC and the C-terminal half of the *P. crispum* AAS. The 70% identity between the *P. crispum* AAS and *T. flavum* TyDC (AAG60665) [12] suggests that their respective AAS and TyDC activities are likely dictated by very limited number of active site residues. Activity analysis of the chimeric enzyme determined that the *T. flavum* -*P. crispum* hybrid has typical AAS activity. The resulting aldehyde synthase activity indicates that residues located in the mutant's C-terminal half are predominantly responsible for activity differentiation. Next, analyses of published crystal structures were preformed to identify putative activity differentiating residues within plant AAAD and AAS enzymes. Several structures were analyzed, but due to the strong plant AAAD homology, the conservation of active site residues, and substantial electron density of an active site proximal catalytic loop (absent from other AAAD structures), the *Human* histidine decarboxylase *(hu*HDC) structure was chosen as the primary model [16]. Investigation of the *Human* HDC (PDB 4E1O) crystal structure identified residues located with in 6 angstroms of the pyridoxal-5'-phosphate inhibitor adduct. Comparison of these active site residues to their homologous residues in characterized plant AAAD and AAS sequences enabled the identification of active site residues potentially responsible for activity differentiation. Analysis of residues conserved in arylalkylamines synthesizing AAADs and absent in aromatic acetaldehyde synthesizing AASs enabled the exclusion of all but one putative activity dictating residue. The resulting analyses enabled the identification of a putative residue located in a catalytic loop proximal to the active site. The candidate residue is represented by a tyrosine 347 in the *T. flavum* enzyme and as a phenylalanine 346 in the *P. crispum* enzyme. Mutation of this candidate residue from phenylalanine to tyrosine within the *Arabidopsis thaliana* (NP_849999) and the *P. crispum* (Q06086) aldehyde synthases converts the enzymes activities from decarboxylation-oxidative deamination to decarboxylation. Mutation of the homologous tyrosine

residue in *Catharanthus roseus* TDC (P17770) and *Papaver Somniferum* TYDC 9 (AAC61842) converted the enzymes activities from decarboxylation to decarboxylation-oxidative deamination. Our data demonstrated that the active site tyrosine and phenylalanine in the flexible loop of plant AAADs plays a primary role for true AAAD activity and AAS activity, respectively. Our progress represents a major step forward towards achieving a comprehensive understanding of substrate specificity and catalytic reactions in plant AAAD proteins.

3.4 Materials and Methods

Reagents

Acetonitrile, 2-mercaptoethanol, formic acid, tryptophan, tryptamine, indole-3-acetaldehyde–sodium bisulfite complex, indole-3-ethanol, phenylalanine, phenylethylamine, phthaldialdehyde, pyridoxal 5-phsophate (PLP), sodium bisulfite, and sodium borohydride were purchased from Sigma (St. Louis, MO). The IMPACT-CN protein expression system was obtained from New England Biolabs (Ipswich, MA).

Plant material and growth conditions

P. crispum seeds, *T. flavum* seeds, *P. Somniferum* seeds, and *C. roseus* seeds were obtained from www.burpee.com, www.dianeseeds.com, www.onestoppoppyshoppe.com, and www.horizonherbs.com, respectively. *A. thaliana* seeds (wild type [CS60000], Columbia ecotype) were from [The *Arabidopsis* Biological Resource Center (Columbus, Ohio)]. Seeds from these plants were germinated in Sunshine Pro Premium potting soil and grown under a 16 h photoperiod at 23 ºC at 100 microeinsteins.

RNA isolation, cDNA amplification, and mutagenesis

Total RNA samples were isolated from 12 week old *A. thaliana*, *C. roseus*, *P. Somniferum, P. crispum and T. flavum* plants using an Ambion® mirVana™ miRNA Isolation Kit. These RNA samples were treated with DNase (Ambion TURBO DNA-free™ Kit). First strand cDNAs were synthesized by RT-PCR of total RNA samples using Invitrogen™ SuperScript™ III and a poly T17- primer. Specific primer pairs (Table 3.1), designed based on coding sequences (CDS) of *A. thaliana* AAS (NP 849999), *P. crispum* AAS (Q06086), *T. flavum* (AAG60665), *P. Somniferum* TyDC (AAC61842), and *C. Roseus* TDC (P17770) were synthesized and used for the amplification of the respective coding sequences. Amplified full-length CDS cDNA were subsequently ligated into IMPACT-CN expression vector for protein expression. Completed expression vectors were used as templates to produce the AAS to AAAD and AAAD to AAS mutants.

Table 3.1.

Primer sequences for the amplification and mutagenesis of AAAD and AAS proteins

The bold and italic font represents the restriction sites

Primer Name	Sequence
Arabidopsis thaliana AAS forward	ACTG***ACTAGT***ATGGAAAATGGAAGCGG
Arabidopsis thaliana AAS reverse	ACTG***CTCGAG***TTACTTGTGAAGCAAGTAAG
Arabidopsis thaliana AAS mutagenesis forward	AAA***GCTCTTCTTAT***CTCAAAAACAAGGCCTCTC
Arabidopsis thaliana AAS mutagenesis reverse	AAA***GCTCTTCTATA***CTCTGGATTTGTTGAAAGAGC
Catharanthus roseus TDC forward	ACT***GGAATGCT***ATGGGCAGCATTGATTCAAC
Catharanthus roseus TDC reverse	ACTG***CTCGAG***TCAAGCTTCTTTGAGCAAATC
Catharanthus roseus TDC mutagenesis forward	AAA***GCTCTTCTTTT***TTAAAAAATAAACAGAGTGATTTAGAC
Catharanthus roseus TDC mutagenesis reverse	AAA***GCTCTTCTAAA***CTCAGGATTCGTAGTGAGTG
Papaver Somniferum TyDC forward	ACTG***GGAATGCT****ATGGGAAGCCTTCCGAC*
Papaver Somniferum TyDC reverse	*ACTG****CTCGAG****CTAGGCACCAAGTATGGCAT*
Papaver Somniferum TyDC mutagenesis *forward*	*AAA****GCTCTTCTTTT****TTGAAGAACAAAGCAACGG*
Papaver Somniferum TyDC mutagenesis *reverse*	*AAA****GCTCTTCTAAA****TTCTGCACTTGTTGATAATGC*
Petroselinum crispum AAS forward	ACTG***ACTAGT***ATGGGCTCCATCGATAATC
Petroselinum crispum AAS reverse	ACTG***CTCGAG***TTTATGATAATACTTCCACGAGC
Petroselinum crispum AAS mutagenesis forward	AAA***GCTCTTCTTAC***TTGAAGAATAATGCTAGTGAAACAAAC
Petroselinum crispum AAS mutagenesis reverse	AAA***GCTCTTCGTA***CTCAGGATATGTGGAAAGAGAC
Hybrid *Petroselinum crispum* C-Term forward	AAA*G****CTCTTCTCGA***CAGTATCTTGACGGTGTGG
Thalictrum flavum TyDC forward	ACTG***ACTAGT***ATGGGTAGCCTCCATGTT
Thalictrum flavum TyDC reverse	ACTG***CTCGAG***TTAAAATGTAGCAAGTACAGCATC
Hybrid *Thalictrum flavum* N-Term reverse	AAA***GCTCTTCTTCG***AAACTCTGGACATATACATG

To generate *T. flavum*-*P. crispum* chimeric enzyme, a specific reverse primer based on codons for *T. flavum* TyDC (AAG60665) residues 294-300 and a forward primer based on *P. crispum* AAS (Q06086) residues 300-306 (with both primers containing a SapI restriction site) were synthesized (Table 3.1). The new *T. flavum* reverse primer was paired with the original *T. flavum* forward primer and the new *P. crispum* forward primer was pared with original *P. crispum* AAS reverse primer to amplify (using the respective full-length *T. flavum* TyDC and full-length *P. crispum* AAS CDS sequences as template) a DNA fragment encoding for the first 300 amino acid of *T. flavum* TyDC and a DNA fragment encoding for the *P. crispum* residues 300-514, respectively. The two cDNA fragments were digested with SapI to generate cohesive 3-end for the *T. flavum* cDNA fragment and cohesive 5-end for the *P. crispum* cDNA fragment. The two digested fragments were ligated together with the aid of T4 DNA ligase to produced a chimeric CDS coding for the 300 N-terminal side residues of the *T. flavum* TyDC and 214 C-terminal site of the *P. crispum* AAS [17].

Full-length CDS cDNA containing the F338Y mutation in *A. thaliana* AAS, the F346Y mutation in *P. crispum* AAS, the Y348F mutation in *C. roseus* TDC, and the Y350F mutation in *P. somniferum* TyDC were generated using a SapI mutagenesis procedure similar to that described for the production of the chimeric *T. flavum* - *P. crispum* enzyme. The variable region of the SapI restriction site was used to generate codon mutagenesis (Table 3.1).

Protein expression and purification

All cDNA products encoding for wild type TyDCs, AASs, TDCs and their mutants were individually ligated into IMPACT-CN bacterial expression plasmids. DNA sequencing was utilized to verify the sequence and frame of each cDNA insert. Recombinant IMPACT-CN

plasmids were utilized to transform *E. coli* DE3. Transformed bacterial colonies, expressing the target proteins, were selected and used for large-scale expression (16-20 liters of *E. coli* cells) of individual recombinant proteins. The detailed conditions for recombinant protein expression and purification were essentially the same as previously described [18].

Activity assays

Typical reaction mixtures of 100 or 200 μl, containing 20-30 μg of recombinant TyDC, TDC, AAS, hybrid enzyme or mutant protein and 5 mM of substrate (tyrosine, dopa, tryptophan or phenylalanine) were prepared in 50 mM potassium phosphate buffer (pH, 7.5) and incubated at 25 ^{o}C in a water bath. The reactions were stopped (at a time point between 5 and 60 min) through the addition of an equal volume of 0.8 M formic acid. Supernatants of the reaction mixtures, obtained by centrifugation, were analyzed with (Aqueous) Pierce Quantitative Peroxide Assay Kit to determine AAS activity. The supernatants were also analyzed by High-performance liquid chromatography (HPLC) with electrochemical detection (HPLC-EC) or HPLC with ultraviolet detection (HPLC-UV). Details of HPLC-EC or HPLC-UV conditions were described in figure captions. Product production was verified though the comparison of various aromatic amine standards under identical chromatography conditions.

AAAD mutant product verification by Liquid chromatography/Tandem mass spectrometry (HPLC/MS/MS)

To further verify the identity of the mutant enzymatic products, reaction mixtures containing physiological substrates and mutant enzymes were analyzed by LC/MS/MS. Reaction mixtures of 100 μl, containing 30 μg of *C. roseus* TDC Y348F and 10 mM of tryptophan, or 30 μg of *A. thaliana* AAS F338Y and 10 mM of phenylalanine were prepared in 50 mM of phosphate buffer (pH, 7.5) and incubated at 25 ^{o}C in a water bath for 30 minutes. Reactions were stopped by

mixing an equal volume of 0.8 M of formic acid. Prior to injection, indole-3-acetaldehyde, generated in the *C. roseus* TDC Y348F mutant and 10 mM tryptophan reaction mixture, was derivatized to indole-3-acetaldehyde–sodium bisulfite addition compound using sodium bisulfite. Samples were analyzed by a LC-3200 Q Trap MS/MS system (AB Sciex) in either positive and negative ion mode, as appropriate. Identification of phenylethylamine from the *A. thaliana* AAS F338Y mutant reaction mixture and indole-3-acetaldehyde–sodium bisulfite addition compound from the derivatized *C. Roseus* TDC Y348F mutant reaction mixture was based on their retention time and MS/MS spectra in comparison with those produced from authentic phenylethylamine and indole-3-acetaldehyde–sodium bisulfite addition compound standards at identical analytic conditions.

Kinetic analysis

After the substrate specificity and catalytic reaction of enzymes were verified, their kinetic parameters were evaluated. The *A. thaliana* AAS (NP_849999) wild type and F338Y mutant enzymes were evaluated using phenylalanine as a substrate. The *C. Roseus* TDC (P17770) wild type and Y348Y mutant enzymes were evaluated using tryptophan as a substrate. Kinetic data points were performed in triplicate and kinetic values were evaluated by hyperbolic regression. Reaction mixtures of 100 μl containing 5 μg of enzyme recombinant protein and varying concentrations of substrate (0.1 – 40 mM of phenylalanine, 0.005 – 16 mM of tryptophan) were prepared in 50 mM phosphate buffer (pH 7.5) and incubated at 25 ^{o}C. To detect phenylethylamine generated by *A. thaliana* F338Y, two volumes of 100% ethanol were added to the reaction mixtures (to stop the reaction) at 5 min after incubation and supernatants, obtained by centrifugation (14,000g for 5 min at 4 ^{o}C), were derivatized using OPT reagent and then analyzed by HPLC-EC and quantitated based on standard curve generated using authentic OPT derivatized phenylethylamine [19]. Tryptamine generated by wild type *C. Roseus* TDC was

measured by stopping the reaction mixture using an equal volume of 0.8 M formic acid, obtaining the supernatant via centrifugation, and analyzing by HPLC-EC against a standard curve of tryptamine. To determine the AAS activity for the *C. Roseus* TDC mutant and the wild type *A. thaliana* enzyme, an equal volume of 0.8 M formic acid was added to the reaction mixtures and supernatants (obtained by centrifugation) were analyzed with (Aqueous) Pierce Quantitative Peroxide Assay Kit to measure peroxide production. The amounts of H_2O_2 product in each reaction mixture was quantitated based on a standard curve generated using authentic peroxide.

3.5 Results

AAAD/AAS chimeric mutant analysis

To narrow the location of the AAAD vs AAS activity differentiating residue/residues, a chimeric (hybrid) protein composed of *T. flavum* TyDC (AAG60665) residues 1-300 and *P. crispum AAS (*Q06086*)* residues 300-514 was generated and its catalytic reaction was assessed with tyrosine as a substrate. Incubation of the *T. flavum -P. crispum* chimeric enzyme in the presence of tyrosine resulted in the detection of a major broad peak overlapping with a minor sharp peak during HPLC-EC analysis (Fig. 3.2A).

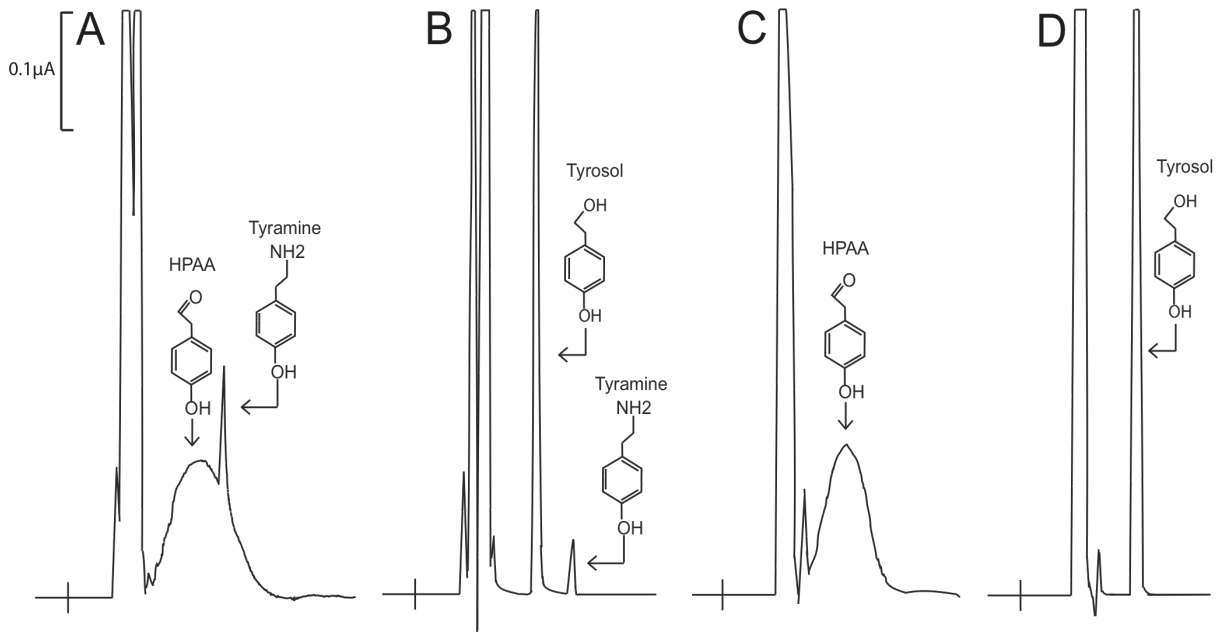

FIGURE 3.2. HPLC-EC analysis of *T. flavum* - *P. crispum* chimeric enzyme and *P. crispum* AAS activity with tyrosine as a substrate. Reaction mixtures of 100 µl containing either 30 µg of *T. flavum* - *P. crispum* chimeric enzyme or 20 µg of wild type AAS and 5 mM of tyrosine were incubated at 25 ^{o}C and their reaction was stop at 40 min after incubation by adding an equal volume of 0.8 M of formic acid into the reaction mixture. The mixtures were centrifuged for 5 min at 14,000g and supernatants were injected for HPLC-EC analysis. To reduce HPAA to HPEA, some reaction mixtures were treated with an equal volume of 100% ethanol saturated with borohydride after 40 min incubation. The borohydride treated mixtures were incubated for

10 min on ice, treated with 0.8 M of formic acid and centrifuged to obtain supernatants. Supernatants were injected for HPLC-EC analysis. Chromatograms (A & B) illustrate the accumulation of HPAA and tyramine in a *T. flavum* - *P. crispum* chimeric enzyme and tyrosine reaction mixture at 40 min after incubation and the reduction of 4-HPAA to 4-HPEA (tyrosol) in a borohydride treated reaction mixture. Chromatograms C and D show the production of 4-HPAA in a wild type *P. crispum* AAS and tyrosine reaction mixture at 40 min after incubation and the reduction of HPAA to HPEA (tyrosol) in a borohydride treated reaction mixture.

The broad peak was considered to be *p*-hydroxyphenylacetaldehyde (HPAA) because it displayed the same chromatographic behavior as the HPAA formed in the wild type *P. crispum* AAS and tyrosine reaction mixture (Fig. 3.2C). When both the hybrid enzyme and the wild type *P. crispum* enzyme reaction mixtures were treated with borohydride prior to HPLC-EC analysis, the broad product peaks (Fig. 3.2A and Fig. 3.2C respectively) were converted to sharp product peaks (Fig. 3.2B and Fig. 3.2D respectively) that coeluted with authentic 4-hydroxyphenylethanol (tyrosol) at different chromatographic conditions. Unlike the wild type AAS and tyrosine reaction mixture, a small amount of tyramine was formed in the mutant enzyme and tyrosine reaction mixture (Fig. 3.2A & 3.2B). Despite this minor activity, the hybrid enzyme behaved primarily as a wild type *P. crispum* AAS. These results suggested that residues in the C-terminal half of plant AAADs are likely responsible for constraining decarboxylation and aldehyde synthase reactions.

C-terminal active site structural analysis and sequence comparison

To impact the catalytic reaction, the activity dictating C-terminal residues should be in close proximity to the active site internal aldimine bond (that subsequent interacts with incoming substrate, leading to the formation of the external aldimine intermediate during catalysis). To elucidate active site proximal residues, the recently released mammalian histidine decarboxylase

(*hu*HDC) (NP_002103) [16] was investigated in Pymol [20] to identify C-terminal residues located within 6 angstroms of the external aldimine inhibitor complex. The catalytic domain of HDC is homologous to that of plant AAADs. Additionally, most of the substrate interacting residues in AAADs are conserved in HDCs. Moreover, the active site loop of a ligand bound HDC complex displayed substantial electron density (absent from other AAAD structures). Results identified 13 active site proximal residues from the C-terminal portion of the *hu*HDC structure. A multiple sequence alignment of the *hu*HDC sequence, 4 characterized plant AAAD sequences, and 3 characterized plant AAS sequences was performed to identify homologous active site proximal residues from plant AAAD and AAS sequences (Fig. 3.3).

```
A. Thaliana AAS     ------------------------------------------MENGSGKV-------LKPMDSEQLREYGHLMVDFIADYYKTIED----FPVLSQVQPGY
Rosa hybrid AAS     ----------------------------------MGSFPFHRDLQEIASSQL-----TKALDPEEFRKQGHMVINFIADYYQNIEK----YPVLSRVEPGY
P. Crispum AAS      ----------------------------------MGSIDNL-TEKLASQFP------MNTLEPEEFRRQGHMMIDFLADYYRKVEN----YPVRSQVSPGY
P. Somniferum AAAD  ----------------------------------MGSLPTN-NLESISLCS------QNPLDPDEFRRQGHMIIDFLADYYKNVEN----YPVRSQVEPGY
T. Flavum AAAD      ----------------------------------MGSLHVE-DLDNISKCTV-----ENPLDPEEFRRQGHMMIDFLADYYRDIEK----YPVRSQVEPGY
A. Thaliana AAAD    MFKPQHMYDREFGTGNGYSNGNGYTNGNGHTNGNGNYNGNGHVNGNGKANGAKVVKMKPMDSELLREQGHIMVDFIADYYKNLQDSPQDFPVLSQVQPGY
O. Sativa AAAD      ----------------------------------MGSLDTNPTAFSAFPAGEGE--TFQPLNADDVRSYLHKAVDFISDYYKSVES----MPVLPNVKPGY
C. Roseus AAAD      ----------------------------------MGSIDSTNVAMSNSPVG-----EFKPLEAEEFRKQAHRMVDFIADYYKNVET----YPVLSEVEPGY
Human HDC 4E1O      ----------------------------------GPLG---------------------SMEPEEYRERGRGREMVDYICQYLSTVRE----RRVTPDVQPGY

A. Thaliana AAS     LHKLLPDSAPDHPETLDQVLDDVRAKILPGVTHWQSPSFFAYYPSNSSVAGFLGEMLSAGLGIVGFSWVTSPAATELEMIVLDWVAKLLNLPEQFMSKGN
Rosa hybrid AAS     LKKCLPVSAPYDPEPISTILRDVQNHIVPGLTHWQSPNFFAYFSSTASTAGFLGEILTTGFNVVGFNWVSSPAATELENIVMDWLGDMLQLPKSFHFSGN
P. Crispum AAS      LREILPESAPYNPESLETILQDVQTKIIPGITHWQSPNFFAYFPSSGSTAGFLGEMLSTGFNVVGFNWMVSPAATELENVVTDWFGKMLQLPKSFLFSGG
P. Somniferum AAAD  LKKRLPESAPYNPESIETILEDVTNDIIPGLTHWQSPNYFAYFPSSGSIAGFLGEMLSTGFNVVGFNWMSSPAATELESIVMNWLGQMLTLPKSFLFSSD
T. Flavum AAAD      LRKEIPDSAPYNPESIETILEDVHKQIIPGITHWQSPNYFAYFPSSGSVAGFLGEMLSTGFNVVGFNWMSSPAATELESIVMDWLGKMLKLPKSFLFSGN
A. Thaliana AAAD    LRDMLPDSAPERPESLKELLDDVSKKIMPGITHWQSPSYFAYYASSTSVAGFLGEMLNAGLSVVGFTWLTSPAATELEIIVLDWLAKLLQLPDHFLSTGN
O. Sativa AAAD      LQDELRASPPTYSAPFDVTMKELRSSVVPGMTHWASPNFFAFFPSTNSAAAIAGDLIASAMNTVGFTWQASPAATEMEVLALDWLAQMLNLPTSFMNRTG
C. Roseus AAAD      LRKRIPETAPYLPEPLDDIMKDIQKDIIPGMTNWMSPNFYAFFPATVSSAAFLGEMLSTALNSVGFTWVSSPAATELEMIVMDWLAQILKLPKSFMFS—
Human HDC 4E1O      LRAQLPESAPEDPDSWDSIFGDIERIIMPGVVHWQSPHMHAYYPALTSWPSLLGDMLADAINCLGFTWASSPACTELEMNVMDWLAKMLGLPEHFLHHHP

A. Thaliana AAS     -----GGGVIQGSASEAVLVVLIAAR-DKVLRSVGKNALE-------KLVVYSSDQTHSALQKACQIAGIHPENCRVLTTDSSTNYALRPESLQEAVSRD
Rosa hybrid AAS     -----GGGVLHGSTCEAIVCTMVAAR-DQMLRRIGSENLG-------KLVVYGSDQTHSTLQKATQIVGINTENFRAIKTTKSTGFALSPEMLRLTISSD
P. Crispum AAS      -----GGGVLQGTTCEAILCTLVAAR-DKNLRQHGMDNIG-------KLVVYCSDQTHSALQKAAKIAGIDPKNFRAIETTKSSNFQLCPKRLESAILHD
P. Somniferum AAAD  GS-SGGGGVLQGTTCEAILCTLTAAR-DKMLNKIGRENIN-------KLVVYASNQTHCALQKAAQIAGINPKNVRAIKTSKATNFGLSPNSLQSAILAD
T. Flavum AAAD      -----GGGVLQGTTCEAILCTLTAAR-DRMLNKIGRENIC-------KLVVYGSDQTHCALQKAAQIAGIHPNNFRAVPTTKANDYGLSASALRSTILED
A. Thaliana AAAD    -----GGGVIQGTGCEAVLVVVLAAR-DRILKKVGKTLLP-------QLVVYGSDQTHSSFRKACLIGGIHEENIRLLKTDSSTNYGMPPESLEEAISHD
O. Sativa AAAD      EGRGTGGGVILGTTSEAMLVTLVAAR-DAALRRSGSDGVAGLH----RLAVYAADQTHSTFFKACRLAGFDPANIRSIPTGAETDYGLDPARLLEAMQAD
C. Roseus AAAD      ---GTGGGVIQNTTSESILCTIIAAR-ERALEKLGPDSIG-------KLVCYGSDQTHTMFPKTCKLAGIYPNNIRLIPTTVETDFGISPQVLRKMVEDD
4E1O_Human_HDC      SS--QGGGVLQSTVSESTLIALLAARKNKILEMKTSEPDADESSLNARLVAYASDQAHSSVEKAGLIS---LVKMKFLPVD--DNFSLRGEALQKAIEED

A. Thaliana AAS     LEAGLIPFFLCANVGTTSSTAVDPLAALGKIANSNGIWFHVDAAYAGSACICPEYRQYIDGVETADSFNMNAHKWFLTNFDCSLLWVKDQDSLTLALSTN
Rosa hybrid AAS     LEKGLVPLFLCATIGTTATTAIDPLEALCHVAKEYGVWVHVDAAYAGSACICPEFRHFINGVEGANSFSFNPHKWLFTGMDCCCLWVKNPSVLASSLSTN
P. Crispum AAS      LQNGLIPLYLCATVGTTSSTTVDPLPALTEVAKKYDLWVHVDAAYAGSACICPEFRQYLDGVENADSFSLNAHKWFLTTLDCCCLWVRNPSALIKSLSTY
P. Somniferum AAAD  IESGLVPLFLCATVGTTSSTAVDPIGPLCAVAKLYGIWVHIDAAYAGSACICPEFRHFIDGVEDADSFSLNAHKWFFTTLDCCCLWVKDSDSLVKALSTS
T. Flavum AAAD      IEAGLVPLFLCATVGTTSSTAVDPIGPLCKVASDYSIWVHVDAAYAGSACICPEFRHFIDGVENADSFSLNAHKWFFTTLDCCCLWVKEPSALIKALSTN
A. Thaliana AAAD    LAKGFIPFFICATVGTTSSAAVDPLVPLGNIAKKYGIWLHVDAAYAGNACICPEYRKFIDGIENADSFNMNAHKWLFANQTCSPLWVKDRYSLIDALKTN
O. Sativa AAAD      ADAGLVPTYVCATVGTTSSNAVDPVGAVADVAARFAAWVHVDAAYAGSACICPEFRHHLDGVERVDSISMSPHKWLMTCLDCTCLYVRDTHRLTGSLETN
C. Roseus AAAD      VAAGYVPLFLCATLGTTSTTATDPVDSLSEIANEFGIWIHVDAAYAGSACICPEFRHYLDGIERVDSLSLSPHKWLLAYLDCTCLWVKQPHLLLRALTTN
4E1O_Human_HDC      KQRGLVPVFVCATLGTTGVCAFDCLSELGPICAREGLWLHIDAAYAGTAFLCPEFRGFLKGIEYADSFTFNPSKWMMVHFDCTGFWVKDKYKLQQTFSVN

A. Thaliana AAS     PEFLKN--KASQANLVVDYKDWQIPLGRRFRSLKLWMVLRLYGSETLKSYIRNHIKLAKEFEQLVSQDPNFEIVTPRIFALVCFRLVP------VKD---
Rosa hybrid AAS     PEFLRN--KASDSKQVVDYKDWQIALSRRFRALKLWLVLRSYGVANLRNFIRIHVKMAKTFEGLVRMDKRFEILVPRNFSLVCFRISP---SALISSNED
P. Crispum AAS      PEFLKN--NASETNKVVDYKDWQIMLSRRFRALKLWFVLRSYGVGQLREFIRGHVGMAKYFEGLVNMDKRFEVVAPRLFSMVCFRIKP---SAMIGKN--
P. Somniferum AAAD  AEYLKN--KATESKQVIDYKDWQIALSRRFRSMKLWLVLRSYGVANLRTFLRSHVKMAKHFQGLMGMDNRFEIVVPRTFAMVCFRLKP---AAIFKQKIV
T. Flavum AAAD      PEYLRN--KATESHQVVDYKDWQIALSRRFRAMKLWLVLRSYGVANLRNFLRSHVKMAKNFEGFIALDKRFEIVVPRTFAMVCFRLLPPRSPLIIKTNGY
A. Thaliana AAAD    PEYLEFKVKVSKKDTVVNYKDWQISLSRRFRSLKLWMVLRLYGSENLRNFIRDHVNLAKHFEDYVAQDPSFEVVTTRYFSLVCFRLAP------VDG---
O. Sativa AAAD      PEYLKN--HASDSGEVTDLKDMQVGVGRRFRGLKLWMVMRTYGVAKLQEHIRSDVAMAKVFEDLVRGDDRFEVVVPRNFALVCFRIRAGAGAAAAT----
C. Roseus AAAD      PEYLKN--KQSDLDKVVDFKNWQIATGRKFRSLKLWLILRSYGVVNLQSHIRSDVAMGKMFEEWVRSDSRFEIVVPRNFSLVCFRLKP-----DVS----
4E1O_Human_HDC      PIYLRH----ANSGVATDFMHWQIPLSRRFRSVKLWFVIRSFGVKNLQAHVRHGTEMAKYFESLVRNDPSFEIPAKRHLGLVVFRLKG------------

A. Thaliana AAS     ---------EEKKCNNRNRELLDAVNSSGKLFMSHTALSGKIVLRCAIGAPLTEEKHVKEAWKIIQEEASYLLHK------------
Rosa hybrid AAS     D---------EIGMVNEVNCKLLEAINASGKAYMTHAVVGGLYVLRCAVGATLTEEKHIVEAWNVVQDHAQAILSTY-----------
P. Crispum AAS      ---------DEDEVNEINRKLLESVNDSGRIYVSHTVLGGIYVIRFAIGGTLTDINHVSAAWKVLQDHAGALLDDTFTSNKLVEVLS
P. Somniferum AAAD  DND---YIEDQT--NEVNAKLLESVNASGKIYMTHAVVGGVYMIRFAVGATLTEERHVTGAWKVVQEHTDAILGA------------
T. Flavum AAAD      QNGNGVYHKDESRANELNRRLLESINASGSAYMTHSMVGGVYMIRFAVGASLTEERHVILAWKVVQEHADAVLATF-----------
A. Thaliana AAAD    ---------DEDQCNERNRELLAAVNSTGKIFISHTALSGKFVLRFAVGAPLTEEKHVTEAWQIIQKHASKFTRNDHY---------
```

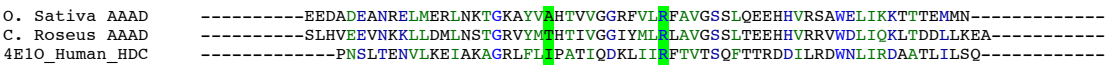

Figure 3.3.

Sequence alignment of a *P. crispum* AAS (Q06086), *Rosa hybrid cultivar* AAS (ABB04522), *A. thaliana* AAS (NP_849999), *C. roseus* TDC (P17770), *O. sativa* TDC (AK069031), *P. Somniferum* TYDC 9 (AAC61842), *T. flavum* TyDC (AAG60665), *A. thaliana* TYDC (NP_001078461), and *Human* HDC (4E1O). The decarboxylation dictating tyrosine and the aldehyde synthase dictating phenylalanine are highlighted in yellow. The C-terminal residues with in 6 angstroms of the pyridoxal-5'-phosphate inhibitor adduct from the *Human* HDC (4E1O) crystal structure and their homologous residues with in plant AAAD and AAS sequences are highlighted in green. The *Thalictrum*-parsley hybrid protein is composed of the underlined sequence.

The majority of these putative activity-dictating residues were subsequently dismissed as activity dictating residues due to inter activity conservation or lack of intra activity conservation. Ultimately, it became apparent that *T. flavum* TyDC Tyr347 was stringently conserved in all identified TyDC and TDC (as well as many other predicted AAADs), while the similar position was occupied by phenylalanine in identified AAS proteins (one verified Rosa AAS contained a valine at the corresponding position) [10]. The correlation between these hypothetical activity differentiating residues and their corresponding catalytic functions can be illustrated by viewing

the multiple alignments of five characterized AAADs and 3 characterized AASs (Fig. 3.4).

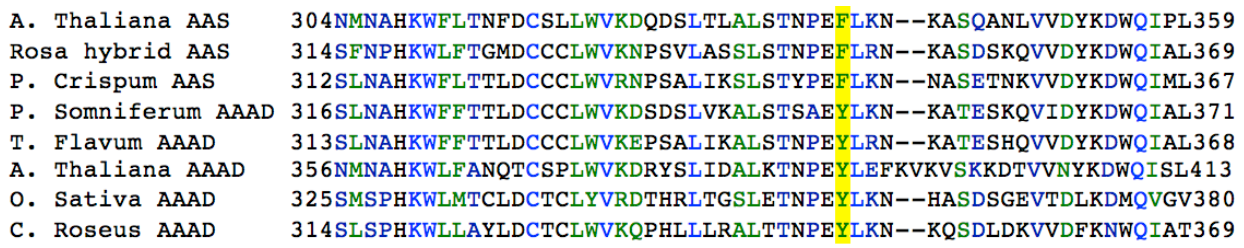

FIGURE 3.4. Sequence alignment of *A. thaliana* AAS (NP_849999), *Rosa hybrid cultivar* AAS (ABB04522), *P. crispum* AAS (Q06086), , *P. Somniferum* TYDC 9 (AAC61842), *T. flavum* TyDC (AAG60665), *A. thaliana* TYDC (NP_001078461), *C. roseus* TDC (P17770), and *O. sativa* TDC (AK069031). The aforementioned plant sequences maintain an average 56% identity. The decarboxylation dictating tyrosine and the aldehyde synthase dictating phenylalanine are highlighted in yellow.

These analyses suggested that this tyrosine and/or phenylalanine might have an impact on AAAD and AAS catalytic reactions.

Conversion of A. thaliana and P. crispum AASs into AAADs through mutation

To compare with *P. crispum* AAS, we previously expressed *A. thaliana* AAS (NP_849999) and verified its activity [12] (the activity of the *A. thaliana* AAS enzyme has previously been investigated) [11]. The *A. thaliana* AAS has a Phe338 occupying the same position as the conserved tyrosine in the TyDC and TDC enzymes flexible loop region. To test the role this positional residue plays in catalysis, the *A. thaliana* AAS Phe338 was mutated to Tyr338 and its mutant protein was expressed, purified, and compared with the wild type AAS in catalytic reaction with phenylalanine as a substrate. After the F338Y mutant was incubated for different time periods with phenylalanine and then assessed for the production of H_2O_2 in the reaction

mixtures, no apparent H_2O_2 accumulation was observed in the reaction mixtures (Fig. 3.5, mutant curve).

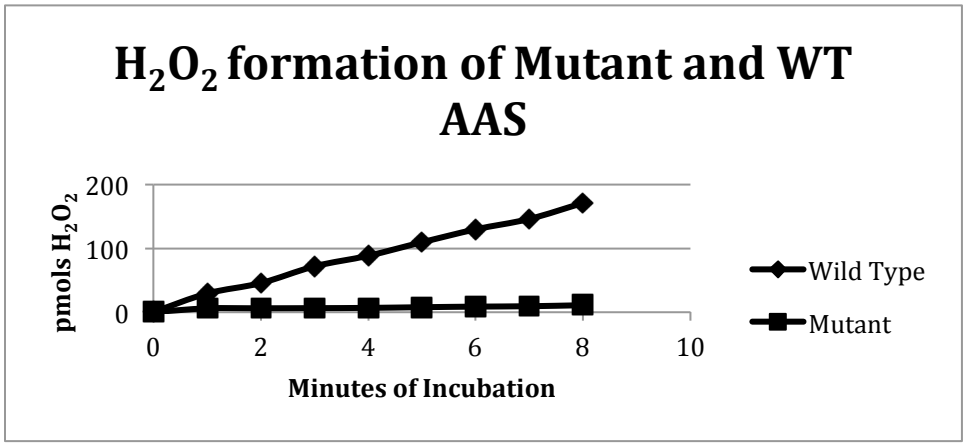

FIGURE 3.5. Analysis of hydrogen peroxide production in reaction mixtures containing phenylalanine and wild type *A. thaliana* AAS or its F338Y mutant. Reaction mixtures of 0.2 ml containing 5 mM phenylalanine and 20 μg of the wild type *A. thaliana* AAS or 20 μg of its F338Y mutant were prepared in 50 mM phosphate buffer, pH 7.5. The reaction mixtures were incubated at 25^{o}C. At each 1 min interval, 20 μl reaction mixture was withdrawn and mixed into 150 μl Pierce peroxide assay reagents solution. The "Wild Type" curve and "mutant" curve illustrate the amount of H_2O_2 accumulated in 20 μl of reaction mixture at 1 – 8 min incubation periods.

In contrast, production of H_2O_2 was observed in the wide-type *A. thaliana* AAS and phenylalanine reaction mixtures and the relative amounts of H_2O_2 were approximately proportional to the incubation periods (Fig. 3.5, wild-type curve). Inability to produce H_2O_2 in the *A. thaliana* AAS F338Y mutant phenylalanine reaction mixtures suggests that this particularly phenylalanine residue is important for the AAS activity of the *A. thaliana* enzyme.

Based on high conservation of the active loop tyrosine in TyDC and TDC at the corresponding position, the generated *A. thaliana* F338Y mutation might result in mutant decarboxylase

activity. When the phenylalanine and *A. thaliana* AAS F338Y mutant reaction mixtures were analyzed by HPLC with UV detection at 265 nm at the described HPLC-EC separation conditions, a product with a retention time of 4.41 min was observed. The relative amounts of the product formed were approximately proportional to the incubation periods of the reaction mixtures (Fig. 3.6A-3.6C).

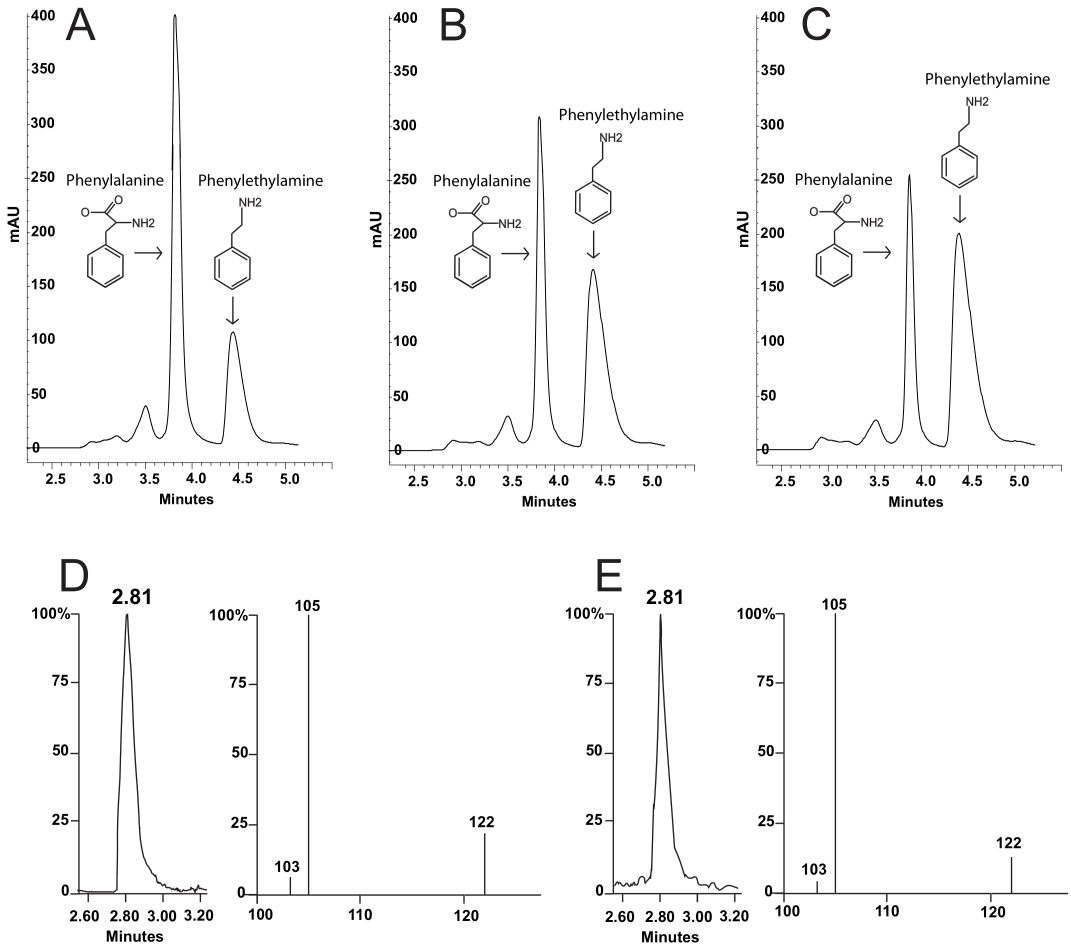

FIGURE 3.6. Detection of phenylethylamine produced in *A. thaliana* AAS F338Y mutant and phenylalanine reaction mixtures by HPLC-UV and LC/MS/MS. Reaction mixtures of 0.1 ml containing 0.1 mg of *Arabidopsis* AAS F338Y mutant and 20 mM of phenylalanine were prepared in 100 mM of phosphate buffer (pH, 7.5). The reaction was stopped after incubation by addition of 0.8 M of formic acid. Supernatants from centrifuged mixtures were then injected for HPLC-UV analysis. Chromatograms (A-C) illustrate the relative amount of phenylethylamine

(4.41-min peak) formed in the reaction mixtures at 5, 10 and 15 min after incubation, respectively. Chromatogram and MS/MS spectrum (D) illustrate the MH+ ion (122) and daughter ions of the product formed in *A. thaliana* AAS F338Y mutant and phenylalanine reaction mixture in comparison with those (E) produced by phenylethylamine standard under identical conditions of LC/MS/MS analysis.

The product has an identical retention time to the authentic phenylethylamine at the same HPLC separation conditions. HPLC/MS/MS analysis in positive ion mode of an *A. thaliana* AAS F338Y mutant and phenylalanine reaction mixture revealed that the products of the MH^+ ion m/z 122.1 and the relative intensities of its tandem spectrum (MS/MS spectrum) were identical to those generated using authentic phenylethylamine at identical conditions (Fig. 3.6D-3.6E). In addition, the product reacted with OPA-thio reagent producing an electrochemically active compound as other primary amines, further verifying the presence of free primary amine of the product. To further verify the decarboxylation activity-dictating role of this active site tyrosine, we performed an additional phenylalanine to tyrosine mutation on the 346-phenylalanine residue of *P. crispum* AAS (Q06086). HPLC-EC comparison of the wild type enzyme versus the F346Y mutant confirmed an alteration in the primary activity from decarboxylation-deamination to decarboxylation (Fig. 3.7).

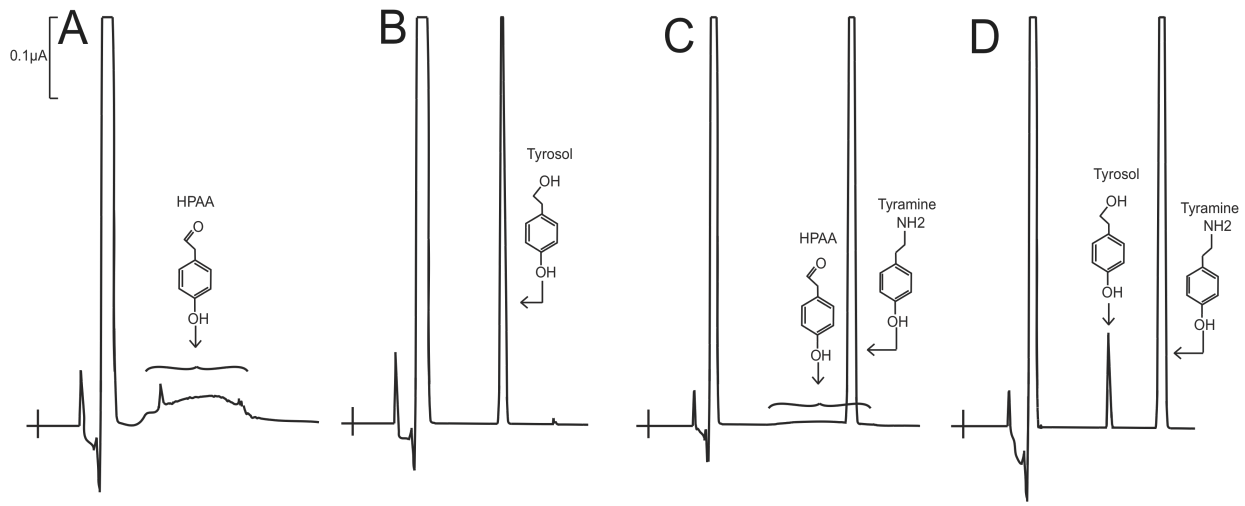

Figure 3.7. HPLC-EC analysis of *P. crispum* wild type and F350Y enzymes with tyrosine as a substrate. Y-axis represents the output in microamps, the x-axis represents retention time. Reaction mixtures of 100 μl containing either 15 μg of *P. crispum* wild type or mutant enzyme were incubated at 25 ^{o}C and their reaction was stop at 40 min after incubation by adding an equal volume of 0.8 M of formic acid into the reaction mixture. The mixtures were centrifuged for 5 min at 14,000g and supernatants were injected for HPLC-EC analysis. To reduce HPAA to HPEA, some reaction mixtures were treated with an equal volume of 100% ethanol saturated with borohydride after 40 min incubation. The borohydride treated mixtures were incubated for 10 min on ice, treated with 0.8 M of formic acid to decompose remaining borohydride and centrifuged to obtain supernatants. Supernatants were injected for HPLC-EC analysis. Chromatograms (A & B) illustrate the accumulation of HPAA (the major broad peak) in the *P. crispum* wild type enzyme and tyrosine reaction mixture at 40 min after incubation and the reduction of 4-HPAA to 4-HPEA (tyrosol) in a borohydride treated reaction mixture. Chromatograms C and D show the production of tyramine in the F350Y *P. crispum* mutant and tyrosine reaction mixture at 40 min after incubation and the reduction of HPAA to HPEA (tyrosol) in a borohydride treated reaction mixture.

In addition to the primary decarboxylation activity, the *P. crispum* F346Y mutant retained a small percentage of decarboxylation-deamination activity. The change from AAS activity to true AAAD activity in the *A. thaliana* AAS F338Y and the P. *crispum* F350Y mutants, in conjunction with the strict conservation of Tyr338 equivalent with in identified TyDCs and TDCs (Fig. 3.4), indicates that this loop region tyrosine residue plays a primarily role in the typical decarboxylation reaction in plant AAADs.

Mutagenic conversion of C. roseus TDC and P. somniferum TyDC into an indole-3-acetaldehyde synthase and a 4-hydroxyphenylacetaldehyde synthase respectively

We have previously expressed a *C. roseus* TDC (P17770) and verified its substrate specificity to primarily tryptophan and also 5-HTP at a reduced rate [12] (the activity of the *C. roseus* TDC enzyme has previously been investigated) [9]. This TDC, like other verified TDC and TyDC, contains the conserved Tyr348 at the position equivalent to Phe338 of the *A. thaliana* AAS. To determine its role in the catalytic reaction, a Y348F mutant of the *C. roseus* TDC was produced and its catalytic reaction was assessed with tryptophan as a substrate. Similar to those obtained during analysis of the *P. crispum* AAS and tyrosine reaction mixtures (Fig. 3.2C), HPLC-EC analysis of the *C. roseus* TDC Y348F mutant and tryptophan reaction mixtures resulted in the detection of a very broad peak (Fig. 3.8A) and treatment of the reaction mixture with borohydride converted the broad peak to a sharp peak (Fig. 3.8B), which contrasts to the typical tryptophan decarboxylation reaction by the wild type *C. roseus* TDC (Fig. 3.8C).

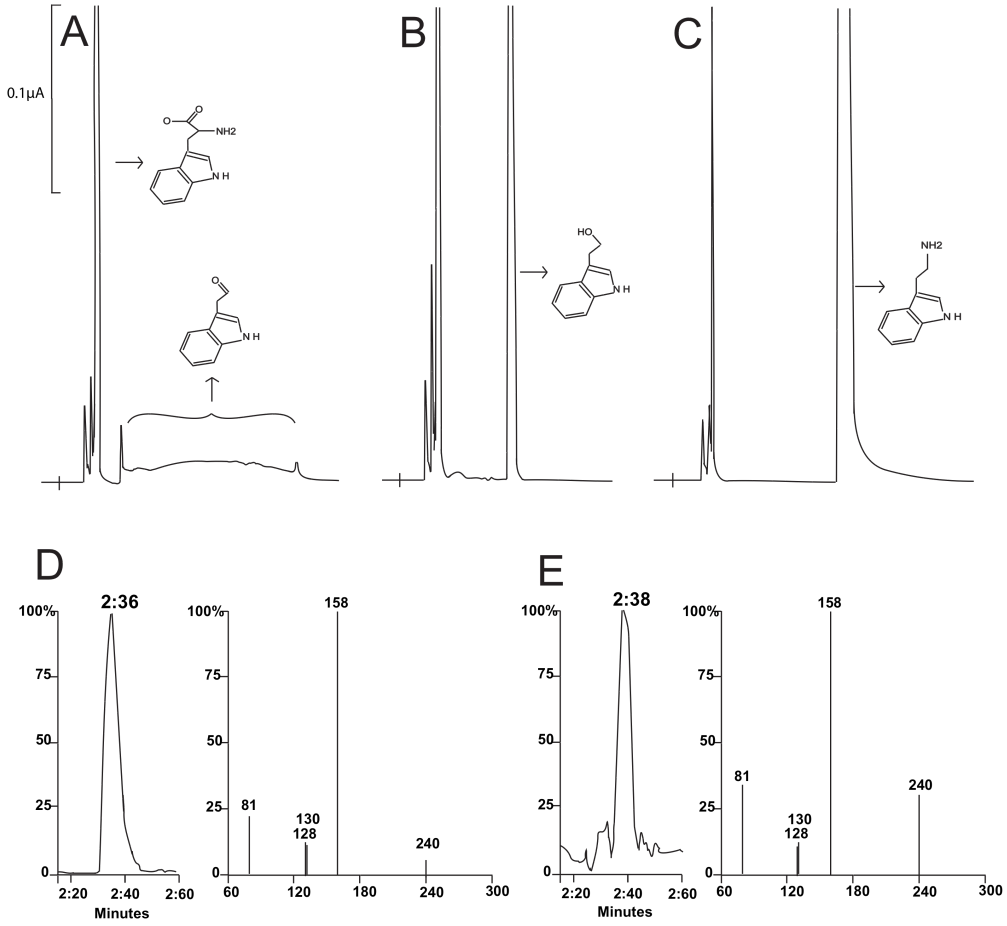

FIGURE 3.8. HPLC-EC and LC/MS/MS detection of indole-3-acetaldehyde generated from *C. roseus* TDC Y348F mutant and tryptophan reaction mixtures. (Chromatograms A-C). Reaction mixtures contain 5 mM of tryptophan and 20 µg of enzyme. The reactions were incubated at 25 ^{o}C and stopped with 0.8 M formic acid. Chromatograms (A and B) illustrate the indole-3-acetaldehyde formed in a TDC Y348F mutant and tryptophan reaction mixtures and the detection of indole-3-ethanol in a borohydride treated reaction. Chromatogram (C) shows the detection of tryptamine in a wild type TDC and tryptophan reaction mixture. Chromatogram and MS/MS

spectrum (D) illustrate the [M-H]- ion (240) and daughter ions of the bisulfite derivatized product formed in bisulfite-treated *A. thaliana* AAS F338Y mutant and phenylalanine reaction mixture in comparison with those (E) produced by indole-3-acetaldehyde–bisulfite standard under identical conditions of HPLC/MS/MS analysis.

The sharp peak, detected in the borohydride-treated reaction mixture, had identical retention time as authentic indole-3-ethanol under the same conditions of HPLC-EC analysis and coeluted with the standard at different mobile phase conditions during HPLC-EC analysis (not shown). Indole-3-ethanol is not charged easily by electrospray ionization, but the indole-3-acetaldehyde-bisulfite adduct (formed easily by reacting indole-3-acetaldehyde with bisulfite in aqueous solution) is negatively charged in aqueous solution even at relatively acidic pH. Analysis of a sodium bisulfite-treated *C. roseus* TDC Y348F mutant and tryptophan reaction mixture by HPLC/MS/MS in negative mode verified that the MS-MS spectrum of $[M-H]^-$ precursor ion of the adduct m/z 240.1 was identical to those of authentic indole-3-acetaldehyde–bisulfite under identical analysis conditions (Fig. 3.8D & 3.8E). The detection of a broad peak during HPLC-EC analysis of the TDC Y348F mutant and tryptophan reaction mixture, the conversion of the broad peak to a sharp peak by borohydride reduction, the coelution of the sharp peak with indole-3-ethanol, the reaction of the enzymatic product with bisulfite (indicative for the presence of aldehyde group) and the identical MS and MS/MS spectra of the its bisulfite adduct with those of indole-3-acetaldehyde-disulfite standards provide convincing evidences for the TDC Y348F enzymatic production of indole-3-acetaldehyde. Accordingly, mutation of Tyr348 to Phe348 changed *C. roseus* TDC into a tryptophan to indole-3-acetaldehyde catalyzing AAS. In addition to indole-3-acetaldehyde, a small amount of tryptamine was also detected in TDC Y348F mutant and tryptophan reaction mixture. In order to substantiate the claim that this active site

phenylalanine is responsible for decarboxylation-deamination activity, an additional tyrosine to phenylalanine mutation was performed upon the *P. Somniferum* tyrosine-350 residue. Evaluation of the *P. Somniferum* wild type and Y350F mutant enzyme activities demonstrates a conversion of activity from decarboxylation to decarboxylation-deamination (Fig. 3.9).

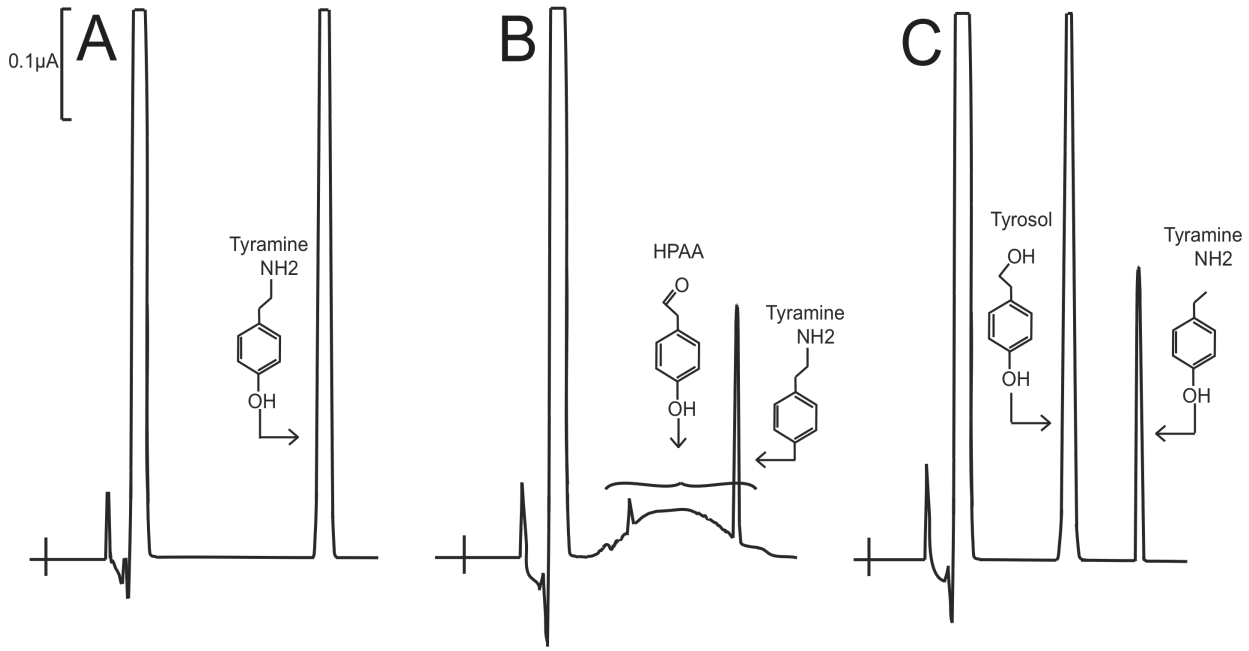

Figure 3.9. HPLC-EC analysis of *P. somniferum* wild type and Y346F enzymes with tyrosine as a substrate. Reaction mixtures of 100 μl containing either 15 μg of *P. somniferum* wild type or mutant enzyme were incubated at 25 ^{o}C and their reaction was stop at 40 min after incubation by adding 0.8 M of formic acid. The mixtures were centrifuged for 5 min at 14,000g and supernatants were injected for HPLC-EC analysis. To reduce HPAA to HPEA, some reaction mixtures were treated with an equal volume of 100% ethanol saturated with borohydride after 40 min incubation. The borohydride treated mixtures were incubated for 10 min on ice, treated with 0.8 M of formic acid to decompose remaining borohydride and centrifuged to obtain supernatants. Supernatants were injected for HPLC-EC analysis. Chromatogram A shows the production of tyramine in the wild type *P. somniferum* mutant and tyrosine reaction mixture at 40 min after incubation. Chromatograms B and C illustrate the accumulation of HPAA and tyramine in the *P. somniferum* Y346F enzyme and tyrosine reaction mixture at 40 min after incubation and the reduction of 4-HPAA to 4-HPEA in a borohydride treated reaction mixture.

In addition to the primary decarboxylation-deamination activity, the *P. Somniferum* Y350F

mutant retained a small percentage of its original decarboxylation activity. Changes of the catalytic reactions in the *C. roseus* and *P. Somniferum* tyrosine to phenylalanine mutants, in conjunction with that of the *P. crispum* and *A. thaliana* phenylalanine to tyrosine mutants, further support the role the active site tyrosine and phenylalanine play in decarboxylation and decarboxylation-deamination activity, respectively.

Substrate specificity and kinetic analysis

The typical substrate of wild-type enzymes was used for activity assays of the mutant enzymes. After the change of catalytic reaction for the mutant enzymes was established, they were screened for activity against other aromatic amino acids. Similar to wild type *A. thaliana* AAS, its F338Y mutant displayed a very low activity to tyrosine (~5% of its activity to phenylalanine) and strong activity to dopa (Fig. 3.10), but showed no detectable activity to tryptophan and 5-HTP; while *C. roseus* TDC Y348F mutant showed activity to tryptophan and 5-HTP with no detectable activity to phenylalanine, tyrosine and dopa (not shown).

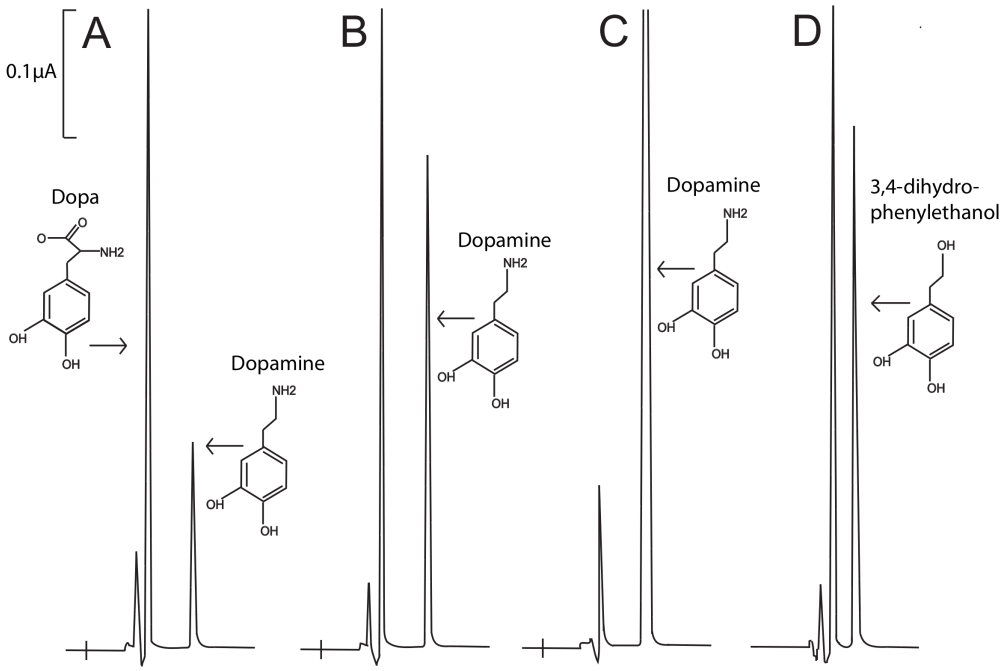

FIGURE 3.10. HPLC-EC detection of dopamine and 3,4-dihydrophenylethanol produced in *A. thaliana* AAS F338Y mutant and wild type reaction mixtures respectively. Y-axis represents the output in microamps and the x-axis represents retention time. Reaction mixtures of 0.1 ml containing 30 µg of *A. thaliana* AAS F338Y mutant or wild type and 5 mM of dopa were prepared in 100 mM of phosphate buffer (pH, 7.5). The reaction mixtures were incubated at 25 ^{o}C and the reaction was stopped at different time after incubation by adding an equal volume of 0.8 M of formic acid. Chromatograms (A-C) illustrate the relative amount of dopamine formed in the reaction mixtures at 4, 12 and 24 min after incubation, respectively. Chromatogram D illustrates wild type enzyme and dopa reaction mixture at 24 min after incubation and the reduction of 3,4-dihydroxylphenylacetaldehyde to 3,4-dihydrophenylethanol in a borohydride treated reaction mixture. In the mutant enzyme reaction mixtures, the rate of product formation was decreased as dopamine accumulated in the reaction mixtures, the reaction could proceed basically to completion (CO_2 is released, so no equilibrium is reached during reaction). At the applied conditions, essentially all dopa was converted to dopamine, but no indication for further oxidative deamination of the dopamine product was observed.

These analyses established that although the catalytic reaction of these mutants was changed, their substrate specificity were the same as their wild type enzymes [9, 11].

Kinetic evaluations were conducted for both the wild type and mutant *A. thaliana* and *C. roseus* proteins using their respective physiological substrate. Under the applied conditions, *A. thaliana* AAS F338Y mutant and *C. roseus* TDC Y348F mutant displayed a similar affinity to phenylalanine and tryptophan, respectively, as compared to their respective wild type enzymes (Table 3.2).

Table 3.2.

Kinetic parameters of *Arabidopsis thaliana* and *Cataranthus roseus* wild type and mutant enzymes

Organism	Enzyme	V_{max} (nmols/min/mgprotein)	K_m (mM)	Substrate	Activity
Arabidopsis thaliana	PAAS (WT)	112 ± 8	5.10 ± 0.70	Phenylalanine	Aldehyde Synthase
Arabidopsis thaliana	PAAS (F338Y)	341±31	4.60 ± 0.55	Phenylalanine	Decarboxylation
Catharanthus roseus	TDC (WT)	2710 ± 110	0.12 ± 0.02	Tryptophan	Decarboxylation
Catharanthus roseus	TDC (Y348F)	160 ± 14	0.095 ± 0.02	Tryptophan	Aldehyde Synthase

Values represent means ± SE (n=3)

Similar Michaelis constants between wild type and mutant enzymes indicate that the mutation of the active site tyrosine to phenylalanine or vise versa does not apparently alter the substrate binding affinity of the enzymes. In contrast, the specific activities of the mutant enzymes were quite different to those determined for the wild-type enzymes (Table 3.2). The decarboxylase activity of *A. thaliana* AAS F338Y mutant was approximately 3 fold faster than the aldehyde synthase activity of its wild type enzyme to the same substrate, while the specific aldehyde synthase activity of *C. roseus* Y348F mutant was approximately 17 fold slower than the decarboxylase activity of the wild type TDC to tryptophan (Table 3.2). Such alterations in

activity likely are reflected by the complexity of the reactions. The added chemistry necessary for decarboxylation-deamination as opposed to a simpler decarboxylation may result in the observed catalysis rate change.

3.6 Discussion

Based on reactions they catalyze, plant AAADs can be classified as true AAADs (enzymes that catalyze the production of arylalkylamines from their respective aromatic amino acid substrates) or AASs (enzymes that catalyze the production of aromatic acetaldehydes from their respective aromatic amino acid substrates). Within each subclass, these enzymes can be further classified based on their substrate specificity, such as TyDCs and TDCs. Association of the substrate selectivity and catalytic reaction with a given AAAD protein provides relevant functional linkages. Unfortunately, high sequence identity across plant AAADs makes it difficult to accurately assign substrate specificity and catalytic reaction based on a primary sequence. Our conversion of two AASs into AAADs through active site phenylalanine to tyrosine mutation and our conversion of two AAADs into AASs through active site tyrosine to phenylalanine mutation demonstrate that the conserved active site tyrosine and phenylalanine are predominantly responsible for their respective AAAD and AAS catalytic reactions. Although more experimental verification is necessary, our data, in conjunction with the strict conservation of the active site tyrosine in all verified TyDC and TDC, indicate that the presence of active site tyrosine is a genuine criterion to predict the decarboxylation activity of a given member of the AAAD family. We submit that the identification of a homologous active site tyrosine or phenylalanine will enable reliable differentiation of plant AAAD and AAS enzymes from a primary sequence basis. In addition, the identification of an activity implicative residue in AAADs and AASs provides some basis to expand on each of the activities respective reaction mechanisms.

PLP-dependent decarboxylases are believed to proceed by a single reaction mechanism [21]. In this mechanism the external aldimine loses the α-carboxyl group to form the carbanion quinonoid intermediate (due to its interaction with catalytic residues). Subsequent α-carbon protonation by an active site residue generates the product monoamine. Previous investigations of AAAD enzymes suggest that the quinonoid intermediate may become protonated by the catalytic loop tyrosine to form the arylalkylamine product [22]. The same report indicated that in the absence of α-carbon protonation, molecular oxygen is capable of attacking the carbanion of the quinonoid intermediate to generate a peroxide. The peroxy-aldimine transition form will undergo heterolysis of the O–O bond allowing for the regeneration of PLP and formation of an imine complex that spontaneously decomposes to yield an aromatic aldehyde and ammonia. Based on the effective conversion of the two AASs into AAADs upon mutating the active site phenylalanine to tyrosine the proposed tyrosine α-carbon protonation mechanism seem plausible. However, the α-carbon protonation of the intermediate requires the ionization of the tyrosine phenolic hydroxyl group proton. With a pKa around 10, the phenolic hydroxyl group of tyrosine may not ionize easily under physiological conditions. Additionally, a lack of electron density for the loop region in the three available AAAD structures makes it difficult to accurately estimate the probable distance between the side chain hydroxyl group of tyrosine and the α-carbon of the external aldimine. Therefore, it is unknown whether the α-carbon and the catalytic loop tyrosine are within interacting distances.

Analysis of a recently released mammalian HDC (the only type II PLP decarboxylase with electron density for the catalytic loop) enables speculation on the interactions between the substrate α-carbon and the catalytic loop tyrosine ([16]. Careful examination of the HDC active site confirmation revealed that although its Tyr344 from monomer B (the equivalent active site tyrosine in plant AAAD and mammalian DDC) is quite close to the α-carbon of the external

aldimine complex (7.50A), its side chain hydroxyl group is actually much closer to the imidazole amine (ε-amine group) (4.42A) of monomer A His194. Accordingly, within the HDC structure, the hydroxyl group of monomer B Tyr344 should interact more easily with the imidazole of monomer A His194 than it would be with the α-carbon of the external aldimine complex. Such structural observations in conjunction with our experimental verifications of catalytic loop tyrosine mediated decarboxylation enable us to propose a new mechanism of α-carbon protonation. We believe that plant AAADs active site tyrosine does not directly protonate the intermediate α-carbon, but rather play a crucial role in stabilizing the proton transfer from His194 to the α-carbon (in the HDC structure, Tyr344 hydroxyl group is 4.39A from the histidine 194 N2). We propose that the phenolic hydroxyl group from the catalytic loop tyrosine forms a stabilizing hydrogen bond with the N2 histidine to enable the proton transfer from the histidine imidazole to the α-carbanion. The modeled active site conformation of *C. roseus* TDC and *A. thaliana* AAS (using 4E1O as template [16]; generated through Modeler [23]; visualized through Pymol [20]) help illustrating the indirect role the active site tyrosine may play in stabilizing protonation of the α-carbon of the substrate-PLP complex through His194 (Fig. 3.11).

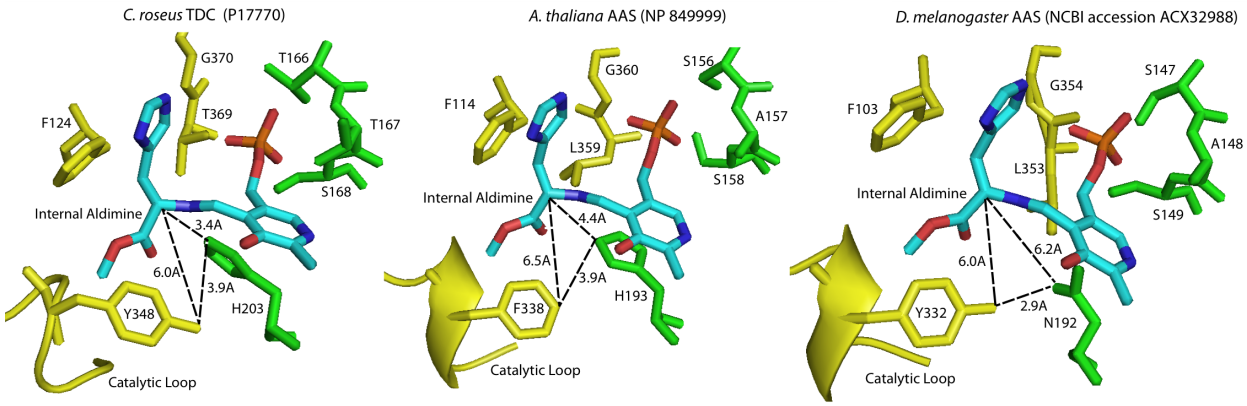

FIGURE 3.11. Models of active site residues and external aldimine interactions. The model on the left shows the relative locations of histidine 203, tyrosine 348, and the external aldimine from

the *C. roseus* TDC model (generated using 4E1O). The model in the middle shows the relative locations of histidine 193, phenylalanine 338, and the external aldimine from the *A. thaliana* AAS model (generated using 4E1O). The model on the right shows the relative locations of asparagine 192, tyrosine 332, and the external aldimine from the *D. melanogaster* AAS model (generated using 4E1O). Residues shown in yellow correspond to the alpha chain whereas residues in green correspond to the beta chain.

This proposed mechanism is further supported by the loss of decarboxylation activity in the tyrosine to phenylalanine AAAD mutants. Upon replacing the catalytic tyrosine with phenylalanine (Y348F mutation in *C. roseus* TDC, Y346F mutation in *P. somniferum* TyDC), there is no electronegative R group atom to stabilize histidine proton transfer. Without such a stabilizing interaction, the substrate α-carbon is not protonated. This leaves the substrate carbanion susceptible to peroxidation and subsequent aromatic acetaldehyde formation.

The above hypothesis regarding the active site tyrosine's role in α-carbon protonation (though reasonable) remains speculative in nature. However, the predicted active site conformation of insect AAS proteins provides a more compelling argument for our mechanistic proposal. Unlike plant AAS proteins that contain an active site phenylalanine, the equivalent position in insect AASs remains as a tyrosine (moreover, this tyrosine residue is stringently conserved in all available insect AAADs, regardless of their substrate specificity and catalytic reactions). This contrasts what is observed in plant AAS proteins. However, analysis of the His194 equivalent in insect AAAD and AAS determined that all typical insect AAADs contain the histidine in the position, but the active site histidine was replaced by an asparagine in all verified insect AAS proteins. Asparagine has a greatly reduced likelihood of proton donation (non ionizable nature of its R group) as compared to histidine. Consequently, in the presence of an active site asparagine in insect AAS, the active site tyrosine does not seem to be able to play a stabilizing role in α-

carbon proton transfer (Fig. 3.11). The presence of tyrosine and absence of histidine within insect AAS enzymes supports the role of tyrosine in promoting typical decarboxylation in plant AAADs through its interaction with the active site histidine. Through these analyses, it seems apparent that the active site tyrosine from insect AAAD and AAS proteins plays a different catalytic role from the tyrosine in plant AAADs. However, this by no mean indicated that this active site tyrosine is not critical for insect AAAD and AAS substrate binding and catalysis. Proximity to the active site and the stringent conservation in all insect AAAD and AAS proteins indicates a probable role in substrate binding or catalysis.

Although our data suggested some apparent similarities in catalytic reactions of plant and non-plant AAADs, there are also considerable differences regarding the structural basis of substrate binding and catalysis. Mammalian DDC has been the most extensively studied AAAD in terms of substrate specificity and catalytic reactions. Based on literature, mammalian DDC can use both dopa and 5-HTP as substrates [24-25], but the plant AAADs or AASs use aromatic amino acids with either indole ring or benzene ring, but never the both [1,8-9]. Other than its typical decarboxylation activity to dopa and 5-HTP, mammalian DDC can also catalyze oxidative deamination of dopamine and 5-hydroxytryptamine (5-HT) [26-27]. However, plant AAADs cannot catalyze any oxidative deamination of tyramine, dopamine or tryptamine (analyzed with two available plant TyDC, one plant TDC and three plant AASs in our laboratory). The same applies to the *A. thaliana* F338Y mutant as well. For example, at the applied assay conditions, essentially all dopa substrate has been converted to dopamine after 24 min incubation. HPLC-EC analyses showed no indication for any further oxidative deamination of dopamine product to its aldehyde derivative in the reaction mixture (Fig. 3.10C). This suggests that arylalkylamines, once released from the catalytic center of plant AAADs or AAS, cannot easily enter into their active site again, or that the external aldimine between the PLP cofactor and arylalkylamines

cannot be easily formed at the active site of plant AAADs. Addition of tyramine at mM concentrations into the wild type *P. crispum* AAS and tyrosine reaction mixtures also did not noticeably slow down the AAS catalyzed PHAA production from tyrosine. Additionally the tyramine levels remained at same level during incubation (not shown), indicating the absence of tyramine oxidative-deamination. This reinforces the notion that the α-carboxyl group is essential for plant AAS substrate binding. Apparently, extensive studies about AAADs are necessary before being able to achieve a better overall understanding of the large AAAD family proteins across species.

The interconversion of AAAD and AAS activities enabled the generation of several unusual plant AAAD and AAS enzyme products. These products include 4-hydroxyphenylacetaldehyde, phenylethylamine, indole-3-acetaldehyde, and 5-hydroxy indole-3-acetaldehyde. 4-hydroxyphenylacetaldehyde has only been documented as a product from a single AAS enzyme [12]. Thus far the physiological function of this AAS product remains unknown. Phenylethylamine has only been observed as plant type II PLP decarboxylase product from a selection of *Solanum lycopersicum* enzymes [28]. Plant AAAD enzymes typically retain approximately 40% identity to one another where as these *S. lycopersicum* enzymes only demonstrate approximately 11% identity to canonical AAADs. Further *S. lycopersicum lycopersicum* type II PLP decarboxylase sequence analysis demonstrates strong homology (approximately 55% identity) to the characterized *Arabidopsis thaliana* (AF389349) and *Brassica napus* (BAA78331) serine decarboxylases (SDCs) [29]. Therefore these *S. lycopersicum* enzymes cannot be viewed as canonical plant AAAD enzymes making phenylethylamine a truly unique plant AAAD product. Finally, the enzymatic conversion of tryptophan to indole-3-acetaldehyde and 5-hydroxytryptophan to 5-hydroxy indole-3-acetaldehyde by the *C. roseus* TDC mutant truly represents novel AAAD enzyme products.

Amongst these unusual products, the *C. roseus* TDC mutant generated indole-3-acetaldehyde is likely the most interesting. Indole-3-acetaldehyde is a proposed intermediate in the original tryptophan dependent indole-3-pyruvic acid (IPA) auxin biosynthetic pathway [30-31]. Although recent biochemical and genetic data has demonstrated a clear alternate IPA pathway (Tryptophan to IPA via tryptophan aminotransferases [32], and IPA to IAA through YUCCA catalyzed oxidative decarboxylation [33-35] (Fig. 3.12)), no experimental data has invalidated indole-3-acetaldehydes role as an alternate IPA pathway intermediate.

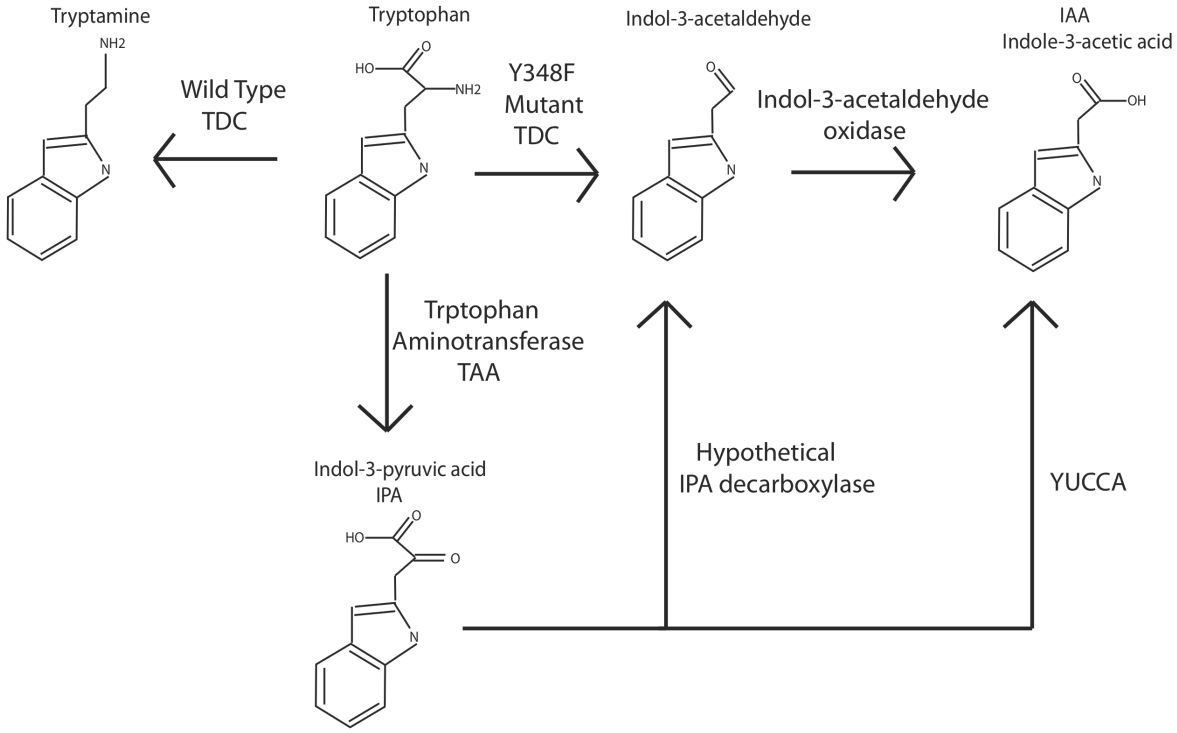

Figure 3.12. Intersection of the *C. roseus* TDC Y348F mutant and the two proposed tryptophan dependent indole-3-pyruvic acid auxin biosynthetic pathway.

Despite references regarding this putative auxin (indole-3-acetic acid) intermediate, no biosynthetic route has been identified. Although there have been verified tryptophan aminotransferases [32] capable of catalyzing the conversion of tryptophan to IPA, there have been no experimental data showing the presence of an IPA decarboxylase (IPA to indole-3-acetaldehyde) in plants. Interestingly, our mutant is capable of performing the function of a tryptophan aminotransferase and the putative IPA decarboxylase (converting tryptophan to indole-3-acetaldehyde) in one step (Fig. 3.12). The final auxin biosynthetic step in this proposed pathway involves the conversion of indole-3-acetaldehyde to indole-3-acetic acid (IAA). This reaction has been demonstrated by aldehyde oxidases [36-37]. Therefore, our TDC Y348F mutation could conceivable convert the standard TDC reaction into one capable of producing a putative intermediate for auxin biosynthesis. The introduction of a stable and active TDC Y348F mutant into wild type and auxin deficient *Arabidopsis* plants should demonstrate the presence/absence of an IPA decarboxylase, demonstrate/disprove in vivo aldehyde oxidases activity, and produce insights into indole-3-acetaldehyde's putative role as an auxin intermediate. Additionally, conversion of a regular TDC enzyme to a tryptophan aldehyde synthase only requires a single nucleotide substitution. One might think that somewhere and some point throughout plant evolution this might have occurred and granted some level of reproductive fitness. Such an enzyme might have evolved in plants and may be producing an alternate auxin biosynthetic route (assuming the original IPA pathway is functional).

In summary, the AAAD family is a great example of protein functional expansion. Based on its ubiquitous distribution, it seems reasonable to consider that the typical DDC or TyDC, present from bacteria to humans, is the prototype of other more specific AAADs. Such divergent

AAADs have likely evolved unique substrate specificities and activities to provide unique physiological requirements. The functions of AAADs vary considerably, depending upon their substrate specificity and catalytic reaction, but their high sequence similarity makes it extremely difficult to tell them apart based on primary sequences. Our data indicated that the presence of the conserved tyrosine or phenylalanine in the active site loop region could serve as signature residues for reliably predicting typical plant AAAD and AAS, respectively. This should help to more precisely distinguish between true AAAD and AAS sequences available in the database and to aid the proper annotation of numerous incoming plant AAAD sequences currently undergoing genome-sequencing projects. Our comparative analyses of active site conformations between different AAAD and AAS proteins lead to a new hypothesis concerning the roles the active site tyrosine and phenylalanine play in their typical decarboxylation reaction and decarboxylation-oxidative deamination reaction, respectively. Although the hypothesis remains to be further substantiated, the proposed mechanism gives some reasonable explanation and insight for AAAD- and AAS-catalyzed reactions, respectively, which should stimulate research in this area. In addition, the ability to catalyze tryptophan to indole-3-acetaldehyde suggests a useful research tool in the investigation of auxin biosynthesis. Overall, our progress in differentiating plant AAAD and AAS proteins is major step forward towards proper classification/annotation of hundreds of individual plant AAADs in the database. However, much still remains to be established regarding the structural components and chemical mechanisms dictating the substrate specificity and variable activities of AAAD- and AAS-mediated reactions.

3.7 Acknowledgements

This study was supported through Virginia Tech Biochemistry college of Agricultural and Life

Sciences funding.

References

1. Facchini, P. J., Huber-Allanach, K. L., and Tari, L. W. (2000) Plant aromatic L-amino acid decarboxylases: evolution, biochemistry, regulation, and metabolic engineering applications. *Phytochemistry* **54**, 121-138.

2. Ellis, B.E. (1983) Production of hydroxyphenylethanol glycosides in suspension-cultures of *Syringa vulgaris*. *Phytochemistr*y **22**, 1941–1943.

3. Leete, E., and Marion, L. (1953) The biogenesis of alkaloids: VI The formation of hordenine and N-methyltyramine from tyrosine in barley. *Can J Chem.* 31, 126–128.

4. Marques, I.A., and Brodelius, P.E. (1988) Elicitor-induced L-tyrosine decarboxylase from plant cell suspension cultures. *Plant Physiol.* **88**, 46–51.

5. Trezzini, G.F., Horrichs, A., and Somssich, I.E. (1993) Isolation of putative defense-related genes from Arabidopsis thaliana and expression in fungal elicitor-treated cells. *Plant Mol. Biol.* **21**, 385–389.

6. Pasquali, G., Goddijn, O.J., de Waal, A., Verpoorte, R., Schilperoot, R.A., Hoge, J.H. and Memelink, J. (1992) *Coordinated regulation of two indole alkaloid biosynthetic genes from cataranthus ruseus by auxin and elicitors*. Plant molecular biology 18(6): 1121-1131

7. Berlin, J., Ruegenhagen, C., Kuzovkina, I.N., Fecker, L.F., and Sasse, F. (1994) Are tissue cultures of Peganum harmala a useful model system for studying how to manipulate the formation of secondary metabolites? *Plant Cell Tissue and Organ Culture* **38**, 289-297.

8. Lehmann, T. and Pollmann, T. (2009) Gene expression and characterization of a stress-induced tyrosine decarboxylase from Arabidopsis thaliana. *FEBS Letters* **583**, 1895–1900

9. Noé, W., Mollenschott, C., and Berlin, J. (1984) Tryptophan decarboxylase from Catharanthus roseus cell suspension cultures: purification, molecular and kinetic data of the homogenous protein. *Plant Molecular Biology* **3** (5), 281-288

10. Kaminaga, Y., Schnepp, J., Peel, G., Kish, C. M., Ben-Nissan, G., Weiss, D., Orlova, I., Lavie, O., Rhodes, D., Wood, K., Porterfield, D. M., Cooper, A. J., Schloss, J. V., Pichersky, E., Vainstein, A., and Dudareva, N. (2006) Plant phenylacetaldehyde synthase is a bifunctional homotetrameric enzyme that catalyzes phenylalanine decarboxylation and oxidation. *J Biol Chem.* **281**, 23357-23366.

11. Gutensohn, M., Klempien, A., Kaminaga, Y., Nagegowda, D. A., Negre-Zakharov, F., Huh, J. H., Luo, H., Weizbauer, R., Mengiste, T., Tholl, D., and Dudareva, N. (2011) Role of aromatic aldehyde synthase in wounding/herbivory response and flower scent production in different Arabidopsis ecotypes. *Plant J* **66**, 591-602.

12. Torrens-Spence, M.P., Gillaspy, G., Zhao, B., Harich, K., White, R.H. and Li, J. (2012) Biochemical evaluation of a parsley tyrosine decarboxylase results in a novel 4-hydroxyphenylacetaldehyde synthase enzyme. *Biochem Biophys Res Commun.* **418**(2), 211-216

13. Vavricka, C., Han, Q., Huan, Y., Huang, Y., Erickson, S.M., Harich, K., Christensen, B.M. and Li, J. (2011) From Dopa to dihydroxyphenylacetaldehyde: a toxic biochemical pathway plays a vital physiological function in insects. *PLoS One* **6**(1), e16124.

14. Park, S., Kang, K., Lee, K., Choi, D., Kim, Y., and Back, K. (2009) Induction of serotonin biosynthesis is uncoupled from the coordinated induction of tryptophan biosynthesis in pepper fruits (Capsicum annuum) upon pathogen infection. *Planta* **230**, 1197-1206

15. Kawalleck, P., Keller, H., Hahlbrok, K., Scheel, D. and Somssich, I.E. (1993) A pathogen-responsive gene of parsley encodes tyrosine decarboxylase. *J Biol Chem.* **268**(3), 2189-2194

16. Komori, H., Nitta, Y., Ueno, H. and Higuchi, Y. (2012) Structural study reveals Ser345 determines substrate specificity on human histidine decarboxylase. *J. Biol. Chem*. **287** (34), 29175-29183

17. Ko, J.K. and Ma, J. (2005) A rapid and efficient PCR-based mutagenesis method applicable to cell physiology study. *Am. J. Physiol. Cell Physiol.* **288**, 1273-1278

18. Han, Q., Ding, H., Robinson, H., Christensen, B.M. and Li, J. (2010) Crystal Structure and Substrate Specificity of Drosophila 3,4-Dihydroxyphenylalanine Decarboxylase. *PLOS ONE* **5** (1), e8826.

19. Buteau, C., Duitschaever, C.L. and Ashton, G.C. (1984) High-performance liquid chromatographic detection and quantitation of amines in must and wine. *J Chromatography A* 284(1), 201-210

20. DeLano, W. L. (2002) The PyMOL Molecular Graphics System, 0.99 Ed., DeLano Scientific, LLC, Palo Alto, CA

21. Eliot, A.C., and Kirsch, J.F (2004) Pyridoxal phosphate enzymes: mechanistic, structural, and evolutionary considerations. *Annu. Rev. Biochem* **73**, 383-415

22. Bertoldi, M., Gonsalvi, M., Contestablile, R. and Borri Voltattorni, C (1998) Mutation of Tyrosine 332 to Phenylalanine Converts Dopa Decarboxylase into a Decarboxylation-dependent Oxidative Deaminase. *J. Biol. Chem* **277** (39), 36357-36362

23. Šali, A., and Blundell, T. L. (1993) Comparative protein modelling by satisfaction of spatial restraints. *J. Mol. Biol*. 234, 779-815

24. Udenfriend, S., Clark, C., and Titus, E. (1953) 5-hydroxytryptophan decarboxylase: a new route of metabolism of tryptophan. *J. Am. Chem. Soc.* 75, 501-502

25. Srinivasan, K., and Awapara, J. (1978) Substrate specificity and other properties of DOPA decarboxylase from guinea pig kidneys. *Biochim Biophys Acta.* 526, 597-604

26. Bertoldi, M., Moore, P. S., Maras, B., Dominici, P., and Borri Voltattorni, C. (1996) Mechanism-based inactivation of dopa decarboxylase by serotonin. *J. Biol. Chem*. 271, 23954–23959

27. Bertoldi, M., Dominici, P., Moore, P. S., Maras, B., and Borri Voltattorni, C. (1998) Reaction of dopa decarboxylase with alpha-methyldopa leads to an oxidative deamination producing 3,4-dihydroxyphenylacetone, an active site directed affinity label. *Biochemistry* 37, 6552–6561

28. Tieman, D., Taylor, M., Schauer, N., Fernie, A.R., Hanson, A.D., and Klee, H.J. (2006) Tomato aromatic amino acid decarboxylases participate in synthesis of the flavor volatiles 2-phenylethanol and 2-phenylacetaldehyde. *PNAS* 103 (210), 8287-8292

29. Rontein, D., Nishida, I., Tashiro, G., Yoshioka, K., Wu, W., Voelker, D.R., Basset, G., and Hanson, A.D. (2001) Plants synthesize ethanolamine by direct decarboxylation of serine using a pyridoxal phosphate enzyme. *J. Biol. Chem.* 276 (38), 35523-35529

30. Woodward, A.W. and Bartel, B. (2005) Auxin: regulation, action, and interaction. *Ann Bot.* 95, 707–735.

31. Koga, J., Adachi, T. and Hidaka, H. (1992) Purification and characterization of indolepyruvate decarboxylase. A novel enzyme for indole-3-acetic acid biosynthesis in Enterobacter cloacae. *J. Biol. Chem.* 267, 15823–15828.

32. Steanova, A.D., Robertson-Hoyt, J., Yun, J., Benavente, L.M., Xie, D. Dozezal, K., Schlereth, A., Jurgens, G., Alonso, J.M. (2008) TAA1-Mediated Auxin Biosynthesis Is Essential for Hormone Crosstalk and Plant Development. *Cell* 133 (1), 177-191

33. Stepanova, A.N., Yun, J., Robles, L.M., Novak, O., He, W., Guo, H., Ljun, K. and Alonso, J.M. (2011) The Arabidopsis YUCCA1 flavin monooxygenase functions in the indole-3-pyruvic acid branch of Auxin biosynthesis. *Plant Cell* 23, 3961-3973

34. Mashiguchi K, Tanaka K, Sakai T, Sugawara S, Kawaide H, Natsume M, Hanada A, Yaeno T, Shirasu K, Yao H, McSteen P, Zhao Y, Hayashi K, Kamiya Y, and Kasahara H. (2011) The main auxin biosynthesis pathway in Arabidopsis. *PNAS* 108 (45), 18512-18517

35. Dia, X., Mashiguchi, K., Chen, Q., Kasahara, H., Kamiya, Y., Ojha, S., DuBois, J., Ballou, D., and Zhao, Y. (2012) The biochemical mechanism of auxin biosynthesis by an Arabidopsis YUCCA flavin-containing monooxygenase. *J. Biol. Chem* M112.424077

36. Seo, M., Akaba, S., Oritani, T., Delarue, M., Bellini, C., Caboche, M., and Koshiba, T. (1998) Higher activity of an aldehyde oxidase in the auxin-overproducing superroot1 mutant of Arabidopsis thaliana. *Plant Physiol*. 116, 687–693.

37. Sekimoto, H., Seo, M., Kawakami, N., Komano, T., Desloire, S., Liotenberg, S., Marion-Poll, A., Caboche, M., Kamiya, Y. and Koshiba, T. (1998) Molecular cloning and

characterization of aldehyde oxidases in Arabidopsis thaliana. *Plant Cell Physiol*. 39, 433–442.

Chapter 4

Investigation of a substrate-specifying residue within *Papaver somniferum* and *Catharanthus roseus* aromatic amino acid decarboxylases.

Submitted to Phytochemistry 04-10-14

Michael P. Torrens-Spence mpspence@vt.edu [1], Michael Lazear lazear@vt.edu[1], Renee von Guggenberg reneev92@vt.edu [1], Haizhen Ding [1] and Jianyong Li lij@vt.edu[1]*

Author Contributions

Michael P. Torrens-Spence[1] wrote the article and performed all the research except for the experiments mentioned below.

Michael Lazear[1] assisted in the cloning, protein expression and protein purification.

Renee vonGuggenberg[1] assisted in the cloning, protein expression and protein purification.

Haizhen Ding[1] assisted in the molecular cloning and protein expression.

Jianyong Li[1] oversaw and directed the research and helped write the article.

[1] Department of Biochemistry, Virginia Tech, Blacksburg, Virginia, United States of America

4.1 Abstract

Plant aromatic amino acid decarboxylases (AAADs) catalyze the decarboxylation of aromatic amino acids with either benzene or indole rings. Because the substrate selectivity of AAADs is intimately related to their physiological functions, primary sequence differentiation could provide significant physiological implications. Due to a general high sequence identity, plant AAAD substrate specificities have been difficult to identify through primary sequence comparison. In this study, we utilized bioinformatic approaches to identify several active site residues within plant AAAD enzymes that may impact substrate specificity. Next we selected a *Papaver somniferum* tyrosine decarboxylase (TyDC) as a model to verify our putative substrate-dictating residues through mutation. Results indicate that the mutagenesis of serine 372 to glycine enables the *P. somniferum* TyDC to use 5-hydroxytryptophan as a substrate and reduces the enzyme activity toward dopa. Additionally, the reverse mutation in a *Catharanthus roseus* tryptophan decarboxylase (TDC) enables the mutant enzyme to utilize tyrosine and dopa as substrates with a reduced affinity toward tryptophan. Molecular modeling and molecular docking of the *P. somniferum* TyDC and the *C. roseus* TDC enzymes provided a structural basis to explain alterations in substrate specificity. Identification of an active site residue that impacts substrate selectivity produces a primary sequence identifier that may help differentiate the indolic and phenolic substrate specificities of individual plant AAADs.

4.2 Keywords

Aromatic amino acid decarboxylase; tyrosine decarboxylases; tryptophan decarboxylases

4.3 Introduction

Aromatic amino acid decarboxylases (AAADs) are a group of economically important and phylogenetically diverse enzymes that are categorically joined through their pyridoxal 5-phosphate (PLP) dependence and sequence homology. This family of enzymes has been studied extensively in mammals where a single enzyme, dopa decarboxylase (DDC), catalyzes the decarboxylation of both phenolic and indolic amino acids to generate their corresponding aromatic amines. Mammalian DDC is responsible for the decarboxylation of dopa and 5-hydroxytryptophan to yield the neurotransmitters dopamine and serotonin, respectively (Srinivasan and Awapara, 1978; Zhu and Juorio, 1995). Unlike the single mammalian DDC enzyme, plant AAADs have evolved with variations in activity and substrate specificity. The resulting paralogs are formally identified as tryptophan decarboxylases (TDCs), tyrosine decarboxylases (TyDCs) and aromatic acetaldehyde synthases (AASs). TDCs catalyze the decarboxylation of tryptophan and 5-hydroxytryptophan (Noé et al., 1984; De Luca et al., 1988; Lopez-Meyer and Nessler, 1997; Yamazaki et al., 2003; Kang et al., 2007; Park et al., 2009), TyDCs catalyze the decarboxylation of tyrosine and dopa (Facchini and De Luca, 1995; Lehmann and Pollmann, 2009; Torrens-Spence et al., 2012; Torrens-Spence et al., 2013) and AASs catalyze a decarboxylation-oxidative deamination of dopa, tyrosine and phenylalanine (Kaminaga et al., 2006; Gutensohn et al., 2011; Torrens-Spence et al., 2012).

Differences in substrate selectivity and activity among plant TyDCs, TDCs and AASs enable individual enzymes to generate specific products with unique physiological functions. For example, plant TDCs are required for synthesis of monoterpenoid indole alkaloids that comprise a diverse group of hundreds of pharmacologically active compounds (Meijer et al., 1993; Berlin et al., 1994; Facchini et al., 2000), TyDCs are known to function in several different metabolic pathways including the biosynthesis of simple alkaloids, complex benzylisoquinoline alkaloids,

and *N*-hydroxycinnamic acid amides (Leete and Marion, 1953; Ellis, 1983; Marques and Brodelius 1988; Trezzini et al., 1993; Facchini et al., 2000) and AAS enzymes catalyze the production of volatile flower scents, floral attractants, and defensive phenolic acetaldehyde secondary metabolites (Kaminaga et al., 2006; Gutensohn et al., 2011; Torrens-Spence et al., 2012). It is clear that the physiological functions of plant AAADs are closely related to their respective activities and substrate specificities; however, due to the subtlety of the enzymatic divergence of plant AAADs, it has historically been difficult to predict the function of any given plant AAAD paralog through sequence comparison. Consequently, being able to distinguish the activity and substrate specificity of individual plant AAADs is of practical significance.

In our previous study, we determined that a single active site residue is capable of dictating the activity of plant TyDCs, TDCs and AASs without altering substrate selectivity. Specifically, the presence of a tyrosine in an active site catalytic loop dictates decarboxylation chemistry while a phenylalanine substitution at the same location dictates aldehyde synthase chemistry (Torrens-Spence et al., 2013). The alteration in enzymatic activity due to a single amino acid substitution suggests that the functional variations in plant AAADs may be dictated by a small number of residues. Such subtle variations in plant AAADs likely explain the difficulty in differentiating plant TyDCs, TDCs and AASs through sequences analysis.

In this study, we attempted to further disambiguate plant AAADs by identifying specific structural identifiers capable of differentiating between the substrate specificity of TDCs and TyDCs. To do so, we have performed bioinformatic analyses of characterized plant AAAD enzymes, predicted several target residues that might potentially impact substrate specificity in plant AAADs and assessed these residues through site-directed mutation using a *Papaver somniferum* TyDC and a *Catharanthus roseus* TDC. Results of the biochemical analyses, in

conjunction with molecular modeling, provide insights into a residue that impacts plant AAAD indole and benzene substrate selectivity.

4.4 Materials and Methods

Reagents

Tyrosine, tyramine, tryptophan, tryptamine, 5-hydroxytryptophan, 5-hydroxytryptamine, dopa, dopamine, phenylalanine, phenylethylamine, pyridoxal 5-phosphate (PLP), phthaldialdehyde, formic acid, and acetonitrile were purchased from Sigma (St. Louis, MO). The IMPACT-CN protein expression system was purchased from New England Biolabs (Ipswich, MA).

Preparation of recombinant proteins

P. somniferum and *C. roseus* RNA extraction, cDNA production, vector cloning and wild type protein expression were conducted as described in our previous publication [12]. Primer pairs were synthesized and used for the amplification and SapI mutagenesis of the expression mutants (Table 4.1).

Primer Name	Sequence
TyDC Forward Cloning	ACTG***CATATG***ATGGGAAGCCTTCCGA
TyDC Reverse Cloning	ACTG***CTCGAG***CTAGGCACCAAGTATGGCAT
TyDC S101A SapI mutagenesis forward	AAA***GCTCTTCT***GCGAGTGGTTCCATTGCTGG
TyDC S101A SapI mutagenesis reverse	AAA***GCTCTTCT***CGCAGGAAAGTAAGCAAAGTAATTTGG
TyDC C170S SapI mutagenesis forward	AAA***GCTCTTCT***TCTGAAGCCATTTTATGTACTCTAACTGC
TyDC C170S SapI mutagenesis reverse	AAA***GCTCTTCT***AGAAGTAGTCCCTTGCAAAACACC
TyDC N318S SapI mutagenesis forward	AAA***GCTCTTCT***AGCGCACACAAGTGGTTCTTCACTACA
TyDC N318S SapI mutagenesis reverse	AAA***GCTCTTCT***GCTTAGACTAAATGAATCTGCATCTTCC
TyDC A319P SapI mutagenesis forward	AAA***GCTCTTCT***CCGCACAAGTGGTTCTTCACTACATTG
TyDC A319P SapI mutagenesis reverse	AAA***GCTCTTCT***CGGATTTAGACTAAATGAATCTGCATCT
TyDC S372G SapI mutagenesis forward	AAA***GCTCTTCT***GGCAGAAGATTCCGATCCATGAAAC
TyDC S372G SapI mutagenesis reverse	AAA***GCTCTTCT***GCCGAGAGCTATTTGCCAGTCTTTG
TDC Forward Cloning	ACTG***GAATGCT***ATGGGCAGCATTGATTCAAC
TDC Reverse Cloning	ACTG***CTCGAG***TCAAGCTTCTTTGAGCAAATC
TDC G370S SapI mutagenesis forward	AAA***GCTCTTCT***AGCCGAAAATTTCGGTCGC
TDC G370S SapI mutagenesis reverse	AAA***GCTCTTCT***GCT CGTTGCGATTTGCCA

TyDC represents the *P. somniferum* TyDC sequence while TDC represents the *C. roseus* sequence. The bold and italic font represents the restriction sites

Table 4.1. Cloning and mutagenesis primers for *P. somniferum* TyDC wild type, *P. somniferum* TyDC S372G, C. *roseus* wild type and *C. roseus* G370S

The resulting PCR products were ligated together into IMPACT-CN bacterial expression plasmids. DNA sequencing was utilized to verify the sequence and frame of each mutant cDNA insert. Transformed bacterial colonies, expressing the wild type and mutant proteins, were selected and used for large-scale expression of individual recombinant proteins. Bacterial cells were cultured at 37 ^{o}C. After induction with 0.15 mM IPTG, the cells were cultured at 15 ^{o}C for 24 hrs. The soluble fusion proteins were applied to a column packed with chitin beads and subsequently hydrolyzed under reducing conditions. The affinity purification resulted in the isolation of each individual recombinant protein at about 85% purity. Further purifications of the recombinant proteins were achieved by Mono-Q and gel filtration chromatographies. Purified recombinant enzymes were concentrated to approximately 10 mg/ml protein in 25 mM HEPES (pH 7), containing 0.04 mM PLP using a Centricon YM-50 concentrator (Millipore). Purity of the recombinant proteins was evaluated by SDS-PAGE. The concentrations of the purified recombinant proteins were determined by a Bio-Rad protein assay kit (Hercules, CA) using bovine serum albumin as a standard.

Homology modeling and ligand superimposition

Modeller [18] was utilized to produce ten *P. somniferum* TyDC and *C. roseus* TDC homology models for the substrate analog bound protein data bank models 1JS3 [19]. The model from each PDB template with the optimal molpdf and DOPE score were selected for further evaluation. Mutant homology models were generated in the same manor from the optimal wild type models. Pymol was utilized to align the PLP coenzyme and the appropriate substrate analog from 1JS3 [19] onto the corresponding homology models and to visualize the active site residues. The residues proximal to the ligand from the homology models were then compared with their homologous residues from characterized TyDC and TDC enzymes to identify potential substrate specifying residues.

Kinetic analysis

The specific activity of the wild type *P. somniferum* TyDC towards tyrosine and dopa was analyzed in 50 μl phosphate buffer (pH 7.5) containing 2 mM substrate with 2 μg of enzyme for an incubation time of 2.5 minutes. This analysis determined that the wild type enzyme possessed typical TyDC activity. The S372G mutant displayed both typical TyDC activity and novel decarboxylation activity towards 5-HTP. The kinetic parameters of the *P. somniferum* TyDC wild type, *P. somniferum* S372G mutant, *C. roseus* TDC wild type and *C. roseus* TDC G370S mutant enzymes were subsequently analyzed. Reaction mixtures of 50 μl containing recombinant protein (25 μg for *P. somniferum* TyDC 5-hydroxytryptophan assay, 3 μg for the *P. somniferum* TyDC dopa assay, 25 μg for C. *roseus* TDC dopa assay and 3 μg for the *C. roseus* TDC tryptophan assay) and varying concentration of substrate (0.05 – 20 mM of 5-hydroxytryptophan, 0.005 – 5 mM of tryptophan and 0.05 – 15 mM of dopa) were prepared in 50 mM phosphate

buffer (pH 7.5) and incubated at 25^{o} C. An equal volume of 0.8 M formic acid was added to each reaction mixture (15 min for *P. somniferum* TyDC 5-hydroxytryptophan assays, 2.5 min for *P. somniferum* dopa assays, 15 min for *C. roseus* TDC dopa assays and 2.5 min for *C. roseus* tryptophan assays) and supernatant was injected for HPLC-electrochemical analysis. Kinetic data points were performed in triplicate and kinetic values were evaluated by hyperbolic regression. An isocratic running buffer consisting of 50 mM phosphate buffer pH 4.3, 25% acetonitrile, and 0.5 mM octyl sulfate was used for the 5-hydroxytryptophan characterization, whereas an isocratic running buffer consisting of 50 mM phosphate buffer pH 4.3, 15% acetonitrile, and 0.5 mM octyl sulfate was used for the dopa characterization. The amounts of products in reaction mixtures containing different concentrations of substrate were quantified based on a standard curve generated using authentic standards at identical conditions of HPLC-electrochemical analysis.

4.5 Results

Primary sequence investigation of recombinantly characterized TyDC and TDC sequences

To begin our investigation of residues that might impact substrate specificity of plant AAAD enzymes, we performed a primary sequence evaluation of essentially all the characterized plant TyDC and TDC sequences. The analyzed sequences included *Cyanea acuminata* TDC [5], *Capsicum annuum* TDC 1 [8], *C. annuum* TDC 2 [8], *Ophiorrhiza pumila* TDC [6], *Oryza sativa* TDC 1 [7], *O. sativa* TDC 2 [7], *C. roseus* TDC [3-4], *P. somniferum* TYDC 9 [12], *P. somniferum* TyDC 7 [12], *Thalictrum flavum* TyDC [11], and *Arabidopsis thaliana* TyDC [10]. The *Petroselinum crispum* [20], *Solanum lycopersicum* AAAD 1A [21], *S. lycopersicum* AAAD 1B [21]*S. lycopersicum* AAAD 2 [21], *P. somniferum* TyDC 1 [9] and *P. somniferum* TyDC 2

[9] sequences were intentionally excluded. *P. crispum* TyDC was excluded because our recent publication demonstrated the mischaracterization of this enzyme [11]. The *S. lycopersicum* AAAD genes were not included due to their atypical sequences. Plant AAAD enzymes typically retain approximately 40% identity to one another where as these *S. lycopersicum* enzymes only demonstrate approximately 11% identity to canonical plant AAADs [21]. The *P. somniferum* TyDC 1 and TyDC 2 genes were excluded due to their extensive identity (greater than 95%) towards the evaluated *P. somniferum* TyDC 7 and TyDC 9 sequences [9]. Pairwise alignments of these characterized plant AAAD enzymes indicate that inter TDC-TyDC class identities are often greater than intra TDC or TyDC class identities. In other words, individual members of the TDC group sometimes share greater identity with enzymes from the TyDC group than they do with other TDC enzymes. For example, despite differences in substrate specificity, the *C. annuum* TDC 2 [8] shares greater homology with the *A. thaliana* TyDC [10] (66% identity) than it does with the *C. acuminata* TDC [5] (56% identity). The sequence ambiguity of plant AAADs can be further illustrated in a dendrogram of characterized TyDC and TDC sequences (Fig 4.1).

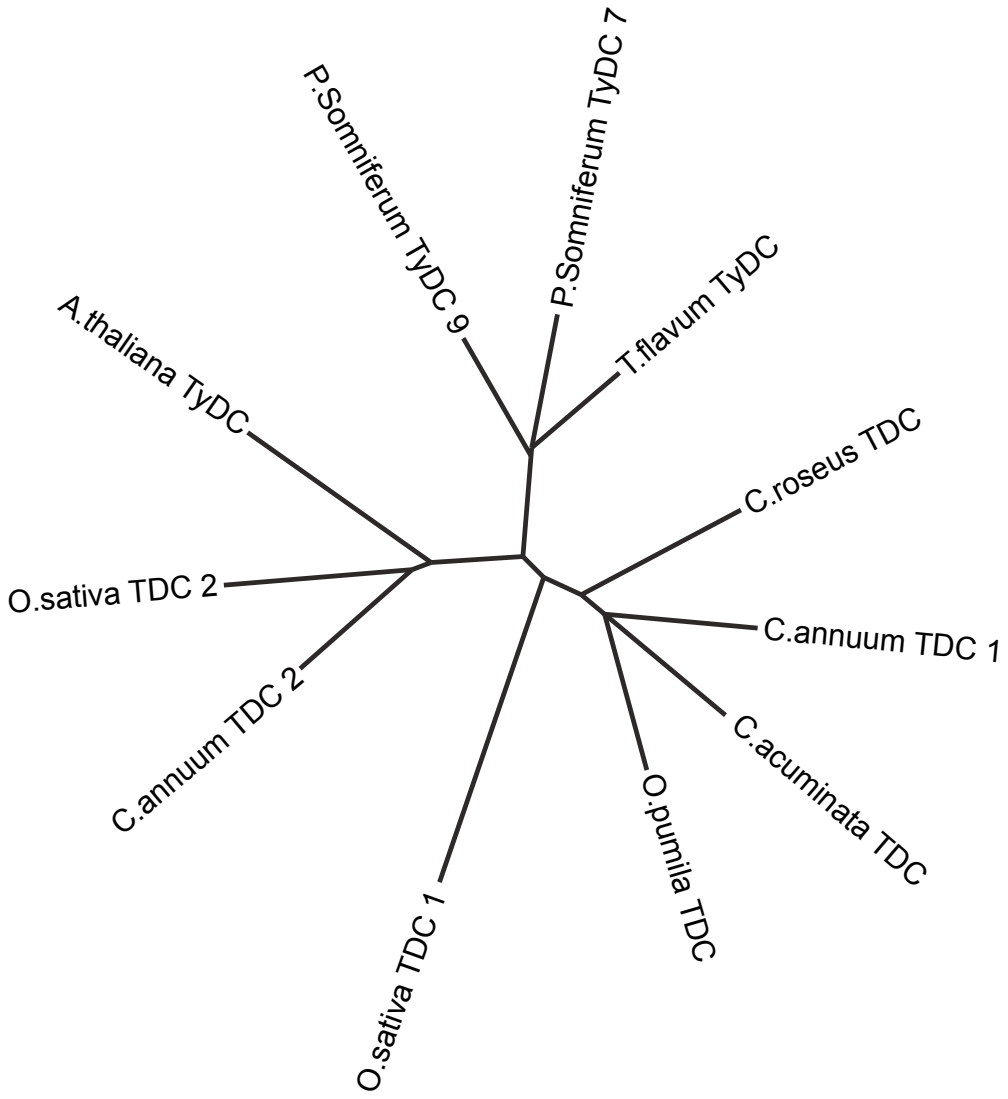

Figure 4.1. Dendrogram of recombinantly characterized plant TyDC and TDC sequences.

As this figure illustrates, TyDC and TDC sequences did not appear to exclusively cluster according to their substrate preference. Despite maintaining identical substrate profiles, the characterized TDC sequences appeared to cluster into two groups. Interestingly, TDC sequences from both *O. sativa* and *C. annuum* appear in both clusters. This suggests that this clustering is not due to evolutionary divergence of plant species but rather the evolutionary divergence of individual AAAD sequences. In addition to the delocalization of TDC sequences, there appears to be inconsistencies in the phylogeny of characterized TyDCs. Although three of the four TyDC

sequence clustered together, the fourth TyDC sequence appeared to cluster with one group of TDC enzymes. The sequence and phylogenetic ambiguity of TyDC and TDC enzymes produces significant challenges in plant AAAD gene annotation.

Multiple sequence alignments of these characterized TyDC and TDC sequences were used to identify putative substrate specifying residues. Twenty-two residues that are conserved between substrate specificities, for 8 or more of the 11 characterized TDC and TyDC sequences, were highlighted in the *P. somniferum* TyDC 9 sequence (subsequently referred to as *P. somniferum* TyDC) [12] (Fig. 4.2).

```
1   MGSLPTNNLE SISLCSQNPL DPDEFRRQGH MIIDFLADYY KNVENYPVRS QVEPGYLKKR
61  LPESAPYNPE SIETILEDVT NDIIPGLTHW QSPNYFAYFP SSGSIAGFLG EMLSTGFNVV
121 GFNWMSSPAA TELESIVMNW LGQMLTLPKS FLFSSDGSSG GGGVLQGTTC EAILCTLTAA
181 RDKMLNKIGR ENINKLVVYA SNQTHCALQK AAQIAGINPK NVRAIKTSKA TNFGLSPNSL
241 QSAILADIES GLVPLFLCAT VGTTSSTAVD PIGPLCAVAK LYGIWVHIDA AYAGSACICP
301 EFRHFIDGVE DADSFSLNAH KWFFTTLDCC CLWVKDSDSL VKALSTSAEY LKNKATESKQ
361 VIDYKDWQIA LSRRFRSMKL WLVLRSYGVA NLRTFLRSHV KMAKHFQGLM GMDNRFEIVV
421 PRTFAMVCFR LKPAAIFKQK IVDNDYIEDQ TNEVNAKLLE SVNASGKIYM THAVVGGVYM
481 IRFAVGATLT EERHVTGAWK VVQEHTDAIL GA
```

Figure 4.2. Putative substrate specifying residues form *P. Somniferum* TyDC 9. Green residues are mostly conserved (residues are conserved between substrate specificities for 8 or more of the 11 characterized TDC and TyDC sequences). Red residues are within 4 angstroms of the carbidopa external aldimine form the TyDC 9 homology model. Yellow residues are amino acids that appear as both green and red residues. Residues in bold and italic indicate amino acids within 4 angstroms of the carbidopa external aldimine from the beta chain of the homodimer.

Next, we modeled our previously characterized *P. somniferum* TyDC (using the crystal structures 1JS3 as a template [19]) and superimposed the carbidopa external aldimine (from 1JS3) into the active site of our model. Residues within four angstroms of the carbidopa external aldimine were highlighted to produce an additional 18 residues potentially involved in substrate recognition (Fig. 4.2). Cross-referencing these active site proximal residues with the partially conserved TyDC/TDC residues (identified through multiple sequences alignments) reduced the hypothetical substrate specifying residues down to 5 amino acids (Fig. 4.2). These residues are

represented as serine 101, cysteine 170, asparagine 318, alanine 319 and serine 372 within the *P. somniferum* TyDC sequence.

2.2 Generation and investigation of putative substrate specifying P. somniferum TyDC mutants

Before evaluating the substrate specifying roles of our select five residues, *P. somniferum* TyDC was first evaluated to determine the substrate range of the wild type enzyme. The wild type enzyme was expressed and purified to homogeneity. Activity assay results showed that the wild type enzyme efficiently catalyzed the decarboxylation of dopa and tyrosine (at 2 mM substrate concentration, the enzyme showed 5910 ± 200 nmol/min/mg protein to dopa and 5350 ± 200 nmol/min/mg protein to tyrosine), but displayed no activity towards phenylalanine or indolic substrates, including 5-hydroxytryptophan and tryptophan. Next, using the *P. somniferum* TyDC as a model, site directed mutations of S101A, C170A, N318S, A319P and S372G were made based on conserved active site proximal residues.

To test perturbations in substrate specificity, the *P. somniferum* TyDC S101A, C170S, N318S, A319P, and S372G mutant enzymes were cloned, expressed, and purified to homogeneity. Next, the activities of the mutant enzymes were tested using dopa, tyrosine, phenylalanine, tryptophan and 5-hydroxytryptophan. Results indicated that the S101A, C170S, N318S and A319P mutants had no obvious alterations in indolic or phenolic substrate specificity. However, the S372G mutant displayed a broader substrate profile. The S372G mutant retained activity towards dopa and tyrosine, had no measurable activity towards tryptophan (Fig 4.3 A-D), but displayed activity towards 5-hydroxytryptophan (Fig 4.4 A-D).

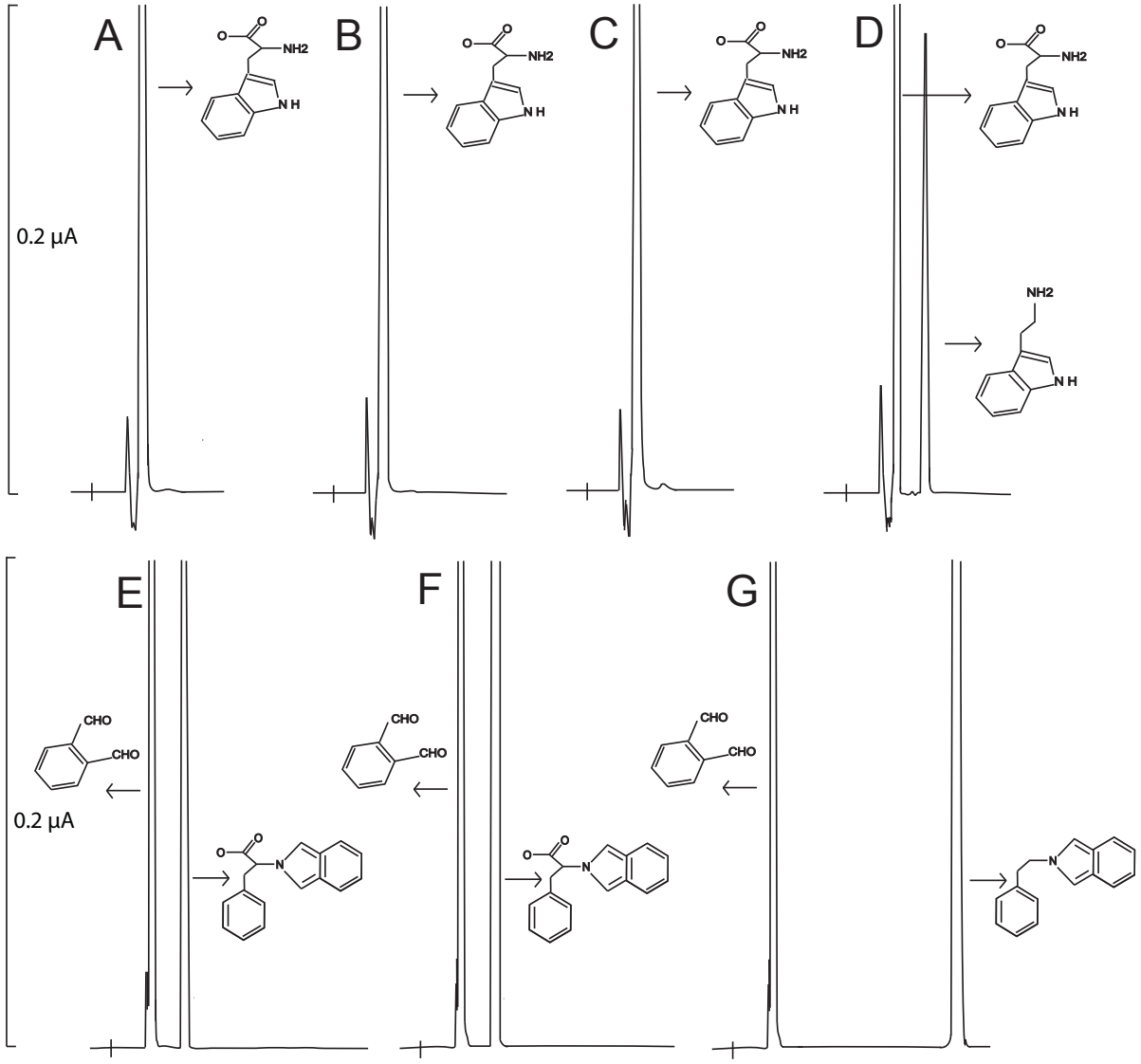

Figure 4.3. The lack of activity of *P. somniferum* TyDC S372G towards tryptophan and the lack of activity of *C. roseus* TDC G370S towards phenylalanine. The Y-axis represents the output in microamps, the x-axis represents retention time. Reaction mixtures of 50 µl containing 5 mM substrate and 20 µg of recombinant enzyme were prepared in 50 mM phosphate buffer (pH, 7.5). The reaction mixtures were incubated at 25 ^{o}C and the reaction was stopped by adding 12.5 µl of 3.2 M of formic acid. The mixtures were centrifuged for 5 min at 14,000g to obtain supernatants that were then injected for HPLC-EC analysis. Reactions corresponding to chromatographs (E-G) were incubated with o-phthalaldehyde reagent prior to injection to generate electrochemically active compounds. Chromatograms (A-C) illustrate lack of product formed from *P. somniferum* TyDC S372G and tryptophan after 5, 10 and 20 minutes of incubation. Chromatogram (D) illustrates the tryptamine product formed from the *C. roseus* wild type enzyme and tryptophan after 10 minutes of incubation. Chromatograms (E-F) illustrate lack of product formed from *P. somniferum* TyDC S372G and phenylalanine after 5 and 20 minutes of incubation. Chromatogram (G) shows the peak generated from the injection of 150 picomoles of phenylethylamine standard.

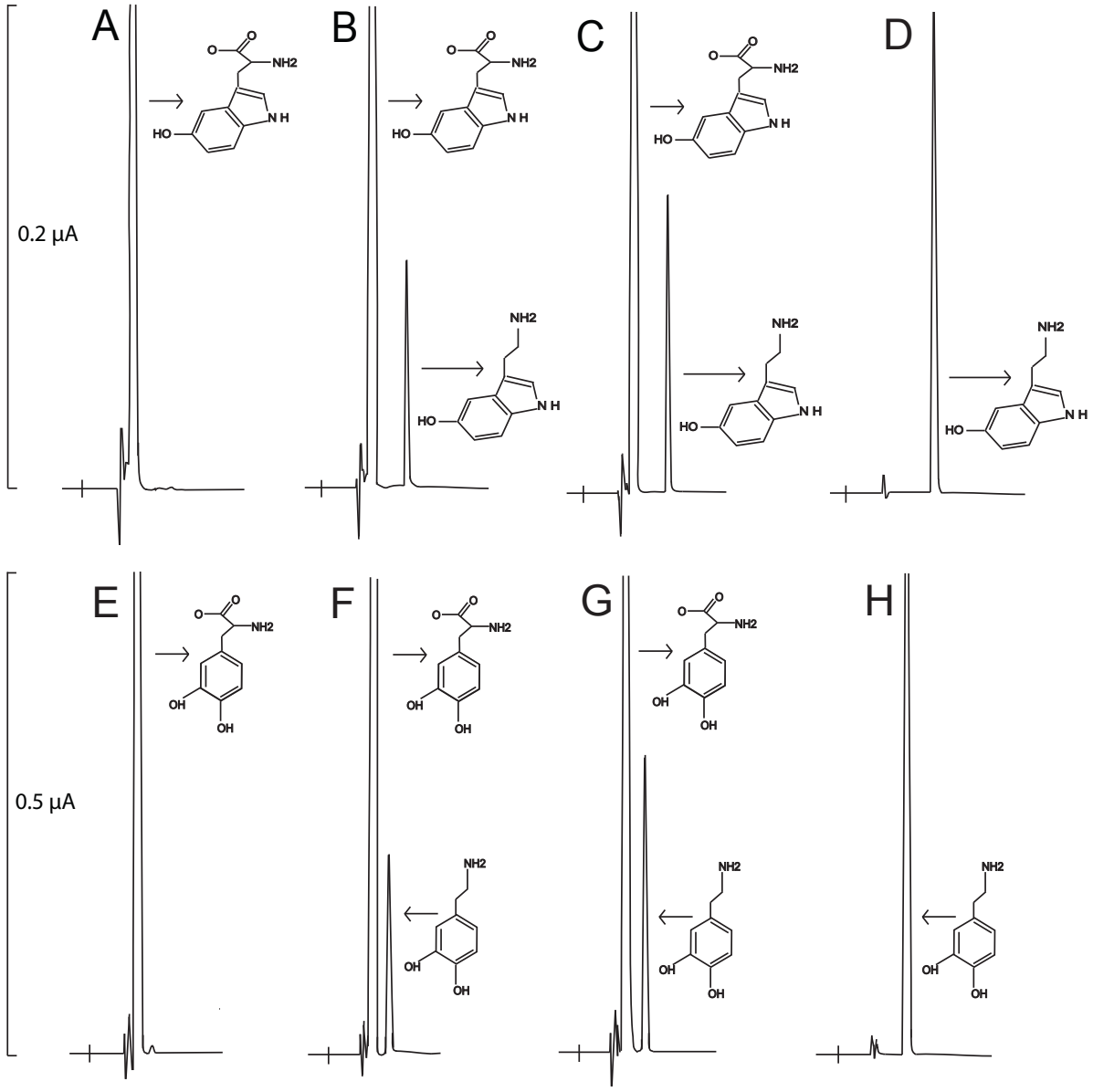

Figure 4.4. HPLC-EC detection of novel chemistry generated from *P. somniferum* TYDC S372G and *C. roseus* TDC G370S mutants. The Y-axis represents the output in microamps, and the x-axis represents retention time. Chromatogram (A) illustrates lack of product formed from *P. somniferum* TyDC wild type and 5-hydroxytryptophan after 20 minutes of incubation. Chromatogram (B) illustrates the formation of 5-hydroxytryptamine generated from 5-hydroxytryptophan and the *P. somniferum* TyDC S372G mutant after 10 minutes of incubation. Chromatogram (C) illustrates the formation of 5-hydroxytryptamine generated from 5-hydroxytryptophan and the *P. somniferum* TyDC S372G after 20 minutes of incubation. Chromatogram (D) shows the peak generated from the injection of 150 picomoles of 5-hydroxytryptamine standard. Chromatogram (E) illustrates the lack of product formed from the *C. roseus* TDC wild type and the dopa reaction mixture after 20 minutes of incubation. Chromatogram (F) illustrates the formation of dopamine generated from incubating dopa and the *C. roseus* TDC G370S mutant for 10 minutes. Chromatogram (G) illustrates the formation of

dopamine generated from dopa and the *C. roseus* TDC G370S mutant after 20 minutes of incubation. Chromatogram (H) shows the peak generated from the injection of 150 picomoles of dopamine standard.

Initial biochemical testing suggests that the *P. somniferum* TyDC serine 372 residue might play a role in differentiating phenolic substrates from indolic substrates. Next, a full kinetic characterization of the S372G and wild type *P. somniferum* TyDC enzymes were performed using dopa and 5-hydroxytryptophan. The calculated kinetic parameters indicated that the mutation reduced the enzymes ability to catalyze the decarboxylation of dopa while granting a newfound ability to decarboxylate 5-hydroxytryptophan (Table 4.2).

Table 4.2. Kinetic parameters of *Papaver somniferum* wild type and mutant TyDC9 enzymes.

Substrate	Enzyme	V_{max} (nmols/min/mgprotein)	kcat (sec)	K_m (mM)
Dopa	PsTyDC (WT)	8520 ± 490	8.02 ± 0.46	0.75 ± 0.10
Dopa	PsTyDC (S372G)	1560 ± 320	1.47 ± 0.30	2.10 ± 0.20
5-Hydroxytryptophan	PsTyDC (WT)	ND	ND	ND
5-Hydroxytryptophan	PsTyDC (S372G)	275 ± 30	0.26 ± 0.03	3.95 ± 0.45
Tryptophan	CrTDC (WT)	2710 ± 110	2.54 ± 0.10	0.12 ± 0.02
Tryptophan	CrTDC (G370S)	1464 ± 120	1.37 ± 0.11	0.21 ± 0.05
Dopa	CrTDC (WT)	ND	ND	ND
Dopa	CrTDC (G370S)	390 ± 15	0.37 ± 0.04	3.40 ± 0.21

Values represent means SE (n=3)
ND, not determined.

No kinetic data was obtainable for the wild type enzyme and 5-hydroxytryptophan due to the lack of measurable product formation. Comparative sequence analysis of residues homologous to the *P. somniferum* TyDC 372 residue revealed that serine was stringently conserved in all experimentally verified TyDC enzymes while glycine was conserved in all experimentally verified TDC enzymes (Fig 4.5).

Enzyme	Organism	Accession	372 Residue
TDC	C. acuminata	AAB39709	QVGTGRRFK
TDC1	C. annuum	ACN62127	QIGTGRKFK
TDC	O. pumila	BAC41515	QIGTGRRFK
TDC	C. roseus	P17770	QIATGRKFR
TDC1	O. sativa	AK069031	QVGVGRRFR
TDC2	C. annuum	ACN62126	QVPLGRRFR
TDC2	O. sativa	AK103253	QIPLGRRFR
TyDC	A. thaliana	NP_001078461	QISLSRRFR
TyDC7	P. somniferum	AAC61843	QIALSRRFR
TyDC	T. flavum	AAG60665	QIALSRRFR
TyDC9	P. somniferum	AAC61842	QIALSRRFR

Figure 4.5. Sequence alignment of a key residue within the characterized TDC and TyDC sequences. Within the TDC sequences, the residue homologous to the TYDC serine 372 is highlighted in red. Within the TyDC sequences, the residue homologous to the TYDC serine 372 is highlighted in yellow.

Generation and investigation of the 370 mutants with in a C. roseus TDC

Results from the aforementioned mutation analysis indicated that the 372 residue impacts the substrate specificity of the *P. somniferum* TyDC enzyme. To investigate this residues role in substrate selectivity of TDCs, a *C. roseus* TDC G370S mutant was expressed, purified, and evaluated for alterations in substrate specificity. This TDC, like other verified TDC, contains the conserved glycine 370 (equivalent to serine 372 of the *P. somniferum* TyDC) (Fig 4.5). An electrochemical HPLC assay determined that, unlike the wild type enzyme, the *C. roseus* TDC G370S mutant was able to catalyze the decarboxylation of dopa (Fig 4.4 E-H) and tyrosine (Fig 4.6 A-D).

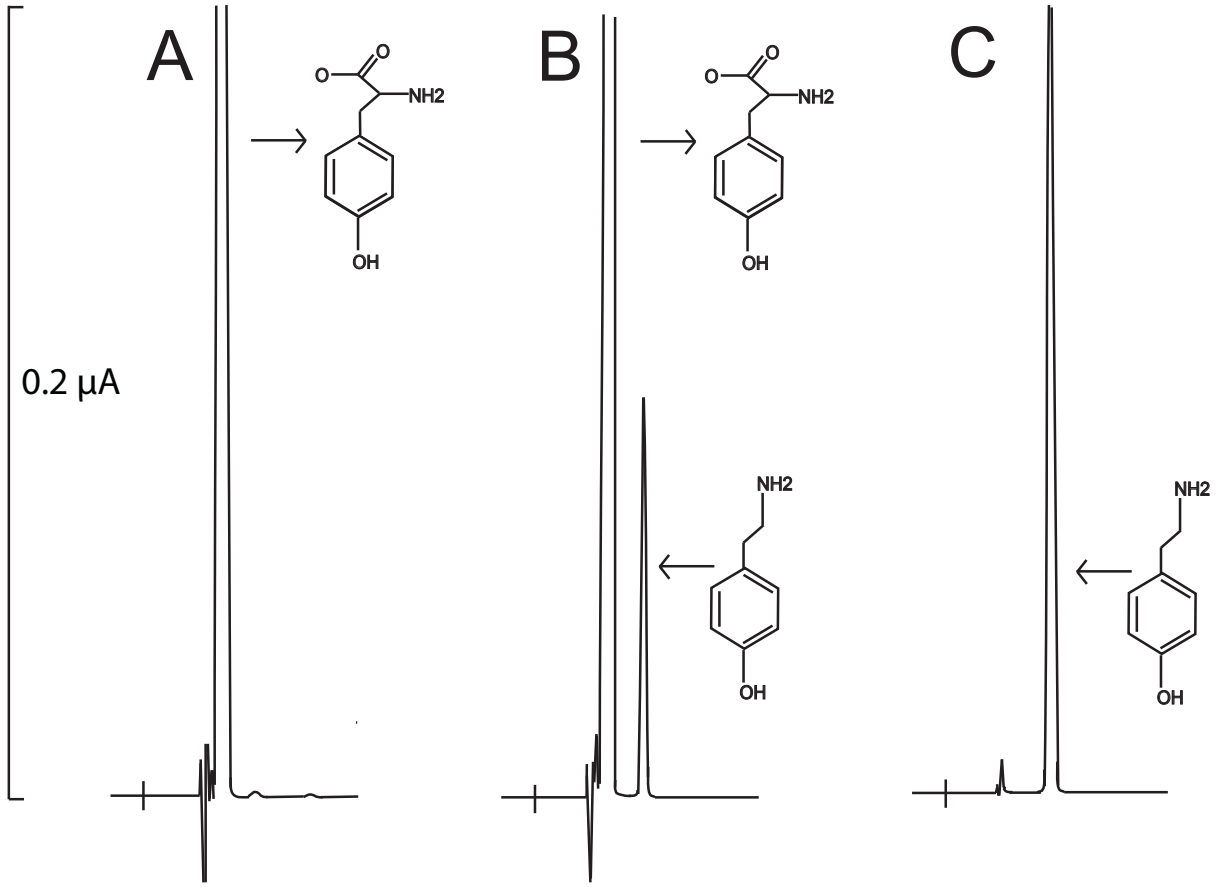

Figure 4.6. HPLC-EC detection of novel chemistry generated from the *C. roseus* TDC G370S mutant. The Y-axis represents the output in microamps, and the x-axis represents retention time. Chromatogram (A) illustrates lack of product formed from *C. roseus* TDC wild type and tyrosine after 10 minutes of incubation. Chromatogram (B) illustrates the formation of tyramine generated from tyrosine and the *C. roseus* TDC G370S mutant after 10 minutes of incubation. Chromatogram (C) shows the peak generated from the injection of 150 picomoles of tyramine standard.

The *C. roseus* TDC G370S enzyme displayed no activity towards phenylalanine (Fig 4.3 E-G). Full kinetic characterization of the G370S and wild type *C. roseus* TDCs showed significant alterations in the enzyme's substrate profile. Comparison of the kinetic values between the wild type TDC and the mutant TDC illustrates that the glycine 370 serine substitution reduces the binding efficiency and the rate of the enzyme towards tryptophan while enabling the enzyme to utilize dopa as a substrate (Table 4.2).

Molecular modeling of the substrate-impacting residue

Homology models of *P. somniferum* TyDC wild type, *P. somniferum* TyDC S372G, *C. roseus* TDC wild type and *C. roseus* TDC G370S were generated and analyzed in an effort to investigate the structure-function relationship of the specificity-impacting residue. To reveal the possible interactions of the enzyme with its substrates, the carbidopa external aldimine (from 1JS3) was superimposed into the active site of our models. Model analysis suggests the likely involvement of the serine 372 (TyDC sequence) and glycine 370 (TDC sequence) in substrate recognition. In the ligand bound models, this residue appeared to be located in the back of the active site approximately three to five angstroms away from the 3 prime hydroxyl of the carbidopa external aldimine (Fig 4.7).

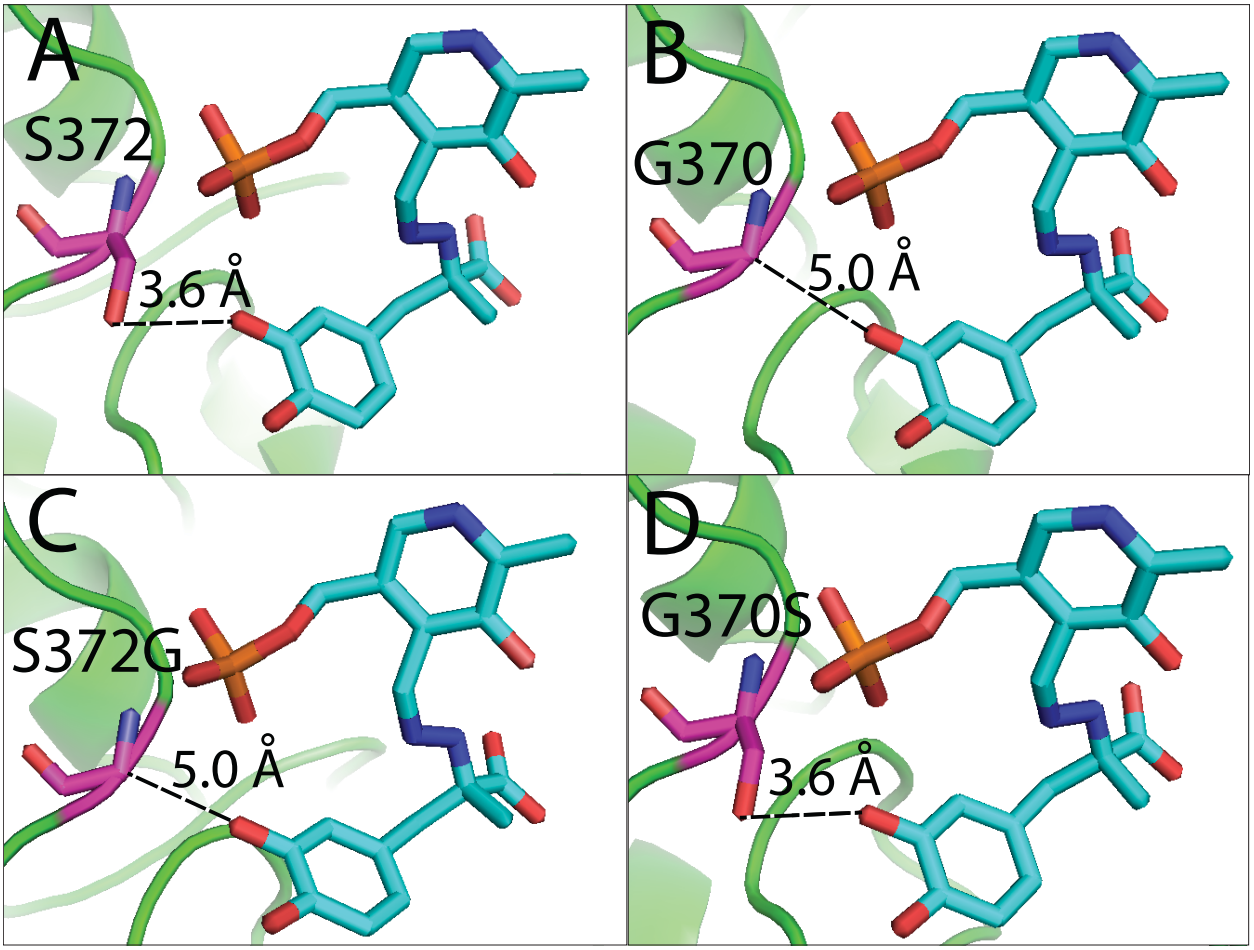

Figure 4.7. Active site analysis of the *P. somniferum* TyDC wild type, the *P. somniferum* TyDC S372G, the *C. roseus* TDC wild type and the *C. roseus* TDC G370S mutant. Ligands and models were generated using the PDB model 1JS3. The blue structure represents the external aldimine of carbidopa and PLP. The magenta residue represents the substrate impacting amino acid. Model

(A) illustrates the distance between the ligand and *P. somniferum* TyDC wild type 372 residue. Model (B) illustrates the distance between the ligand and *C. roseus* TDC wild type 370 residue. Model (C) illustrates the distance between the ligand and *P. somniferum* TyDC mutant residue 372. Model (D) illustrates the distance between the ligand and *C. roseus* TDC mutant residue 370.

Comparison of the wild type and mutant models indicated that the mutations altered the size of the active site pocket by approximately one and a half angstroms. For example, within the *P. somniferum* TyDC model, the serine 372 glycine mutation increases the distance between the 3 prime hydroxyl group of the carbidopa ligand and the 372 residue from 3.6 Å to 5.0 Å. Conversely, the reverse mutation in the *C. roseus* TDC enzyme, decreases the distance from 5.0 Å to 3.6 Å. The theoretical alterations in active site volume might enable the accommodation of specific sizes of substrates. The structurally larger serine residues may reduce the active site pocket to accommodate phenolic substrates while the structurally smaller glycine may increase the size of the active site to accommodate larger indolic compounds. Biochemical characterization of the substrate-impacting residue, in coordination with ligand bound homology model analyses, helps illuminate the functional roles of these active site residues.

4.6 Discussion

Our previous work illustrated the primary sequence differentiation of decarboxylation-oxidative deamination catalyzing aromatic acetaldehyde synthases (AAS) enzymes from the decarboxylation catalyzing aromatic amino acid decarboxylase enzymes [12]. The resulting research provides a tangible basis to suggest that specific active site residues can be used to differentiate homologous plant type II PLP decarboxylases. TDC and TyDC play different physiological functions; therefore being able to distinguish their substrate selectivity without lab-intensive experimental verification is highly useful. In this study, attempts were made to identify key residues capable for differentiating the phenolic selective tyrosine decarboxylases from indolic selective tryptophan decarboxylases. Extensive comparative analyses of characterized

TyDC and TDC sequences enabled us to select several potential target residues. Site-directed mutagenesis of these residues with in two model enzymes provided evidence to suggest that the *P. somniferum* TyDC 372 residue and the *C. roseus* TDC 370 residue collectively impact substrate selectivity. The newly found activity of the *P. somniferum* S372G TyDC towards 5-hydroxytryptophan and the *C. roseus* G370S TDC towards dopa appears to be significant. The kinetic values of these mutant enzymes and their new substrates are comparable to some characterized AAAD enzymes. For example, the V_{max} of the two mutant enzymes towards their new substrates are larger than the V_{max} of *C. annuum* TDC 1 and *C. annuum* TDC 2 [8] towards tryptophan. Moreover, the substrate specificity of the mutants towards their new substrates is comparable to those of an investigated orphan TDC enzyme (K_m 3.0 mM towards tryptophan) [22]. Although both mutations enabled expanded substrate profiles, the substitutions did not lead to the loss of their original activities. However, it is reasonable to suggest that this active site residue is a key amino acid responsible for impacting substrate specificity. This hypothesis is supported by the glycine conservation in verified TDCs and the serine conservation in verified TyDCs (Fig. 4.5).

Subsequent analysis of the active site conformation of the *C. roseus* TDC and *P. somniferum* TyDC ligand bound homology models provides some structural basis for alterations in substrate profiles. We propose that the mutation of the *P. somniferum* 372 residue, from serine to glycine, enables broader substrate selectivity by increasing the active site cavity to accommodate structurally large substrates like 5-hydroxytryptophan while the *C. roseus* G370S mutation reduces the size of the active site to accommodate the structurally smaller dopa. Molecular interaction measurements support this hypothesis. The two mutants illustrate an alteration of active site pocket by 1.4 angstroms. The altered volume of the active site could enable structurally different compounds to enter the active site and form the external aldimine with the

PLP cofactor.

A brief database evaluation of this AAAD dictating 372 residue has been performed in an effort to annotate none characterized plant AAAD sequences using the results from this study. An analysis of the NCBI plants (taxid: 3193) database enables us to tentatively identify several sequences annotated as TyDCs that are likely TDC enzymes. For example, based on the conservation of the homologous G372 residue (implicating indolic substrate specificity) and the presence of the homologous Y350 residue (implicating decarboxylation activity and not aldehyde synthase activity) [12], we speculate that the annotated *Fragaria vesca* TyDC, *Medicago truncatula* TyDC, *Setaria italica* TyDC and *Theobroma cacao* TyDC sequences are all likely TDC enzymes. Such primary sequence annotation illustrates the practicality of substrate specificity and activity differentiation within plant type II PLP decarboxylases. Our study is one step forwards toward better classification of plant TyDC and TDC.

The functional evolution of AAAD enzymes within different branches of the phylogenetic tree reflects the physiological needs of different species. In plants, AAADs are an integral part of the pathways for the biosynthesis of numerous chemical compounds responsible for mitigating interactions with their biotic and abiotic environments (many of these compounds represent novel therapeutic functions) [13-16, 23-24]. For example, *P. somniferum* contains approximately 15 TyDC sequences that play roles in the production of benzylisoquinoline alkaloids such as the pharmacologically active morphine, codeine and papaverine [9 13]. However, despite variable functions plant TyDC and TDC do not have easily recognizable motifs in primary sequences. Although it is sometimes possible to classify the substrate specificity of a given AAAD through extensive sequence comparison, this means of plant AAAD differentiation remain quite speculative. Our finding regarding the S372G and G370S mutants indicates that the phenolic and

indolic substrate selectively in plant AAADs could be primarily dictated by this single active site amino acid. The stringent conservation for serine and glycine in verified plant TyDC and TDC, respectively, support this consideration (Fig 4.5). Future research is needed to fully reveal the active site conformations and residues invariably conserved amongst distinct plant AAAD classes. Upon completion, AAAD fingerprints should enable the proper annotation of AAAD and AAS genes without expensive and laborious enzyme expression and characterization.

4.7 Sequence data

All of the following accession numbers are from the NCBI Genbank

C. acuminata TDC [AAB39709], *C. annuum* TDC 1 [ACN62127], *C. annuum* TDC 2 [ACN62126], *O. pumila* TDC [BAC41515], *O. sativa* TDC 1 [AK069031], *O. sativa* TDC 2 [AK103253], *C. roseus* TDC [P17770], *P. somniferum* TYDC 9 [AAC61842], *P. somniferum* TyDC 7 [AAC61843], *T. flavum* TyDC [AAG60665], and *A. thaliana* TyDC [NP_001078461], *P. crispum* TyDC [Q06086], *S. lycopersicum* AAAD 1A [NP_001233845], *S. lycopersicum* AAAD 1B [NP_001233852], *S. lycopersicum* AAAD 2 [NP_001233859], *P. somniferum* TyDC 1 [P54768], *P. somniferum* TyDC 2 [P54769], *Fragaria vesca* TyDC [XP_004292248], *Medicago truncatula* TyDC [XP_003625397], *Setaria italica* TyDC [XP_004956078] and *Theobroma cacao* TyDC [EOX99271].

4.8 Acknowledgements

This study was supported through Virginia Tech Biochemistry college of Agricultural and Life Sciences funding.

References

[1] Srinivasan, K. and Awapara, J. (1978) Substrate specificity and other properties of DOPA decarboxylases from guinea pig kidneys. BBA enzymology. 526: 597-604

[2] Zhu M-Y. and Juorio A.V. (1995) Aromatic L-amino acid decarboxylase: Biological characterization and functional role. General Pharmacology: The vascular system 26: 681-696

[3] Noé, W., Mollenschott, C. and Berlin, J. (1984) Tryptophan decarboxylase from Catharanthus roseus cell suspension cultures: purification, molecular and kinetic data of the homogenous protein. Plant Molecular Biology 3: (5) 281-288

[4] De Luca, V., Marineau, C. and Brisson, N. (1988) Molecular cloning and analysis of cDNA encoding a plant tryptophan decarboxylase: Comparison with animal dopa decarboxylase PNAS 86 (8), 2582-2586

[5] Lopez-Meyer, M. and Nessler, C.L. (1997) Tryptophan decarboxylase is encoded by two autonomously regulated genes in Camptotheca acuminata which are differentially expressed during development and stress. The plant journal. 11: 1167-1175

[6] Yamazaki, Y., Sudo, H., Yamazaki, M., Aimi, N., and Saito, K. (2003) Camptothecin Biosynthetic genes in hairy roots of ophiorrhiza pumila: cloning, characterization and differential expression in tissues and by stress compounds. Plant Cell Physiol. 44: 395-403

[7] Kang, S., Kang, K., Lee, K. and Back, K. (2007) Characterization of rice tryptophan decarboxylases and their direct involvement in serotonin biosynthesis in transgenic rice. Planta 227: 263-272

[8] Park, S., Kang, K., Lee, K., Choi, D., Kim, Y. and Back, K. (2009) Induction of serotonin biosynthesis is uncoupled from the coordinated induction of tryptophan biosynthesis in pepper fruits (Capsicum annuum) upon pathogen infection. Planta. 230: 1197-1206

[9] Facchini, P.J. and De Luca, V. (1995) Expression in Echerichia coli and partial characterization of two tyrosine/dopa decarboxylases from opium poppy. Phytochemistry 38: 1119-1126

[10] Lehmann, T. and Pollmann, T. (2009) Gene expression and characterization of a stress-induced tyrosine decarboxylase from Arabidopsis thaliana. FEBS Letters. 583: 1895–1900

[11] Torrens-Spence MP, Gillaspy G, Zhao B, Harich K, White RH, and Li J. (2012) Biochemical evaluation of a parsley tyrosine decarboxylase results in a novel 4-hydroxyphenylacetaldehyde synthase enzyme. Biochem Biophys Res Commun. 2: 211-216

[12] Torrens-Spence, M.P., Liu, P., Ding, H., Harich, K., Gillaspy, G. and Li, J. (2013) Biochemical evaluation of the decarboxylation and decarboxylation-deamination activities of plant aromatic amino acid decarboxylases. J Biol Chem. 288: 2376-2387

[13] Facchini, P. J., Huber-Allanach, K. L. and Tari, L. W. (2000) Plant aromatic L-amino acid decarboxylases: evolution, biochemistry, regulation, and metabolic engineering applications. Phytochemistry 54: 121-138.

[14] Meijer, A.H., Verpoorte, R. and Hoge, J.H.C. (1993) Regulation of enzymes and genes involved in terpenoid indole alkaloid biosynthesis in Catharanthus roseus. Journal of Plant Research. 3: 145-164.

[15] Berlin, J., Ruegenhagen, C., Kuzovkina, I.N., Fecker, L.F. and Sasse, F. (1994) Are tissue cultures of Peganum harmala a useful model system for studying how to manipulate the formation of secondary metabolites? Plant Cell Tissue and Organ Culture 38: 289-297.

[16] Leete, E. and Marion, L. (1953) The biogenesis of alkaloids: VI The formation of hordenine and N-methyltyramine from tyrosine in barley. Can J Chem. 31: 126–128.

[17] Marques, I.A., and Brodelius, P.E. (1988) Elicitor-induced L-tyrosine decarboxylase from plant cell suspension cultures. *Plant Physiol.* **88**, 46–51.

[18] Šali, A. and Blundell, T. L. (1993) Comparative protein modelling by satisfaction of spatial restraints. J. Mol. Biol. 234: 779-815

[19] Burkhard, P., Dominica, P,. Borri-Voltattorni, C., Jansonius, J.N. and Malashkevich, V.N. (2001) Structural insight into Parkinson's disease treatment from drug-inhibited DOPA decarboxylase. Nature structural biology 8: (11) 963-967

[20] Kawalleck, P., Keller, H., Hahlbrok, K., Scheelet, D. and Somssich, I.E. (1993) A pathogen-responsive gene of parsley encodes tyrosine decarboxylase, J. Biol. Chem. 268: (3) 2189–2194.

[21] Tieman, D., Taylor, M., Schauer, N., Fernie, A.R., Hanson, A.D. and Klee, H.J. (2006) Tomato aromatic amino acid decarboxylases participate in synthesis of the flavor volatiles 2-phenylethanol and 2-phenylacetaldehyde. PNAS. 103: 8287-92.

[22] Gibson, R.A., Barret, G. and Wightman, F. (1972) Biosynthesis and Metabolism of Indol-3yl-acetic Acid: III. Partial purification and properties of a tryptamine-forming L-tryptophan

[23] decarboxylase from tomato shoots. Journal of Experimental Botany: 23 (3) 775-789.

[24] Ellis, B.E. (1983) Production of hydroxyphenylethanol glycosides in suspension-cultures of Syringa vulgaris. Phytochemistry 22: 1941–1943.

[25] Trezzini, G.F., Horrichs, A. and Somssich, I.E. (1993) Isolation of putative defense-related genes from Arabidopsis thaliana and expression in fungal elicitor-treated cells. Plant Mol. Biol. 21: 385–389.

Chapter 5

Diverse functional evolution of type II pyridoxal 5'-phosphate decarboxylases: Detection of two novel acetaldehyde synthases that uses hydrophobic amino acids as substrates.

Submitted to BMC Plant Biology 05-22-14

Michael P. Torrens-Spence1 mpspence@vt.edu, Renee von Guggenberg1 reneev92@vt.edu, Michael Lazear1 lazear@vt.edu, Haizhen Ding1 dingh@vt.edu and Jianyong Li1 lij@vt.edu*

1 Department of Biochemistry, Virginia Tech, Blacksburg, Virginia, United States of America

*Corresponding Author

Author Contributions

Michael P. Torrens-Spence$_1$ wrote the article and performed all the research except for the experiments mentioned below.

Renee vonGuggenberg$_1$ assisted in the cloning, protein expression and protein purification.

Michael Lazear$_1$ assisted in the cloning, protein expression and protein purification.

Haizhen Ding$_1$ assisted in the molecular cloning and protein expression.

Jianyong Li$_1$ oversaw and directed the research and helped write the article.

$_1$ Department of Biochemistry, Virginia Tech, Blacksburg, Virginia, United States of America

5.1 Abstract

Type II pyridoxal 5'-phosphate decarboxylases are an important group of phylogenetically diverse enzymes involved in amino acid metabolism. Within plants, this group of enzymes is represented by aromatic amino acid decarboxylases, glutamate decarboxylases and serine decarboxylases. Additional evolutionary divergence of plant aromatic amino acid decarboxylases has resulted in further subcategories with distinct substrate specificities and enzymatic activities. Despite shared homology, no such evolutionary divergence has been characterized within GDCs or SDCs. Comparative analysis of two previously characterized SDC-like enzymes demonstrates distinct substrate specificities despite their highly conserved primary sequence. The alternate substrate preference of these homologous SDC-like proteins indicated that functional divergence might have occurred with in SDC-like proteins. In an effort to identify structural features responsible for the alterations in substrate specificity, two uncharacterized SDC-like enzymes were recombinantly expressed and characterized. An extensive biochemical analysis of two SDC-like recombinant proteins led to an interesting discovery; both proteins catalyze the formation of acetaldehyde derivatives from select hydrophobic amino acids substrates. Specifically, *Medicago truncatula* [GenBank: XP_003592128] and *Cicer arietinum* [GenBank: XP_004496485] catalyze the decarboxylation and oxidative deamination of phenylalanine, methionine, leucine and tryptophan to generate their corresponding acetaldehydes. The promiscuous aldehyde synthase activity of these proteins yields novel product formation in the synthesis of 4-(methylthio) butanal, 3-methylbutanal (isovaleraldehyde) and indole-3-acetaldehyde from methionine, leucine and tryptophan respectively. A comparative biochemical analysis of the *Medicago truncatula* and *Cicer arietinum* enzymes against two previously characterized SDC-like enzymes further emphasizes the unusual substrate specificity and activity

of these novel aldehyde synthases. This work further elaborates on the functional complexity of plant type II PLP decarboxylases and their roles in secondary metabolite biosynthesis.

5.2 Keywords

Type II PLP decarboxylases; aromatic amino acid decarboxylase; aromatic acetaldehyde syntheses; serine decarboxylases.

5.3 Introduction

Biochemical characterization of a serine decarboxylase (SDC) was first established in *Arabidopsis thaliana* (AtSDC) [1]. It was believed that the enzyme plays a major role in choline synthesis by producing ethanolamine, a major intermediate for choline production [2-3]. Ethanolamine is also a precursor of phosphatidylethanolamine (PE) and phosphatidylcholine (PC); both PE and PC are major phospholipids in eukaryotic membranes [4-6]. The importance of this SDC in *A. thaliana* development has been demonstrated through the investigation of the *AtSDC* deficient mutant. A T-DNA insertion in the single *A. thaliana* SDC gene showed developmental defects, including necrotic leaf lesions, multiple inflorescences and flower sterility [7].

The functional characterization of the *AtSDC* enzyme provided a protein model to predict similar functions of homologous proteins based on their sequence homology without extensive biochemical verification. Indeed, a GenBank search revealed a number of uncharacterized plant SDC-like sequences annotated as SDC proteins or SDC-like proteins. Additionally, it was noticed that many SDC-like proteins also were annotated as histidine decarboxylase (HDC)-like proteins. A literature search revealed that the HDC annotation in plants occurred from the cloning of a truncated tomato ortholog with high similarity towards bacterial HDC sequences [8]. However, a study of two plant HDC-like enzymes *demonstrated their strict decarboxylation activity to serine with no measurable activity towards histidine [1]*. Based upon the functional study of these enzymes, the authors suggest that all plant sequences annotated as HDC likely function as SDCs [1]. In our database search, we also found that some individual *Solanum lycopersicum* SDC-like sequences were annotated as aromatic amino acid decarboxylase (AAAD). Biochemical analysis of one of these SDC-like AAADs sequences (SlAAAD) demonstrated significant decarboxylation activity to tyrosine and phenylalanine [9]. Despite displaying aromatic amino acid decarboxylation activity, these tomato enzymes have limited

homology to other characterized plant AAADs (10-15% identity) [10-13]. Rather, these tomato AAADs share significantly increased homology to the characterized plant AtSDCs (57% identity) [1].

Due to the extensive sequence identity between the functionally different SlAAAD and AtSDC enzymes, it was presumed that these enzymes might share some overlap in substrate specificity. To clarify the biochemical activity of both of these SDC-like sequences, we assessed the AtSDC enzyme for activity towards aromatic amino acids and the SlAAAD enzyme for activity towards serine. Additionally, we expressed and characterized two previously uninvestigated SDC-like enzymes from *Medicago truncatula* and *Cicer arietinum* in an effort to identify overlap in SlAAAD and AtSDC substrate selectivity. Our study of these uncharacterized SDC-like proteins led to an interesting discovery. Our data clearly show that both the *M. truncatula* and *C. arietinum* proteins function as acetaldehyde synthases with substrate preferences for bulky hydrophobic amino acids. In this report, we provide data that describe the substrate specificity, catalytic reaction and kinetic properties of these recombinant enzymes. This study of the novel activity of the *M. truncatula* and *C. arietinum* acetaldehyde synthases provides insights for a better understanding of the functional evolution of plant type II pyridoxal 5'-phosphate decarboxylases.

5.4 Materials and Methods

Reagents

Alanine, arginine, asparagine, aspartic acid, cysteine, glutamine, glutamic acid, glycine, histidine, isoleucine, leucine, lysine, methionine, phenylalanine, proline, serine, threonine, tryptophan, 5-hydroxytryptophan, tyrosine, valine, dopa, pyridoxal 5-phosphate, formic acid, phthaldialdehyde, hydrogen peroxide solution and acetonitrile were purchased from Sigma (St. Louis, MO). The IMPACT-CN protein expression system was purchased from New England Biolabs (Ipswich, MA).

Preparation of the recombinant proteins

M. truncatula cDNA and *S. lycopersicum* cDNA were obtained through Dr. Jiangqi Wen at the Noble Institute and Dr. Richard Veilleux from the Virginia Tech horticulture department, respectively. *C. acuminata* seeds were obtained through Bountiful Gardens. *C. acuminata* seeds were germinated in Sunshine Pro Premium potting soil and were grown under a 16 h photoperiod at 23 ^{o}C. at 100 microeinsteins. Total RNA was isolated from whole plants (12 weeks) Ambion mirVana™ miRNA Isolation Kit. RNA samples were subsequently DNase-treated using Ambion TURBO DNA-free™ Kit. cDNAs were produced using Invitrogen ™ SuperScript™ III First-Strand Synthesis System for RT-PCR. *A. thaliana* cDNA was prepared as previously described [13]. Primer pairs were synthesized and used for the amplification of the *M. truncatula* [GenBank: XP_003592128] MtAAS gene, the *C. arietinum* [GenBank: XP_004496485] CaAAS gene, the *S. lycopersicum* NP_001233845 SlAAAD gene and the *Arabidopsis thaliana* NP_175036 AtSDC gene (Table 5.1).

Table 5.1. Cloning primers.

Primer Name	Sequence
Medicago truncatula XP_003592128 forward	ACTG***CATATG***ATGGCAATGACTTTCATTCCT
Medicago truncatula XP_003592128 reverse	ACTG***CTCGAG***CTAACAATTTCTCGATAAGTTGTGTAT
Cicer arietinum XP_004496485 forward	ACTG***CATATG***GAGAATCAAGTACAAGAAGAC
Cicer arietinum XP_004496485 reverse	*ACTG**CTCGAG**TCAATTGTGCAATGAACAAATAC*
Solanum lycopersicum NP_001233845 forward	AAA***ACTAGT***ATGGGTAGTCTCTCACTTGAAATG
Solanum lycopersicum NP_001233845 reverse	AAA***CTCGAG***CTAAGGACAGATGTAGTCAATCATG
Arabidopsis thaliana NP_175036 forward	ACTG***GAATGCT***ATGGTTGGATCTTTGGAATC
Arabidopsis thaliana NP_175036 reverse	ACTG***CTCGAG***TCACTTGTGAGCTGGACAG

The resulting PCR products were ligated into the pTYB12 IMPACT-CN bacterial expression plasmid. DNA sequencing was utilized to verify the sequences and frame of each cDNA insert. Transformed bacterial colonies were selected and used for large-scale expression of individual recombinant proteins. Bacterial cells were cultured at 37 ^{o}C. After induction with 0.15 mM IPTG, the cells were cultured at 15 ^{o}C for 24 hrs. The soluble fusion proteins were applied to a column packed with chitin beads and subsequently hydrolyzed under reducing conditions. The affinity purification resulted in the isolation of each individual recombinant protein at about 85% purity. Further purifications of the recombinant proteins were achieved by Mono-Q and gel filtration chromatographies (greater than 95% purity). Purity of the recombinant proteins was evaluated by SDS-PAGE. Purified recombinant enzymes were concentrated to 5 mg/ml protein in 20 mM HEPES (pH 7.5), containing 5 mM PLP using a Centricon YM-50 concentrator (Millipore). Using bovine serum albumin as a standard, purified recombinant proteins concentrations were determined by a Bio-Rad protein assay kit (Hercules, CA).

MtAAS and CaAAS *activity assays*

Typical reaction mixtures of 50 μl, containing 25 μg of MtAAS recombinant enzyme and 5 mM substrate (20 proteinogenic amino acids plus 5-hydroxytryptophan and dopa) were prepared in 20 mM HEPES (pH 7.5) and incubated at 25 ^{o}C in a water bath. The reactions were stopped after

20 minutes through the addition of 50 μl of 0.8 M formic acid. Supernatants of the reaction mixtures, obtained by centrifugation, were analyzed with (Aqueous) Pierce Quantitative Peroxide Assay Kit to determine AAS activity. Tryptophan reaction mixtures were also analyzed by high-performance liquid chromatography (HPLC) with electrochemical detection (HPLC-EC). 50 μl reactions containing 25 μg of recombinant enzyme and 8 mM tryptophan were prepared in 20 mM HEPES (pH 7.5) and incubated at 25 ^{o}C in a water bath for 5, 20 or 40 minutes. The reactions were stopped through the addition of 200 μl of 0.8 M formic acid or with 200 μl of borohydride saturated ethanol solution. Separation was achieved through a 50 mM potassium phosphate isocratic running buffer (pH 4.0) with 0.5 mM octyl sulfate and 45% acetonitrile. Indole-3-ethanol was verified though the comparison of authentic standards under identical chromatography conditions.

Kinetic analysis

Initial MtAAS and CaAAS activity assays indicated that at high substrate concentrations (5 mM) several hydrophobic amino acids demonstrated significant activity. To determine the binding affinity and reaction velocity the kinetic parameters of the enzyme were analyzed using leucine, methionine, tryptophan, and phenylalanine. Reaction mixtures of 50 μl containing 5 μg of recombinant protein and varying concentration of substrate (0.0025 – 45 mM; depending on the solubility of individual amino acids) were prepared in 20 mM HEPES (pH 7.5) and incubated at 25^{o} C. An equal volume of 0.8 M formic acid was added to each reaction mixtures after 5 min of incubation and analyzed using the Pierce® Quantitative Peroxide Assay Kit. Product formation was compared to standards generated from 30% (w/w) hydrogen peroxide solution. Kinetic data points were performed in triplicate and kinetic values were evaluated by hyperbolic regression.

MtAAS, CaAAS, AtSDC and SlAAAD activity comparisons

HPLC electrochemical analysis was used to further illustrate the unusual substrate range of MtAAS and CaAAS enzymes. Purified AtSDC and SlAAAD recombinant enzymes were assayed against the preferred substrates of MtAASs and CaAAS (phenylalanine, methionine, leucine and tryptophan) in addition to other common type II PLP decarboxylase substrates (histidine, serine, glutamate, dopa and tyrosine). Reaction mixtures of 50 μl containing 15 μg of recombinant protein and 5 mM substrate were prepared in 20 mM HEPES (pH 7.5) and stopped with an equal volume of 0.8 M formic acid after 10 min of incubation at 25^{o} C. The products (besides tryptophan, 5-hydroxytryptophan, dopa, tyrosine, reactions) were then derivatized with OPA-thiol reagent (to convent amine to electrochemically active compound). Various isocratic running buffers consisting of 50 mM phosphate buffer pH 4.0, 0.5 mM octyl sulfate and a acetonitrile range of 40-55% were used for the OPA-thiol characterization. An isocratic running buffer consisting of 50 mM phosphate buffer pH 4.3, 28% acetonitrile, and 0.5 mM octyl sulfate was used for the tryptamine products. An isocratic running buffer consisting of 50 mM phosphate buffer pH 4.3, 18% acetonitrile, and 0.5 mM octyl sulfate was used for the dopamine and tyramine products.

5.5 Results

Qualitative analysis of AtSDC and SlAAAD activities

Initially, our interest in SDC-like enzymes was aroused from the report of the unusual tomato SDS-like SlAAADs [9]. Although SDCs and AAADs are proposed to have a common evolutionary ancestor, significant evolutionary divergence has occurred between these two groups resulting in limited sequence conservation. While individual enzymes within each group (AAADs and SDCs) retain high sequence identity (typically greater than 50%), enzymes between these related groups maintain significantly reduced identity (typically lower than 15%). Therefore, the high sequence identity (57%) between the aromatic amino acid decarboxylating

SlAAADs and serine decarboxylating AtSDC is quite unusual. In fact, the extensively shared identity of these enzymes led us to believe that there were likely overlaps in substrate specificity. The original characterization of SlAAAD did not test serine as a substrate while the original report of AtSDC did not examine if phenylalanine serves as a potential substrate [1,9]. To investigate their true substrate profiles, both the AtSDC and the SlAAAD were expressed, purified and subjected to decarboxylation activity assays. Analysis of the AtSDCs substrate preference confirmed the results of the original report [1]. AtSDC only has activity towards serine with no measurable decarboxylation of histidine, dopa, tyrosine, phenylalanine, tryptophan or glutamate (Figure 5.1).

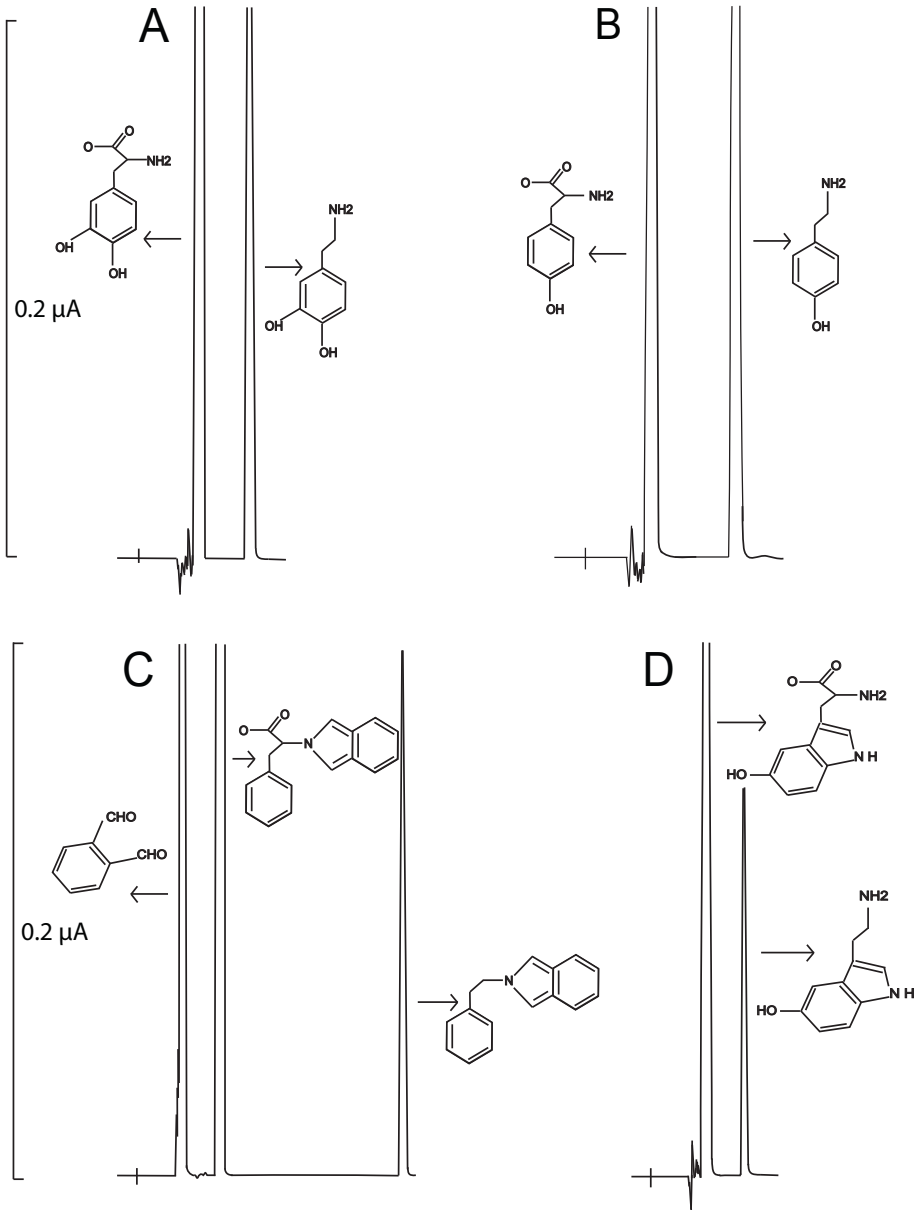

Figure 5.1. HPLC-EC analysis of SlAAAD activity with dopa, tyrosine, phenylalanine and tryptophan as substrates. Y-axis represents the output in microamps and the x-axis represents retention time. Reaction mixtures of 50 µl containing 15 µg of SlAAAD and 5 mM of substrate were incubated at 25 ^{o}C and their reaction was stop at 10 min after incubation by adding an equal volume of 0.8 M of formic acid into the reaction mixture. After stopping the reaction with formic acid, the phenylalanine reaction mixture was treated OPA-thiol reagent to generate an electrochemically active conjugate. The mixtures were centrifuged for 5 min at 14,000g and supernatants were injected for HPLC-EC analysis. Chromatogram (A) illustrates the accumulation of dopamine in a SlAAAD and dopa reaction mixture. Chromatogram (B) illustrates the accumulation of tyramine in a SlAAAD and tyrosine reaction mixture. Chromatogram (C) illustrates the accumulation of phenylethylamine in a SlAAAD and phenylalanine reaction mixture. Chromatogram (D) illustrates the accumulation of tryptamine in a SlAAAD and tryptophan reaction mixture. Various isocratic running buffers consisting of 50 mM phosphate buffer pH 4.0, 0.5 mM octyl sulfate and a acetonitrile range of 18-55% were used for the characterization.

An identical SlAAAD decarboxylation assay demonstrated activity towards tyrosine, dopa, phenylalanine and tryptophan with no activity towards serine, histidine or glutamate (Figure 5.2). These results confirmed the separate functions of these highly homologous enzymes.

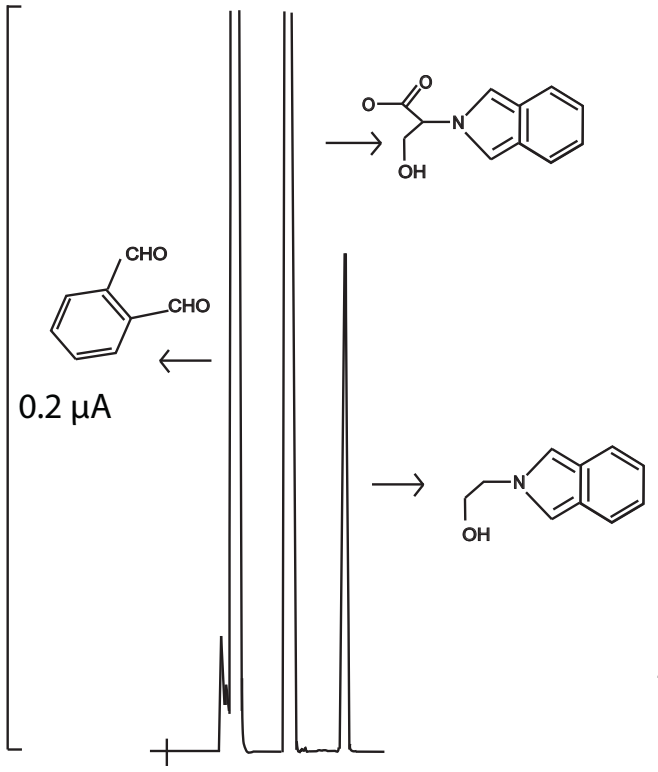

Figure 5.2. HPLC-EC analysis of AtSDC activity with serine as a substrate. Y-axis represents the output in microamps and the x-axis represents retention time. The reaction mixture of 50 µl containing 15 µg of SlAAAD and 5 mM of serine was incubated at 25 ^{o}C and stopped after 10 min of incubation by adding an equal volume of 0.8 M formic acid. Next, the reaction mixture was treated OPA-thiol reagent to generate an electrochemically active conjugate. The mixture was centrifuged for 5 min at 14,000g and supernatant was injected for HPLC-EC analysis. The chromatogram illustrates the accumulation of ethanolamine in an AtSDC and serine reaction mixture. An isocratic running buffer consisting of 50 mM phosphate buffer pH 4.0, 0.5 mM octyl sulfate and 40% acetonitrile was used for the characterization.

Characterization of MtAAS

In an effort to evaluate biophysical characteristics capable of differentiating these functionally divergent enzymes, we have cloned, expressed, and purified a SDC-like enzyme from *Medicago truncatula* (MtAAS) and a SDC-like enzyme from *Cicer arietinum* (CaAAS). MtAAS and CaAAS were initially assayed using known group II amino acid decarboxylase substrates (serine, histidine, glutamate, tyrosine, dopa, tryptophan, and 5-hydroxytryptophan) via an HPLC electrochemical assay [10,13-14]. Despite demonstrating no measurable amine product formation from any of the tested substrates, a very broad peak was detected in the tryptophan reaction mixtures for each enzyme. The peak dimension increased proportionally as the incubation time increased (Figure 5.3A-C), indicating that the broad peak corresponds to the reaction product. The product peak in the recombinant enzymes and tryptophan reaction mixtures appeared to be an aromatic acetaldehyde based on its similar chromatographic behavior to previously investigated aromatic acetaldehydes [13,15-16]. This acetaldehyde-like peak suggested that the MtAAS and CaAAS enzymes might function as aromatic aldehyde synthases rather than a serine decarboxylases. Aldehydes can be reduced to their corresponding alcohol by borohydride [13,15]. When the recombinant protein and tryptophan reaction mixtures were treated with $NaBH_4$ prior to HPLC-ED analysis, the broad product peak (Figure 5.3A-C) was converted to a sharp peak (Figure 5.3D-F).

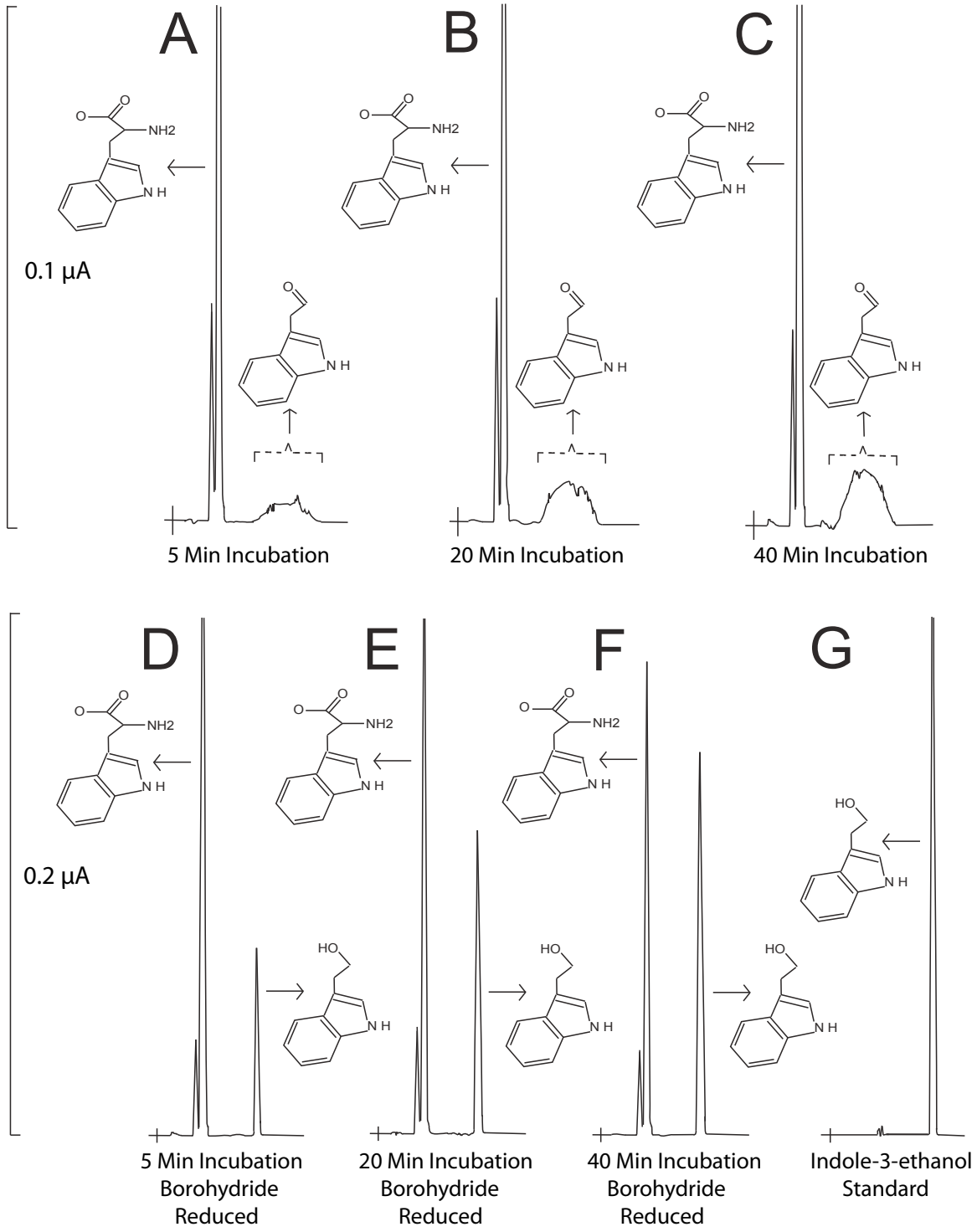

Figure 5.3. HPLC-EC detection of indole-3-acetaldehyde generated from MtAAS and tryptophan reaction mixtures. (Chromatograms A-F) Y-axis represents the output in microamps and the x-axis represents retention time. Chromatograms (A-C) illustrate the indole-3-acetaldehyde (the major broad peak) formed in MtAAS and tryptophan reaction mixtures after 5 min, 20 min and 40 min incubation, respectively. Chromatograms (D-F) illustrate the indole-3-ethanol (tryptophol) formed in borohydride reduced MtAAS and tryptophan reaction mixtures

after 5 min, 20 min and 40 min incubation, respectively. Chromatogram (G) shows the detection of authentic indole-3-ethanol standard.

The sharp peak, detected in the borohydride-treated reaction mixture, had identical retention time as authentic indole-3-ethanol under the same conditions of HPLC-EC analysis and coeluted with the standard at different mobile phase conditions during HPLC-EC analysis (Figure 5.3G). Comparison of the chromatographic behavior of the product and authentic tryptamine further indicated that these enzymes function as a novel aldehyde synthases and not as a decarboxylases (Figure 5.4).

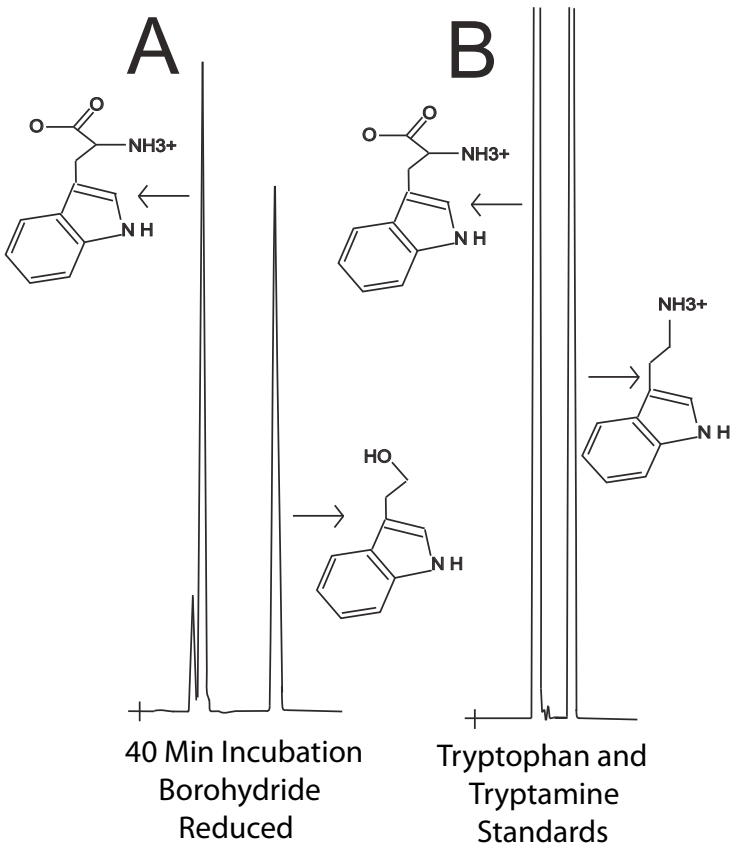

Figure 5.4. HPLC-EC analysis of MtAAS activity with tryptophan as a substrate. Y-axis represents the output in microamps and the x-axis represents retention time. The reaction mixture of 50 µl containing 15 µg of MtAAS and 5 mM of tryptophan was incubated at 25 ^{o}C and stopped after 10 min of incubation by adding an equal volume of 0.8 M of 100% ethanol saturated with borohydride. The mixture was centrifuged for 5 min at 14,000g and supernatant was injected for HPLC-EC analysis. Chromatogram (A) illustrates the accumulation of indole-3-acetaldehyde (subsequently reduced to indole-3-ethanol via borohydride) in an MtAAS and

tryptophan reaction mixture. Chromatogram (B) illustrates a tryptophan and tryptamine standard. An isocratic running buffer consisting of 50 mM phosphate buffer pH 4.0, 0.5 mM octyl sulfate and 28% acetonitrile was used for the characterizations.

To further verify if the recombinant enzymes function as a novel aldehyde synthases (AAS) a peroxide assay was performed against each of the 20-proteinogenic amino acids (plus 5-hydroxytryptophan and dopa). Enzyme reaction mixtures were then assayed through the use of the Pierce® Quantitative Peroxide Assay Kit. AASs catalyze a rather complicated decarboxylation-oxidative deamination process of aromatic amino acids, leading to the production of aromatic acetaldehydes, CO_2, ammonia, and hydrogen peroxide rather than the AAAD derived arylalkylamines and CO_2 (Figure 5.5) [13,15,17-18].

Figure 5.5. Relative activities of aromatic amino acid decarboxylase (AAAD) and aromatic acetaldehyde synthases (AAS).

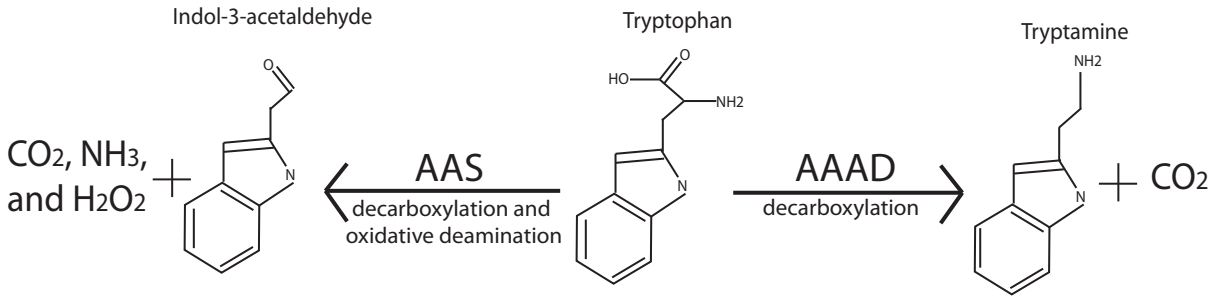

Therefore, the production of hydrogen peroxide can be used as a mechanism to further differentiating AAS and AAAD enzymatic activities. Results for both MtAAS and CaAAS demonstrated very minimal acetaldehyde synthase activity to the majority of tested substrates and significant acetaldehyde synthase activity towards several bulky, non-polar and hydrophobic amino acids (phenylalanine, methionine, leucine and tryptophan).

Kinetic properties of MtAAS and CaAAS

Next, amino acids demonstrating significant specific activity were used in a full kinetic study of the MtAAS and CaAAS enzymes. The profile of kinetically characterized substrates includes phenylalanine, methionine, leucine and tryptophan. Results demonstrated that the aforementioned amino acids function well as substrates (Table 5.2).

Table 5.2. Kinetic parameters

Enzyme	Substrate	kcat (sec^{-1})	K_m (mM)	kcat/Km ($sec^{-1} mM^{-1}$)
MtAAS	Phenylalanine	0.358 ± 0.005	0.02 ± 0.01	17.90 ± 2.29
MtAAS	Methionine	0.144 ± 0.006	1.90 ± 0.20	0.08 ± 0.01
MtAAS	Tryptophan	0.125 ± 0.008	1.70 ± 0.30	0.07 ± 0.01
MtAAS	Leucine	0.197 ± 0.005	7.60 ± 0.70	0.03 ± 0.01
CaAAS	Phenylalanine	0.595 ± 0.009	0.09 ± 0.01	6.60 ± 0.65
CaAAS	Methionine	0.351 ± 0.012	1.62 ± 0.20	0.22 ± 0.01
CaAAS	Tryptophan	0.187 ± 0.016	2.80 ± 0.70	0.07 ± 0.01
CaAAS	Leucine	0.467 ± 0.010	4.60 ± 0.40	0.10 ± 0.01

Values represent means SE (n=3)

All active substrates share similar biophysical characteristics (bulky, non polar, and hydrophobic). This substrate promiscuity is highly atypical of characterized AASs [15, 17-18].

Comparison of substrate promiscuity

Results from the kinetic characterization of MtAAS and CaAAS elaborated on the unusual activity and substrate specificity of the enzymes. To emphasize the promiscuous nature of these AASs, we have tested their preferred substrates against the homologous AtSDC and the SlAAAD enzymes. Literature searches in addition to our own analysis indicate that the AtSDC

and SlAAAD enzymes both maintain stringent substrate specificity [1, 9]. The recombinantly characterized AtSDCs only displayed activity towards serine while the recombinantly characterized SlAAAD catalyzed the decarboxylation of aromatic substrates (phenylalanine, tyrosine, dopa and tryptophan). An HPLC electrochemical assay of SlAAAD and AtSDC using MtAASs preferred substrates (phenylalanine, methionine, leucine and tryptophan) further verify the previous reported AtSDC and SlAAAD activity. Results indicate that AtSDC lacks measurable activity towards any of the MtAAS and CaAAS substrates while the SlAAAD lacks activity towards leucine and methionine. In addition to divergent substrate specificities, an AAS hydrogen peroxide assay of AtSDC and SlAAAD towards their preferred substrates (serine and tyrosine respectively) demonstrated no peroxide production (Figure 5.6). The lack of AAS activity and limited substrate profile of AtSDC and SlAAAD serve to highlight the unusual nature of the recombinantly characterized promiscuous MtAAS and CaAAS enzymes.

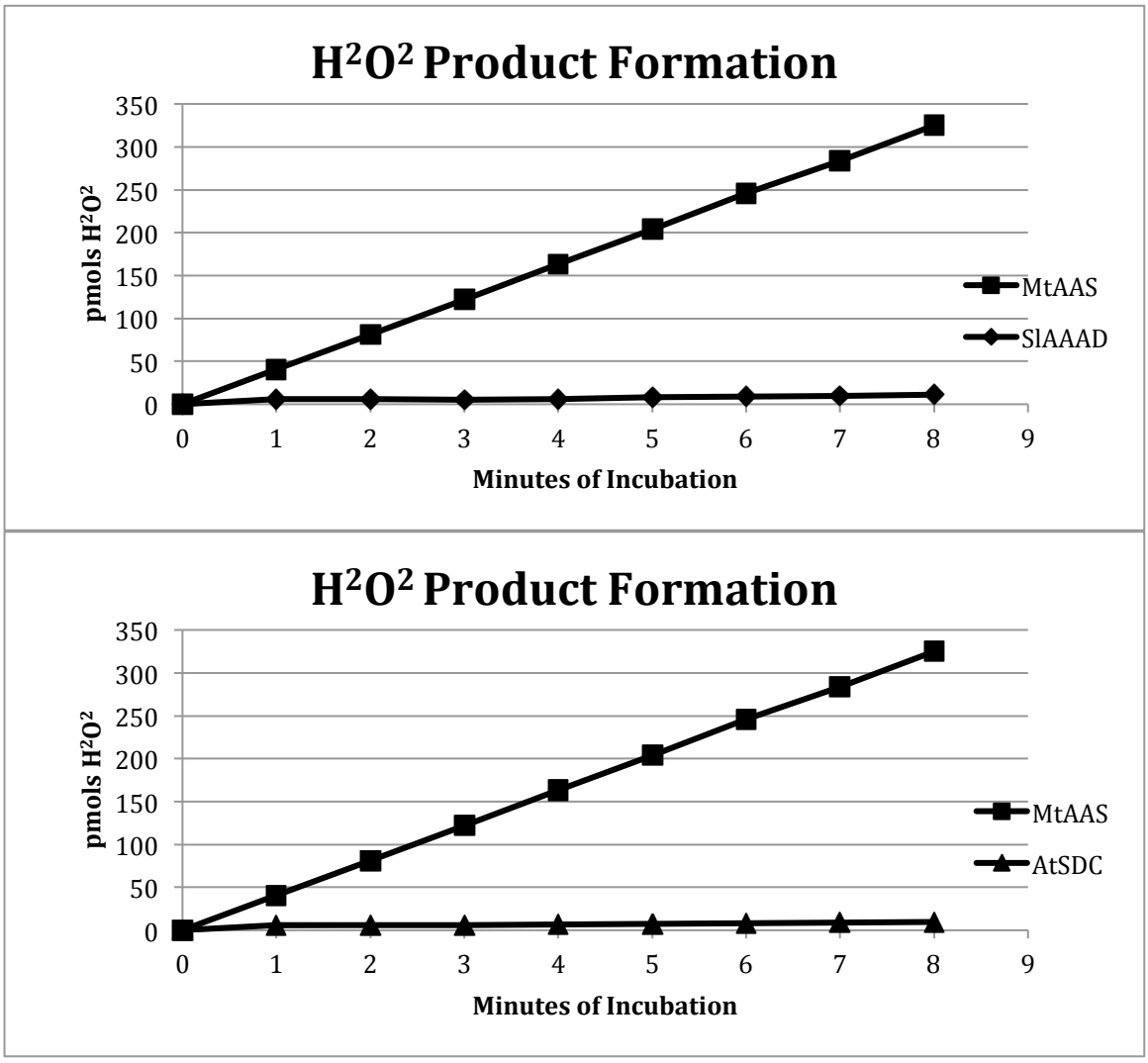

Figure 5.6. Analysis of hydrogen peroxide generated from MtAAS, AtSDC and SlAAAD. The preferred substrate was used for each enzyme. Phenylalanine was used for MtAAS, serine was used for AtSDC and tyrosine was used for SlAAAD. Reaction mixtures of 0.2 ml containing 5 mM substrate and 1ug of recombinant enzyme were prepared in 20 mM HEPES (pH 7.5). The reaction mixtures were incubated at 25 °C. At each 1-min interval, 20 µl of reaction mixture was withdrawn and mixed into 200 µl of Pierce peroxide assay reagents solution. The MtAAS, AtSDC and SlAAAD curves illustrate the amount of H_2O_2 accumulated in 20 µl of reaction mixtures at a 1–8-min incubation periods. Product formation from AtSDC and SlAAAD reaction mixtures are displayed on separate graphs to maintain figure clarity.

5.6 Discussion

Type II pyridoxal 5'-phosphate (PLP)-dependent decarboxylases are a group of enzymes with important roles in amino acid metabolism. This group of enzymes has undergone functional

evolution from a shared ancient evolutionary origin to generate a selection of subfamilies with stringent substrate selectivity's [14]. Plant type II PLP decarboxylases include aromatic amino acid decarboxylases (AAADs), serine decarboxylases (SDCs) and glutamate decarboxylases (GDCs). Plant SDSs catalyze the decarboxylation of serine to ethanolamine [1], GDCs catalyze the decarboxylation of glutamate to γ-aminobutyric acid (GABA) [19] and AAADs catalyze the decarboxylation of aromatic amino acids to generate aromatic arylalkylamines [10-12]. Based on their respective substrate specificities each group is responsible for the biosynthesis of unique products [1,10,19]. Although all plant type II PLP decarboxylases have evolved from a common evolutionary ancestor, significant evolutionary divergence has occurred resulting in limited sequence conservation [14]. While individual enzymes within each group (AAADs, SDCs, and GDCs) maintain high identity (typically greater than 50%), enzymes between these related groups maintain significantly reduced identity (typically lower than 15%). For example, the characterized *Arabidopsis thaliana* enzymes from each class demonstrate 9% identity between GDC (NP_*197235) and SDC (NP*_175036), 5% identity between GDC and AAAD (NP_001078461), and 14% identity between SDC and AAAD.

Unlike other plant type II PLP decarboxylases, plant AAADs have undergone additional functional evolution resulting in multiple paralogs with divergent functions [10]. Plant AAAD subfamilies include tryptophan decarboxylases (TDCs) [12], tyrosine decarboxylases (TyDCs) [11] and aromatic acetaldehyde synthases (AASs) [17]. TDCs and TyDCs catalyze the decarboxylation of indolic and phenolic amino acids respectively to generate their corresponding aromatic arylalkylamines while AAS catalyze a more involved decarboxylation/oxidative deamination reaction to generate aromatic acetaldehydes from their phenolic amino acid substrates. Although this functional divergence is well documented within plant AAADs [10], there has been no reports of similar divergence within plant SDCs or GDCs.

In this study we have investigated plant SDC-like enzymes in an effort to evaluate their functional divergence. To gain additional insight into variations in substrate selectivity, we have analyzed two SDC-like enzymes from *Medicago truncatula* and *Cicer arietinum*. Activity assays and a full kinetic characterization of the MtAAS and CaAAS demonstrated novel aldehyde synthase enzymes with activity towards phenylalanine, methionine, leucine and tryptophan. These SDC-like enzymes are capable of generating phenylacetaldehyde, 4-(methylthio) butanal, 3-methylbutanal (isovaleraldehyde) and indole-3-acetaldehyde from phenylalanine, methionine, leucine and tryptophan respectively. Judging by the respective k_{cat}/K_m values of the MtAAS and CaAAS substrates in addition to the previous characterization of phenylalanine decarboxylation and oxidative deamination enzymes [17-18], it is likely that MtAAS and CaAAS function as a phenylacetaldehyde *synthases* (PAAS) for the *in vivo* production of phenylacetaldehyde (a floral volatile [20-22]). Despite the obvious preference for phenylalanine as a substrate, tryptophan, methionine and leucine have specificity constants comparable to other recombinantly characterized PAAS enzymes. For example the k_{cat}/K_m for the petunia PAAS and the Arabidopsis PAAS towards phenylalanine are k_{cat}/K_m 0.678 sec^{-1} mM^{-1} and k_{cat}/K_m 0.012 sec^{-1} mM^{-1} respectively [17-18]. The physiologically relevant k_{cat}/K_m values of MtAAS and CaAAS towards tryptophan, methionine and leucine indicate that these substrates may be catalyzed to product formation *in vivo.*

If phenylalanine were indeed the preferred physiological substrate of MtAAS and CaAAS, then one might ask, why would these enzymes demonstrate significant and unusual activity towards other biophysically similar amino acids. Two potential explanations occur to us. First, these enzymes do indeed use these amino acid substrates for the production of evolutionary useful compounds. Second, these enzymes have recently (from an evolutionary perspective) diverged from an SDC and are currently in the process of evolving and tuning the enzymes specificity

towards phenylalanine. To analyze the first explanation, we have performed literature searches in an effort to find examples of 4-(methylthio) butanal, 3-methylbutanal (isovaleraldehyde) and indole-3-acetaldehyde product formation. Although 4-(methylthio) butanal and 3-methylbutanal (isovaleraldehyde) proved to be unknown enzyme products, there have been many references regarding the production of indole-3-acetaldehyde [13, 23-24]. Indole-3-acetaldehyde is a proposed intermediate in the original tryptophan dependent indole-3-pyruvic acid (IPA) auxin biosynthetic pathway [23-24]. Although many references suggest indole-3-acetaldehyde as an auxin intermediate, a full indole-3-acetaldehyde dependent biosynthetic pathway has not been identified. Despite the proposition of plant aldehyde oxidases capable of catalyzing the conversion of indole-3-acetaldehyde to indole-3-acetic acid (IAA) there have thus far been no enzymes capable of generating indole-3-acetaldehyde [25-26]. Interestingly, the decarboxylation and oxidative deamination of tryptophan via MtAAS or CaAAS is capable of performing this very function. Therefore, it is reasonable to suggest this enzyme could be a possible link in the biosynthesis of auxin (Figure 5.7.).

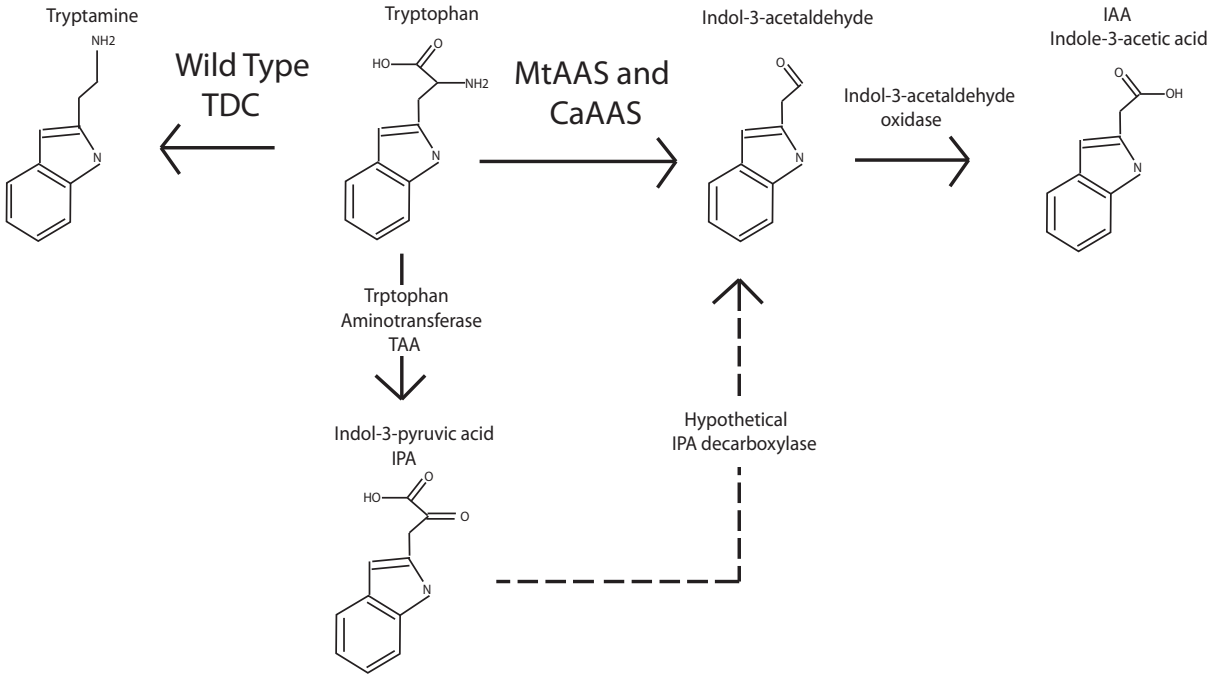

Figure 5.7.

Intersection of the MtAAS and CaAAS enzymes and the proposed tryptophan dependent indole-3-pyruvic acid auxin biosynthetic pathway.

The second explanation regarding unusual product formation of MtAAS suggests that 4-(methylthio) butanal, 3-methylbutanal (isovaleraldehyde) and indole-3-acetaldehyde are unintended byproducts. Such catalytic promiscuity appears to be a common consequence of secondary metabolite biosynthetic enzymes [27-29]. This mechanistic elasticity of secondary metabolite biosynthetic enzymes often results in diminished catalytic efficiency with greater substrate permissiveness [27-29]. Although unintended chemistry and product formation may occur, the synthesis of a product that confers a fitness advantage will still drive the proliferation of the gene. Individual secondary metabolite biosynthetic enzymes do not require exact substrate specificity or chemistry; they only require the synthesis of a useful compound to be maintained in the population. Moreover, such promiscuous substrate specificity may enable individual enzymes to play multiple physiological roles. One of the minor products may subsequently grant a reproductive advantage as the organism is exposed to a fluctuating environment. This work has identified an additional branch of SDC-like enzymes. Through enzymatic divergence this branch has developed novel substrate preferences and chemistry to generate an altered profile of products. In this study, we have characterized two AAS enzyme with unusual aldehyde synthase activity towards phenylalanine, tryptophan, methionine, and leucine. Although it is likely that these enzymes functions as a PAASs for the production of flower volatiles, additional product aldehyde formation opens the options for alternative physiological roles. Additional research is needed to clarify the *in vivo* function of this enzyme. This research serves to demonstrate the complexities of plant type II PLP decarboxylases and the evolution of plant secondary biosynthetic enzymes as a whole.

5.7 Acknowledgements

This study was supported through Virginia Tech Biochemistry college of Agricultural and Life Sciences funding.

References

[1] Rontein D, Nishida I, Tashiro G, Yoshioka K, Wu W, Voelker DR., Basset G, Hanson AD: Plants synthesize ethanolamine by direct decarboxylation of serine using a pyridoxal phosphate enzyme. J. Biol. Chem 2001, 276 (38): 35523-35529

[2] Mudd, S.H. and Datko, A.H. (1989) Synthesis of ethanolamine and its regulation in Lemna paucicostata. Plant Physiol. 91, 587–597.

[3] Rhodes, D. and Hanson, A.D. (1993) Quaternary ammonium and tertiary sulfonium compounds in higher plants. Annu. Rev. Plant Physiol. Plant Mol. Biol. 44, 357–384

[4] Gibellini, F. and Smith, T.K. (2010) The Kennedy pathway-de novo synthesis of phosphatidylethanolamine and phosphatidylcholine. IUBMB Life. 62, 414–428.

[5] Raetz, C.R. (1986) Molecular genetics of membrane phospholipid synthesis. Annu. Rev. Genet. 20, 253–295.

[6] Zinser, E., Sperkagottlieb, C.D.M., Fasch, E.V., Kohlwein, S.D., Paltauf, F. and Daum, G. (1991) Phospholipid synthesis and lipid composition of subcellular membranes in the unicellular membranes in the unicellular eukaryote Saccharomyces cerevisiae. J. Bacteriol. 173, 2026–2034.

[7] Kwon, Y., Yu, S.I., Lee, H., Yim, J.H., Zhu, J.K. and Lee B.H. (2012) Arabidopsis serine decarboxylase mutants implicate the roles of ethanolamine in plant growth and development. International Journal of Molecular Sciences. 13, 3176–3188

[8] Picton, S., Gray, J. E., Payton, S., Barton, S. L., Lowe, A., and Grierson, D. (1993) A histidine decarboxylase-like mRNA is involved in tomato fruit ripening. Plant Mol. Biol. 23, 627–631

[9] Tieman, D., Taylor, M., Schauer, N., Fernie, A.R., Hanson, A.D., and Klee, H.J. (2006) Tomato aromatic amino acid decarboxylases participate in synthesis of the flavor volatiles 2-phenylethanol and 2-phenylacetaldehyde. PNAS 103 (210), 8287-8292

[10] Facchini, P. J., Huber-Allanach, K. L., and Tari, L. W. (2000) Plant aromatic L-amino acid decarboxylases: evolution, biochemistry, regulation, and metabolic engineering applications. Phytochemistry 54, 121-138.

[11] Lehmann, T. and Pollmann, T. (2009) Gene expression and characterization of a stress-induced tyrosine decarboxylase from Arabidopsis thaliana. FEBS Letters 583, 1895–1900

[12] De Luca, V., Marineau, C. and Brisson, N. (1988) Molecular cloning and analysis of cDNA encoding a plant tryptophan decarboxylase: Comparison with animal dopa decarboxylase PNAS 86 (8), 2582-2586

[13] Torrens-Spence MP, Liu P, Ding H, Harich K, Gillaspy G, Li J (2013) Biochemical evaluation of the decarboxylation and decarboxylation–deamination activities of plant aromatic amino acid decarboxylases. J Biol Chem 288(4):2376–2387

[14] Sandmeier, E., Hale, T. I., and Christen, P. (1994) Multiple evolutionary origin of pyridoxal-5'-phosphate-dependent amino acid decarboxylases. Eur. J. Biochem. 221, 997–1002

[15] Torrens-Spence, M.P., Gillaspy, G., Zhao, B., Harich, K., White, R.H. and Li, J. (2012) Biochemical evaluation of a parsley tyrosine decarboxylase results in a novel 4-hydroxyphenylacetaldehyde synthase enzyme. Biochem Biophys Res Commun. 418(2), 211-216

[16] Vavricka C., Han Q., Huan Y., et al. (2011) From Dopa to dihydroxyphenylacetaldehyde: a toxic biochemical pathway plays a vital physiological function in insects. PLoS One 6(1): e16124.

[17] Kaminaga, Y., Schnepp, J., Peel, G., Kish, C. M., Ben-Nissan, G., Weiss, D., Orlova, I., Lavie, O., Rhodes, D., Wood, K., Porterfield, D. M., Cooper, A. J., Schloss, J. V., Pichersky, E., Vainstein, A., and Dudareva, N. (2006) Plant phenylacetaldehyde synthase is a bifunctional homotetrameric enzyme that catalyzes phenylalanine decarboxylation and oxidation. J Biol Chem. 281, 23357-23366.

[18] Gutensohn, M., Klempien, A., Kaminaga, Y., Nagegowda, D. A., Negre-Zakharov, F., Huh, J. H., Luo, H., Weizbauer, R., Mengiste, T., Tholl, D., and Dudareva, N. (2011) Role of aromatic aldehyde synthase in wounding/herbivory response and flower scent production in different Arabidopsis ecotypes. Plant J. 66, 591-602.

[19] Bouché, N., Fait, A., Zik, M. and Fromm, H. (2004) The root-specific glutamate decarboxylase (GAD1) is essential for sustaining GABA levels in Arabidopsis. Plant Mol Biol. 55(3) 315-325

[20] Knudsen, J. T., Tollsten, L., and Bergstrom, G. (1993) Floral scents – a checklist of volatile compounds isolated by head-space techniques. Phytochemistry 33, 253–280

[21] Verdonk, J. C., de Vos, C. H. R., Verhoeven, H. A., Haring, M. A., van Tunen, A. J., and Schuurink, R. C. (2003) Regulation of floral scent production in petunia revealed by targeted metabolomics. Phytochemistry 62, 997–1008

[22] Boatright, J., Negre, F., Chen, X., Kish, C. M., Wood, B., Peel, G., Orlova, I., Gang, D., Rhodes, D., and Dudareva, N. (2004) Understanding in vivo benzenoid metabolism in petunia petal tissue Plant Physiol. 135, 1993–2011

[23] Woodward, A.W. and Bartel, B. (2005) Auxin: regulation, action, and interaction. Ann Bot. **95**, 707–735.

[24] Koga, J., Adachi, T. and Hidaka, H. (1992) Purification and characterization of indolepyruvate decarboxylase. A novel enzyme for indole-3-acetic acid biosynthesis in Enterobacter cloacae. J. Biol. Chem. **267**, 15823–15828.

[25] Seo, M., Akaba, S., Oritani, T., Delarue, M., Bellini, C., Caboche, M., and Koshiba, T. (1998) Higher activity of an aldehyde oxidase in the auxin-overproducing superroot1 mutant of Arabidopsis thaliana. Plant Physiol. **116**, 687–693.

[26] Sekimoto, H., Seo, M., Kawakami, N., Komano, T., Desloire, S., Liotenberg, S., Marion-Poll, A., Caboche, M., Kamiya, Y. and Koshiba, T. (1998) Molecular cloning and characterization of aldehyde oxidases in Arabidopsis thaliana. Plant Cell Physiol. **39**, 433–442.

[27] Weng, J.-K. (2013) The evolutionary paths towards complexity: a metabolic perspective. New Phytol 201, 1141–1149.

[28] Tokuriki, N., Jackson, C.J., Afriat-Jurnou, L., Wyganowski, K.T., Tang, R. and Tawfik, D.S. (2012) Diminishing returns and tradeoffs constrain the laboratory optimization of an enzyme. Nature Communications 3: 1257.

[29] Weng, J.-K. and Noel, J.P. (2012) The Remarkable Pliability and Promiscuity of Specialized Metabolism. Cold Spring Harb. Symp. Quant. Biol. 77, 309-320

Chapter 6

6.1 Conclusions

Aromatic amino acid decarboxylases (AAADs) are a group of economically important and phylogenetically diverse enzymes categorically joined through their pyridoxal-5'-phosphate (PLP) dependence and sequence homology. These enzymes catalyze key reactions in a diverse set of pathways impacting synthesis of neurotransmitters in animals and insects, alkaloid, volatile and hormone production in plants, and egg maturation, immune and muscle development in insects. This family of enzymes has been studied extensively in mammals where the single enzyme Dopa decarboxylase (DDC) catalyzes the decarboxylation of dopa to yield the neurotransmitter dopamine.

Extensive evolutionary divergence of AAADs has occurred in plants to produce multiple AAAD enzymes that fall into different subgroups that have different functions. Plant AAADs can use different substrates and catalyze different reactions (decarboxylation versus decarboxylation-deamination) with these substrates, creating a diverse set of end products. Despite these variations in substrate specificity and catalytic reactions, AAADs in general retain great amino acid homology. Due to this high sequence homology, it is difficult to predict the function of any given plant AAAD through sequence comparison. Of the thousands of predicted plant AAAD sequences in the databases, only a handful have been biochemically characterized. Thus our ability to utilize these enzymes for a better understanding of many different developmental and physiological pathways in plants remains limited.

Our bioinformatic and spectral analysis of several plant AAADs provide a tangible basis to suggest that some active site residues dictate substrate binding/recognition, are different in

distinct AAAD groups, and are identifiable through primary sequence analysis. This suggests that there are intrinsic characteristic residues dictating the substrate specificity and catalysis in each distinct AAAD group. Once biochemical and spectral data for a critical number of characterized AAADs is obtained, group-specific residues or fingerprints can be deciphered through bioinformatic approaches and used to distinguish them from other AAAD groups.

Bioinformatic and biochemical analysis of prospective activity and substrate specifying residues has identified several residues involved in AAAD functional differentiation. Characterization of these residues demonstrates their functional role within their respective enzymes. The resulting data have enabled the production of several mutant AAADs with novel chemistry with potential applications in metabolic engineering. Additionally the characterization of these dictating residues has generated a primary sequence fingerprint capable of differentiating different classes of plant AAADs. Moreover, investigation of these residues in homologous type II PLP decarboxylases has identified additional examples of functional evolution. Overall, the work presented in this document adds to the understanding of AAAD enzyme mechanisms, function, and evolution.